

Copyright
by
Thomas Korff
2005

**The Dissertation Committee for Thomas Korff certifies that this is the approved
version of the following dissertation:**

**Age-Related Differences in Muscular Force Application:
Differentiating Between the Influences of Growth and Maturation of the
Neuro-Motor System**

Committee:

Jody L. Jensen

Lawrence D. Abraham

Jonathan B. Dingwell

Richard R. Neptune

Marcus G. Pandy

**Age-Related Differences in Muscular Force Application:
Differentiating Between the Influences of Growth and Maturation of the
Neuro-Motor System**

by

Thomas Korff, M.S.

Dissertation

Presented to the Faculty of the Graduate School of

The University of Texas at Austin

in Partial Fulfillment

of the Requirements

for the Degree of

Doctor of Philosophy

The University of Texas at Austin

May, 2005

Dedication

Dedicated to my parents Heidemarie and Wilhelm Korff.

Acknowledgements

I express my sincere appreciation and gratitude to Dr. Jody Jensen for her continuous support during my Ph.D. program. She provided me with expert guidance and had faith in me throughout the whole course. I thank Jody not only for her significant contribution to achieving my academic goals, but also for her contribution to shaping my personality. Not only did she inspire me to ask important scientific questions, to obtain “good” data, and to “tell the story” well. She also taught me to be problem-oriented, persistent, and optimistic about my work and about life, in general.

I am greatly indebted to my dissertation committee. I was fortunate to benefit from a broad range of areas of interests and expertise within the committee. I express my sincere gratefulness to:

Dr. Lawrence Abraham who made me think about the “big picture” and the broad implications of the scientific questions that I pursued.

Dr. Jonathan Dingwell who was very helpful and creative in pointing out alternative ways and methods to better answer my questions.

Dr. Richard Neptune who gave me very clear and constructive guidance and advice with regards to scientific questions and methodological issues related to cycling and cycling biomechanics.

Dr. Marcus Pandy who gave me advice with regards to the biomechanical model used in this dissertation.

I express my thanks to all my fellow graduate students who made my time at UT a true and memorable experience. In particular, I thank Ana Almódovar, Mike Decker, Sky Pile, and Ajay Seth. Not only did I enjoy sharing ideas about scientific questions or methodological issues with them. I also appreciated their friendship and moral support throughout the whole program.

I am grateful for the support of my professors and teachers in the Colleges of Education and Engineering, the administrative staff in the Department of Kinesiology and Health Education, and the technical staff in the Departments of Mechanical Engineering and Aerospace Engineering.

I also express my thanks my parents and my sister. Their support and thrust were invaluable for me completing my degree at UT. Finally, I thank Dr. Lesley Brown. Through Lesley, I got exposed to the “world of science” and to the idea of pursuing a career in academia. With her help, I established the link with Dr. Jody Jensen which made possible my acceptance into the doctoral program at the University of Texas at Austin.

**Age-Related Differences in Muscular Force Application:
Differentiating Between the Influences of Growth and Maturation of the
Neuro-Motor System**

Publication No. _____

Thomas Korff, PhD

The University of Texas at Austin, 2005

Supervisor: Jody L. Jensen

As children grow older, multiple factors result in changes in motor behavior. These changes can be revealed in differences in the application of muscular forces, which give us information about the nervous system's contribution to the task. To allow for a valid interpretation of age-related differences in muscular force application, two general methodological assumptions must be made. The method to estimate muscular forces must be suitable, and age-related differences in muscular force application must not be confounded by factors other than those to which observed differences are attributed.

The goal of this dissertation was to distinguish between the contributions of growth and maturation to age-related differences in muscular force application. Distinguishing between these two factors is important because the interpretation of observed differences in muscular force application might be different, depending on their source. Three studies were performed. The first study was an investigation of the effect of growth on muscular force application using two different methods that have been

previously used to answer developmental questions. The results of this study revealed that the answer to the question of how growth affects the application of muscular forces depends on the biomechanical technique used. Based on these results, an analysis of intersegmental dynamics was chosen as the method for Studies 2 and 3. Studies 2 and 3 were designed to differentiate between the influences of growth and maturation of the neuro-motor system on children's adaptability in terms of muscular power production. Results of Study 2 revealed that during pedaling, segmental growth has a significant effect on how muscular power is transferred through the limbs to the crank. Results of Study 3 showed that if children perform a cyclical dynamic task at a high movement speed, a reduction in muscular power production results in a weaker synergy of inter-muscular coordination.

The results of this dissertation increase our understanding about the factors that lead to age-related improvements in adaptation and let us speculate about the factors that are limiting children's performance ranges. They have practical implications for teachers and coaches and are important prerequisites for future research.

Table of Contents

List of Tables	xi
List of Figures	xiii
Chapter 1: General Introduction	1
Chapter 2: Study 1	8
Introduction.....	8
Methods.....	12
Results.....	20
Discussion	27
References.....	31
Chapter 3: Study 2	33
Introduction.....	33
Methods.....	36
Results.....	45
Discussion	53
References.....	57
Chapter 4: Study 3	59
Introduction.....	59
Methods.....	64
Results.....	75
Discussion	95
References.....	103
Chapter 5: General Discussion.....	105
Appendix A: Consent Forms	110
Appendix B: Bicycle-Riding Questionnaires.....	116

Appendix C: Subject Information.....	118
Subject Information Sheet.....	118
Spreadsheet for Estimating Peak Power	119
Appendix D: Pedaling Model	120
Kinematic Constraint Equations	123
Decomposition of mechanical power.....	126
Appendix E: Kautz and Hull’s Decomposition Technique.....	133
Appendix F: Tracking Results – Studies 1 and 2.....	136
Appendix G: Extended Results – Study 2.....	142
Appendix H: Sensitivity Analysis for Bilateral Asymmetry – Study 3	146
Appendix I: Extended Results - Study 3.....	152
Appendix J: Tracking Results – Study 3.....	171
References.....	175
Vita	179

List of Tables

Table 2.1	Anthropometric characteristics of the biomechanical models.	16
Table 2.2.	Statistical analysis of the Age x Method interactions of the MANOVAs on muscular and non-muscular power profiles during the different crank regions (EXT=extensor, FLEX=flexor, TOP=top, and BOT=bottom).	22
Table 2.3.	Statistical analysis of age-related differences in anthropometry on muscular (Mus) and non-muscular (Non-Mus) forces using the pedal force decomposition technique (PFD) and the forward dynamics simulation (FDS).....	22
Table 3.1.	Statistical analysis on the main effect for age on the muscular contributions to crank power (Mus2Crank) and to limb power (Mus2Limbs).....	47
Table 3.2.	Statistical analysis on Age x Cadence interaction with regard to the muscular contribution to limb power (Mus2Limbs).....	47
Table 3.3.	Effect sizes (ES) and percent differences (% difference) in muscular power contributions to limb power between hypothetical age groups.	52
Table 4.1.	Group characteristics of the participants who were included in the final analysis.....	66
Table H1.	Effect of bilateral asymmetry on the dependent variables used in Study 3.	151
Table II.	Effect sizes describing the age group differences in peak power (AD: adults; OC: older children; YC: younger children).....	168

Table I2.	Effect sizes describing the age group differences in net muscular power during the extensor phase (EXT) and during the top phase (TOP).	168
Table I3.	Effect sizes describing the age group differences in the hip power contribution to limb power the during the extensor phase (EXT) and during the top phase (TOP).	169
Table I4.	Effect sizes describing the age group differences in the ankle power contribution to limb power during the extensor phase (EXT) and during the top phase (TOP).	169
Table I5.	Effect sizes describing the age group differences in the knee power contribution to crank power the extensor phase (EXT) and during the top phase (TOP).	170
Table J1.	Tracking errors for younger children quantified as the relative absolute deviation (RAD) in percent.	171
Table J2.	Tracking errors for older children quantified as the relative absolute deviation (RAD) in percent.	172
Table J3.	Tracking errors for adults quantified as the relative absolute deviation (RAD) in percent.	173

List of Figures

Figure 2.1.	Regions of the crank cycle.	19
Figure 2.2.	Profiles of the muscular component of the pedal reaction force using the pedal force decomposition (PFD) and the forward dynamics simulation (FDS).....	23
Figure 2.3.	Profiles of the non-muscular component of the pedal reaction force using the pedal force decomposition (PFD) and the forward dynamics simulation (FDS).....	24
Figure 2.4.	Effect of age-related changes in anthropometry on the averaged normalized muscular forces during the extensor (EXT) and flexor (FLEX) regions of the crank cycle.....	25
Figure 2.5.	Effect of age-related changes in anthropometry on the averaged normalized muscular forces during the top (TOP) and bottom (BOT) regions of the crank cycle.	26
Figure 3.1.	Regions of the crank cycle.	42
Figure 3.2.	Profiles of the muscular power contribution to crank power for hypothetical preadolescents (anthro-PA), older children (anthro-OC) and younger children (anthro-YC) for 60 rpm (A) and 120 rpm (B).	48
Figure 3.3.	Age-group differences in the muscular power contribution to crank power during the extensor phase.....	49
Figure 3.4.	Profiles of the muscular power contribution to limb power for hypothetical preadolescents (anthro-PA), older children (anthro-OC) and younger children (anthro-YC) for 60rpm (A) and 120rpm (B).	50

Figure 3.5.	Age-group differences in the muscular power contribution to limb power during the extensor phase.....	51
Figure 4.1.	Mechanical energy distribution due to all muscles (A), and torques at the hip (B), knee (C), and ankle (D) for an experienced adult cyclist.	63
Figure 4.2.	Effect of cadence on peak power at the ankle (A), knee (B), and hip (C) joints.....	78
Figure 4.3.	Net muscular power for adults (AD), older children (OC), and younger children (YC) at 5 different cadences.	81
Figure 4.4.	Effect of age and cadence on net muscular power during the extensor phase (EXT).....	82
Figure 4.5.	Effect of age and cadence on net muscular power during the top phase (TOP).	82
Figure 4.6.	Effect of age and cadence on the hip power contribution to limb power during the extensor phase (EXT).	85
Figure 4.7.	Effect of age and cadence on the ankle power contribution to limb power during the extensor phase (EXT).	85
Figure 4.8.	Effect of age and cadence on the knee power contribution to crank power during the extensor phase (EXT).	86
Figure 4.9.	Effect of age and cadence on the hip power contribution to limb power during the top phase (TOP). The Age x Cadence interaction was statistically non-significant. Means and standard deviations are plotted for adults (AD), older children (OC), and younger children (YC). ...	88
Figure 4.10.	Effect of age and cadence on the ankle power contribution to limb power during the top phase (TOP). The Age x Cadence interaction was statistically non-significant.	88

Figure 4.11. Effect of age and cadence on the knee power contribution to crank power during the top phase (TOP).....	89
Figure 4.12. Contribution of hip power to limb power for adults (AD), older children (OC), and younger children (YC) at 5 different cadences.	90
Figure 4.13. Ankle power contribution to limb power for adults (AD), older children (OC), and younger children (YC) at 5 different cadences.	91
Figure 4.14. Direct knee power contribution to crank power for adults (AD), older children (OC), and younger children (YC) at 5 different cadences.	92
Figure 4.15. Effect of age and cadence on the crank angular velocities during the extensor (EXT) top (TOP) regions.	94
Figure D1. Planar model of 2-legged pedaling.	120
Figure F1. Experimental and simulated crank angle at 60 rpm.	136
Figure F2. Experimental and simulated thigh angle at 60 rpm.	136
Figure F3. Experimental and simulated crank angular velocity at 60 rpm.	137
Figure F4. Experimental and simulated thigh angular velocity at 60 rpm.	137
Figure F5. Experimental and simulated horizontal forces at 60 rpm.	138
Figure F6. Experimental and simulated vertical forces at 60 rpm.	138
Figure F7. Experimental and simulated crank angle at 120 rpm.	139
Figure F8. Experimental and simulated thigh angle at 120 rpm.	139
Figure F9. Experimental and simulated crank angular velocity at 120 rpm.	140
Figure F10. Experimental and simulated thigh angular velocity at 120 rpm.	140
Figure F11. Experimental and simulated horizontal forces at 120 rpm.	141
Figure F12. Experimental and simulated vertical forces at 120 rpm.	141
Figure G1. Age-group differences in the muscular power contribution to crank power during the extensor phase.	142

Figure G2.	Age-group differences in the muscular power contribution to crank power during the flexor phase.....	142
Figure G3.	Age-group differences in the muscular power contribution to crank power during the top phase.....	143
Figure G4.	Age-group differences in the muscular power contribution to crank power during the bottom phase.....	143
Figure G5.	Age-group differences in the muscular power contribution to limb power during the extensor phase.....	144
Figure G6.	Age-group differences in the muscular power contribution to limb power during the flexor phase.....	144
Figure G7.	Age-group differences in the muscular power contribution to limb power during the top phase.....	145
Figure G8.	Age-group differences in the muscular power contribution to limb power during the bottom phase.....	145
Figure H1.	Net muscular power at the ankle joint for the three asymmetry conditions.....	147
Figure H2.	Net muscular power at the knee joint for the three asymmetry conditions.....	147
Figure H3.	Net muscular power at the hip joint for the three asymmetry conditions.	148
Figure H4.	Net muscular power for the three asymmetry conditions.....	148
Figure H5.	Hip power contribution to limb power for the three asymmetry conditions.....	149
Figure H6.	Ankle power contribution to limb power for the three asymmetry conditions.....	149

Figure H7.	Direct knee power contribution to crank power for the three asymmetry conditions.....	150
Figure I1.	Net muscular power at the ankle joint for adults (AD), older children (OC), and younger children (YC) at 5 different cadences.	152
Figure I2.	Net muscular power at the knee joint for adults (AD), older children (OC), and younger children (YC) at 5 different cadences.	153
Figure I3.	Net muscular power at the hip joint for adults (AD), older children (OC), and younger children (YC) at 5 different cadences.	154
Figure I4.	Effect of cadence on peak power at the ankle (A), knee (B), and hip (C) joints.....	155
Figure I5.	Net muscular power for adults (AD), older children (OC), and younger children (YC) at 5 different cadences.	156
Figure I6.	Effect of age and cadence on net muscular power during the extensor phase (EXT).....	157
Figure I7.	Effect of age and cadence on net muscular power during the flexor phase (FLEX).....	157
Figure I8.	Effect of age and cadence on net muscular power during the top phase (TOP).	158
Figure I9.	Effect of age and cadence on net muscular power during the bottom phase (BOT).....	158
Figure I10.	Hip power contribution to limb power for adults (AD), older children (OC), and younger children (YC) at 5 different cadences.	159
Figure I11.	Effect of age and cadence on the hip power contribution to limb power during the extensor phase (EXT).	160

Figure I12. Effect of age and cadence on the hip power contribution to limb power during the flexor phase (FLEX).....	160
Figure I13. Effect of age and cadence on the hip power contribution to limb power during the top phase (TOP).....	161
Figure I14. Effect of age and cadence on the hip power contribution to limb power during the bottom phase (BOT).	161
Figure I15. Knee joint power contribution to crank power for adults (AD), older children (OC), and younger children (YC) at 5 different cadences.	162
Figure I16. Effect of age and cadence on the knee power contribution to crank power during the extensor phase (EXT).	163
Figure I17. Effect of age and cadence on the knee power contribution to crank power during the flexor phase (FLEX).....	163
Figure I18. Effect of age and cadence on the knee power contribution to crank power during the top phase (TOP).....	164
Figure I19. Effect of age and cadence on the knee power contribution to crank power during the bottom phase (BOT).	164
Figure I20. Ankle power contribution to limb power (AD), older children (OC), and younger children (YC) at 5 different cadences.	165
Figure I21. Effect of age and cadence on the ankle power contribution to limb power during the extensor phase (EXT).	166
Figure I22. Effect of age and cadence on the ankle power contribution to limb power during the flexor phase (FLEX).....	166
Figure I23. Effect of age and cadence on the ankle power contribution to limb power during the top phase (TOP).....	167

Figure I24. Effect of age and cadence on the ankle power contribution to limb power during the bottom phase (BOT).	167
--	-----

Chapter 1: General Introduction

The study of motor development is the investigation of changes in motor behavior and their underlying mechanisms across the life span. Motor development during childhood is marked by considerable change in motor performance. This change is due to changes in the factors that set boundaries to the behavior. These factors or constraints can be broadly classified into three categories: organism, task, and environment (Newell, 1986). Organismic constraints are factors within the human system, environmental and task constraints are external factors that set boundaries to the movement of interest. In order to understand the underlying mechanisms of differences in motor behavior, we need to investigate how changing constraints lead to behavioral change. From a developmental perspective, we are particularly interested in how factors within the system (organismic constraints) change during childhood and how these changes lead to differences in motor behavior.

There are two distinct organismic constraints that result in developmental changes in motor behavior: physical growth and physical maturation. “Physical growth is an increase in size or body mass resulting from an increase in complete, already formed body parts” (Timiras, 1972 as cited in Haywood & Getchell, 2001, p.5). “Physical or physiological maturation is a qualitative advance or biological advance in biological makeup and may refer to cell, organ, or system advancement in biochemical composition rather than to size alone” (Teeple, 1978 as cited in Haywood & Getchell, 2001, p.5)¹. Depending on which organismic constraint causes age-related changes in motor behavior, the interpretation of these changes could be very different. Distinguishing between the

¹ The original definitions for physical growth by Timiras (1972) and for physical maturation by Teeple (1978) were slightly modified by Haywood and Getchell (2001). These modified definitions are used as working definitions in this dissertation.

effects of growth and maturation on motor behavior is of particular importance because it allows us to assess whether observed age-related differences in motor behavior are immature or functional. The reason for this and the importance of distinguishing between physical growth and physical maturation is explained in the remainder of this chapter. The structure of this dissertation is described in the context of this distinction. It is the goal of this dissertation to distinguish between the effects of growth and maturation on the construction of a motor task.

Force Construction During Human Movement - The Importance of Muscular Forces

According to Newton's second law, human movement is a result of all forces acting on the human system. If the human body is modeled as a dynamic system, the equations of motion give an explicit mathematical relationship between the forces acting within and on the system and the resulting motion (Equation 1.1). In general, the equation of motion can be written in the following form:

$$M(q)\ddot{q} + C(q)\dot{q}^2 + G(q) + R(q)F^{MT} + E(q, \dot{q}) = 0 \quad (1.1)$$

where

q is a vector of the generalized coordinates

$M(q)$ is the system mass matrix

$C(q)\dot{q}^2$ is a vector of centrifugal and Coriolis forces and torques

$G(q)$ is a vector containing gravitational terms

F^{MT} is a vector containing muscular forces

$R(q)$ is the matrix of muscle moment arms

$E(q, \dot{q})$ is a vector of external forces and torques

Solving Equation 1.1 for the accelerations (Equation 1.2) illustrates that both, muscular and non-muscular forces contribute to segmental acceleration.

$$\ddot{q} = \underbrace{M^{-1}(q)[-R(q)F^{MT}]}_{\text{Muscular contribution}} + \underbrace{M^{-1}(q)[-C(q)\dot{q}^2 - G(q) - E(q, \dot{q})]}_{\text{Non-Muscular contribution}} \quad (1.2)$$

It has been well documented that both muscular and non-muscular forces act in concert to produce the movement outcome (Bothner & Jensen, 2001; Fregly & Zajac, 1996; Hoy & Zernicke, 1986; Kautz & Hull, 1993; Schneider, Zernicke, Ulrich, Jensen, & Thelen, 1990). Muscular forces and torques are of particular importance because they represent the nervous system's contribution to movement. Winter (1989) remarks that muscular torques are the “final common mechanical pathway [of the central nervous system]” (p.338). In a developmental context, age-related changes in muscular force application can give us insight into how changing organismic constraints lead to changes in motor behavior.

The Effect of Segmental Growth on Motor Behavior

In addition to showing the force construction of movement, Equation 1.2 also demonstrates an explicit relationship between the construction of the task and the anthropometry of the performer. The matrices M, C, G, and R contain the anthropometric properties of the human body: segmental masses, segmental moments of inertia, segmental center of mass locations, and muscular moment arms. This implies that the contributions of both muscular and non-muscular forces to human movement depend on the anthropometry of the performer. The relationship between anthropometry, non-muscular, and muscular forces, and the movement outcome is non-linear, even during

simple motor tasks. If anthropometry changes, non-muscular forces change in a non-linear fashion, which implies that muscular forces have to be adjusted if the movement outcome is to be the same.

The anthropometric changes that take place during childhood have been well documented. In addition to absolute changes in body mass and length (Asmussen & Hebøll-Nielsen, 1955), relative anthropometric parameters, such as segmental mass proportions, relative center of mass locations, and radii of gyration change during childhood (Jensen, 1981, 1986, 1989; Schneider & Zernicke, 1992; Sun & Jensen, 1994). As a result of these relative changes, muscular forces have to be applied differently for any given movement, even if the task is appropriately scaled to the individual participant's size. Depending on the movement and its characteristics, this need to match muscular forces to non-muscular forces may be more or less significant. For example, one might expect that anthropometry has a greater influence on the distribution between muscular and non-muscular forces if large motion-dependent forces are present (e.g., at high movement speeds). The differences in anthropometry pose a possible confounding factor if observed age-related differences in muscular force application are to be attributed to an immaturity of features of the neuro-motor system. The reason for this is that age-related differences in muscular force application can be interpreted as a functional adjustment (Brown & Jensen, 2003; Jensen, 1989) and may in fact represent a mature response of the neuro-motor system if they are due to differences in anthropometry.

In Chapter 3, an investigation of the effect of non-linear changes in anthropometry on muscular force production is described across various task demands. It was the goal of this investigation to determine the practical relevance of this effect.

Age-Related Differences in Features of the Neuro-Motor System and Their Effect on Movement and Adaptation

Maturation of the neuro-motor system includes age-related changes in muscle-intrinsic properties (Asai & Aoki, 1996; Lexell, Sjöström, Nordlund, & Taylor, 1992; Lin, Brown, & Walsh, 1994, 1997) and neural processes (Forssberg, 1982, 1985; Gibbs, Harrison, & Stevens, 1997). These changes can also lead to age-related differences in muscular force application. Forssberg (1985), for example, found a deficiency in children's abilities to produce forward progression during walking. This deficiency was revealed in smaller relative shear forces in children when compared to those of adults. The author attributed these differences in the ground reaction forces to an immaturity of neural circuits at young ages.

Differences in features of the neuro-motor system are often revealed in the way children respond to changes in the task demand, or when the task is scaled to the participants' performance limits. Researchers have demonstrated that when children perform motor tasks at their performance limits, there is a reduction in their ability to develop muscular forces quickly (Asai & Aoki, 1996) or to produce muscular power (Martin, Farrar, Wagner, & Spirduso, 2000).

In Chapter 4, an investigation about children's capacity to adapt in terms of muscular power production is described. It was hypothesized that a reduction in muscular power production in children would result in a different adaptive strategy. This effect was hypothesized to be most apparent at high movement speeds because during such circumstances, children are known to be less successful than adults (Chao, Rabago, Korff, & Jensen, 2002).

Biomechanical Techniques to Estimate Muscular Forces

On a methodological level, the quantification of muscular force application depends not only on the constraints that set the boundaries to the behavior, but also on the suitability of the method being employed. Since it is difficult to measure muscular forces directly, we make use of biomechanical principles to estimate forces and torques that are produced by muscles. The validity of the inferences from observed differences in muscular force application depends on the accuracy of the method being employed.

Biomechanical techniques for estimating muscular forces include both inverse and forward dynamics techniques (Pandy, 2001). During inverse dynamics, muscular torques are estimated from the observed movement and measured reaction forces (Hof, 1992; Hull & Jorge, 1985; Winter, 1990; Winter & Robertson, 1978). During forward dynamics simulations, muscular forces or torques actuate the biomechanical model, which produces the movement of the system (Anderson & Pandy, 2001, 2003; Fregly & Zajac, 1996; Neptune & Hull, 1998). Although Hatze (2000) argues that inverse dynamics techniques are inaccurate and should not be used at all, in some cases these techniques can give us the best available representation of muscular forces or torques, especially when complicated and computationally expensive forward models are not available. In pedaling, the task studied in this dissertation, both inverse dynamics (Hull & Jorge, 1985; van Ingen Schenau, et al., 1995; Kautz & Hull, 1993; Marsh, Martin, & Sanderson, 2000) and forward dynamics (Fregly & Zajac, 1996; Neptune & Hull, 1998; Raasch, Zajac, Ma, & Levine, 1997) techniques have been used to estimate muscular forces, or torques. Forward dynamics simulations have also been used in developmental research (Korff & Jensen, 2004). One particular method that has been used in the developmental literature to study muscular force application is the pedal force decomposition technique described by Kautz and Hull (1993) (Brown & Jensen, 2003;

Korff & Jensen, 2003a, 2003b). In order to put the present investigations into the context of this developmental literature, a comparison between the pedal force decomposition technique and the forward dynamics simulation was performed and is described in Chapter 2.

Purpose of the Dissertation

The purpose of this series of studies is to determine age-related changes in muscular force application and attribute these changes to changing features of the neuro-motor system, independent of simple changes in body size. Three studies are presented. Study 1 is an identification of a suitable method that allows for an accurate quantification of muscular forces (Chapter 2). Study 2 is an investigation of the effect of differences in anthropometry on muscular force application (Chapter 3). Results of this study allow us to quantify the possible confounding effect of growth on muscular force application when observed differences are to be attributed to the maturation of the neuro-motor system. Study 3 is an investigation of age-related differences in muscular force application in terms of adaptation to changes in the task demands (Chapter 4).

Chapter 2: Study 1

INTRODUCTION

During dynamic movements, muscular forces act in concert with non-muscular forces such as gravity or motion-dependent forces in order to achieve a resultant force that complies with the goals of the task. From a developmental perspective, this ability to match muscular to non-muscular forces can be an indicator of skillfulness. Researchers have shown that children become more proficient in matching muscular to non-muscular forces with increasing age (Jensen, Ulrich, Thelen, Schneider, & Zernicke, 1994; Konczak, Borutta, & Dichgans, 1997; Schneider, Zernicke, Ulrich, Jensen, & Thelen, 1990). Where in these cases age-related differences in muscular force application may be attributed to a maturing neuro-motor system, such differences may also be a simple consequence of segmental growth. Changes in anthropometry change the magnitude of gravitational and motion-dependent forces. Therefore, differences in anthropometry between performers may lead to differences in non-muscular forces. If the resultant force (the sum of muscular and non-muscular forces) is to be the same, muscular forces must be adjusted to compensate for anthropometry-driven changes in the non-muscular forces.

The interaction between muscular and non-muscular forces in the performance of voluntary, purposeful movement is of particular interest in developmental studies. In asking questions about the development of motor control, one must confront the confounding factor of increasing physical size.

Brown (2000) and Korff and Jensen (2004) present conflicting results with regard to the influence of age-related changes in anthropometry on the distribution of muscular and non-muscular forces during pedaling. Brown (2000) speculated that age-related differences in anthropometry might influence the mechanical force construction during

pedaling. This speculation received support when adding mass to children's limbs resulted in a more adult-like force construction (Brown, 2000). In contrast, Korff and Jensen (2004) found that mathematically manipulating anthropometric characteristics of a biomechanical model had no significant effect on the force construction of the task.

Where both studies sought to determine the effect of changes in anthropometry between 6 and 10 years of age on the distribution between muscular and non-muscular forces, two major differences between these two studies need to be pointed out: a different experimental design and a different technique to decompose the reaction force into muscular and non-muscular components.

Brown (2000) performed an experimental manipulation of anthropometry where the manipulation performed by Korff and Jensen (2004) was mathematical. However, it is unlikely that this difference in the experimental design led to the conflicting results. In both studies, the authors controlled for the kinematics of the behavior and the total reaction forces applied to the pedal. With these factors controlled, differences in the distribution between muscular and non-muscular components of the pedal reaction force can be attributed to differences in anthropometry.

The second methodological difference between the studies by Brown (2000) and Korff and Jensen (2004) was that two different techniques were employed to decompose the pedal reaction force into muscular and non-muscular contributions. Where Brown (2000) used the pedal force decomposition (PFD) described by Kautz and Hull (1993), Korff and Jensen (2004) used a forward dynamics simulation (FDS) to decompose the pedal reaction force into muscular and non-muscular components.

In this investigation, we asked if differences in the decomposition technique being employed (PFD vs. FDS) could lead to different answers to the question of whether age-related differences in anthropometry affect the force construction of the task.

What is common to the PFD and the FDS is that the crank of the bicycle combined with the lower segments of the rider on the ipsilateral side is modeled as a 5-bar linkage. The reaction force at the pedal is decomposed into muscular and non-muscular components. Due to the kinematic indeterminacy of such a model, inherent assumptions have to be made in order to decompose the total pedal reaction force. The indeterminacy problem arises from the fact that at a given crank angle, the configuration of the system can change. The discrepancies in the techniques begin to emerge in how the issues of indeterminacy are resolved.

Kautz and Hull (1993) proposed to solve the indeterminacy problem by adding a hypothetical external moment at the foot in order to create static equilibrium of the leg at each instant in time. This external moment prevents the configuration of the system from changing during the instant of interest. Thus, when using the PFD, muscular or non-muscular forces may be erroneously attributed to the pedal reaction force even though they also contribute to accelerating the segments of the dynamical system.

Using the FDS, one can instantaneously set all muscle moments to zero and quantify how non-muscular forces contribute to the pedal reaction force. Similarly, one can set motion-dependent or gravitational terms to zero and quantify the muscular contribution to the pedal reaction force. Using such a technique, we also assume static equilibrium, although the system is accelerating. Thus, when using the FDS, muscular or non-muscular forces may erroneously be attributed to accelerations of the segments even though they also contribute to the reaction force at the pedal.

It becomes clear, then, that due to the differences in the inherent assumptions, each technique introduces potential error to the estimation of muscular and non-muscular components of the pedal reaction force. The purpose of this study was to determine the effect of age-related changes in anthropometry on the force construction of the task using

two different methods. Where Brown (2000) found this effect to be significant when using the PFD, Korff and Jensen (2004) found this effect to be insignificant when using the FDS. Thus, in a direct comparison of methods, we hypothesized that age-related differences in the muscular and non-muscular components of the pedal reaction force are greater if the PFD is used when compared to the FDS.

METHODS

Planar Model of Cycling

Two different methods to decompose the pedal reaction force were performed. To guarantee that differences between the two techniques were not confounded by differences in kinematics, the angular accelerations, velocities, and positions obtained from the FDS were also used for the PFD.

A torque-driven planar model of 2-legged stationary cycling was developed (Fregly & Zajac, 1996). The model consisted of two 5-bar linkages. The configuration of the model was described by seven angles (thigh, shank, and foot angles of the right and left limbs, as well as crank angle, see Figure D1 in Appendix D). The model was kinematically constrained by fixing in space the position of the hip and the crank axis of rotation. These constraints yielded a model with three degrees of freedom. The crank angle, and the right and left thigh angles were chosen as the free degrees of freedom. The foot and the shank angles were the dependent degrees of freedom and were constrained to satisfy the configuration constraints of the system (Appendix D). The corresponding angular velocities and accelerations were constrained to satisfy the kinematic constraint equations (Appendix D). The model was driven by muscular torques about the hip, knee, and ankle joints of the right and left legs. The resistance due to frictional forces was modeled using an effective inertial load and an effective frictional load (Fregly, Zajac, & Dairaghi, 2000). The equations of motion were derived using Autolev (Online Dynamics, Inc., CA) and analyzed in Matlab (Mathworks, Inc., MI).

Experimental Data

Experimental data were collected from one male experienced cyclist (age: 21 years; mass: 61 kg; height: 177 cm). Prior to testing, the participant provided written

consent. He rode a stationary ergometer (Monark, Model 829E) for 15 s at a speed of 60 revolutions per minute (rpm) and 96 W external power output. This power output corresponded to 10% of the participant's predicted peak power which was estimated from lean thigh volume (Martin, Farrar, Wagner, & Spirduso, 2000). This percentage of predicted peak power was chosen because it is commonly used in developmental research and represents a resistance at which children can perform the task successfully (Brown & Jensen, 2003; Jensen & Korff, 2004).

Kinematic data were collected at 60 Hz using a 5-camera Vicon 250 motion analysis system (Oxford Metrics, UK). Before data collection, the cameras were calibrated. The calibration residual for each camera was less than 0.6 mm. Reflective markers were placed on the pedal, the lateral malleolus, the lateral femoral epicondyle, the greater trochanter, and the anterior superior iliac spine (ASIS) of the right side of the body. Pedal reaction forces normal and tangential to the pedal were collected at 600 Hz using a custom-made pedal with two tri-axial piezoelectric force sensors (Kistler, model 9251AQ01).

Kinematic data were low pass filtered at 10 Hz with no phase lag using a second order Butterworth filter. The hip joint center was estimated using the marker of the greater trochanter and the ASIS according to a method presented by Neptune and Hull (1995). Force data were low-pass filtered at a cutoff frequency of 20 Hz with no phase lag using a second order Butterworth filter. The force data were then downsampled in order to match kinematic data. Kinematic and force data were averaged across 5 revolutions.

A gradient-based optimization algorithm (`fminsearch`, Mathworks, Inc., MI) found the joint positions that complied with the kinematic constraints of the model and differed minimally from those obtained experimentally. Segmental angles (crank, foot,

shank, and thigh) were calculated based on these optimal joint positions and defined as the angle of the corresponding segment with respect to the horizontal axis of the inertial reference frame (see Figure D1 in Appendix D). Positive angles were defined counterclockwise. For the contralateral leg, the model tracked joint angles that were 180 degrees out of phase with those of the ipsilateral leg.

Modification of Anthropometric Characteristics

The anthropometric parameters of the model were scaled to represent those of children of 5, 7.5, and 10 years of age. The mass of the participant was 61 kg. The masses of the children's models were scaled to 18 kg, 24 kg, and 32 kg for the three age groups, respectively. These values were determined using the growth charts published by the Centers for Disease Control and Prevention (<http://www.cdc.gov/growthcharts>). From the masses of the children's models, scaling factors S_M were determined that describe the ratio of the masses in adults and the corresponding children's models. Segment lengths (including the crank length and the distance between the crank axis of rotation and the hip joint) were scaled using dimensionality theory. According to dimensionality theory, the growth rate of a specific anthropometric parameter depends on its Euclidean dimension. Measures of length are one-dimensional where measures of mass are three-dimensional (Rowland, 2003). According to dimensionality theory, the following relationships hold:

$$S_M = S_L^3 \quad (2.1)$$

which is equivalent to

$$S_L = S_M^{(1/3)} \quad (2.2)$$

S_M is the scaling factor that described the ratio of masses between individuals and S_L is the scaling factor that describes the ratio between segment lengths. The scaling factor S_L was determined using equation (2.2). Using such manipulations, we assumed

that different segment lengths change at a constant rate. This allowed us to keep the (angular) kinematics identical between all participants and to eliminate the possible confound of differences in the kinematics on muscular force application.

Segmental mass proportions, center of mass locations, and radii of gyration were obtained using the regression equations presented by Jensen (1989). Jensen (1989) showed that these relative measures of anthropometry change during childhood. In particular, the relative mass proportions of the thigh and foot, the relative center of mass location of the shank and its radius of gyration change between 4 and 20 years of age. In order to model inter-individual variability in anthropometry within age groups, we created 20 hypothetical participants in each age group. Segmental mass proportions, relative center of mass locations, and radii of gyration were randomly varied ± 3 times the standard error for each measure reported by Jensen (1989). Means and standard deviations for relative mass proportions, segmental center of mass locations, and radii of gyration for all hypothetical age groups can be found in Table 2.1. In the remainder of this chapter the hypothetical groups of 5, 7.5, and 10-year-old children will be, respectively, referred to as younger children (“anthro-YC”), older children (“anthro-OC”), and preadolescents (“anthro-PA”).

The total pedal reaction forces to be produced were scaled by the same factor which was used to scale the total body mass of the corresponding model. As body mass appears as a linear factor in the equations of motion, this procedure ensured that the effect of relative (and not absolute) differences in anthropometry on the distribution between muscular and non-muscular forces was isolated.

Table 2.1 Anthropometric characteristics of the biomechanical models. For each age group, mean values (M) and standard deviations (SD) are shown (anthro-PA=preadolescents, anthro-OC=older children, anthro-YC=younger children). Segmental mass proportions are given as a percentage of body mass. Segmental center of mass locations are expressed as the distance between the segmental center of mass and the proximal joint as a percentage of segment length. The radii of gyration are dimensionless.

		anthro-PA		anthro-OC		anthro-YC	
		M	SD	M	SD	M	SD
Thigh	Mass Proportion	10.24	0.54	9.58	0.61	7.88	0.69
	Segmental Center of Mass Location	45.48	2.80	44.47	3.56	44.01	3.63
	Radius of Gyration	0.29	0.02	0.29	0.02	0.29	0.02
Shank	Mass Proportion	4.98	0.75	5.03	0.69	4.47	0.61
	Segmental Center of Mass Location	42.09	0.97	42.46	1.08	43.22	0.77
	Radius of Gyration	0.29	0.01	0.29	0.01	0.29	0.01
Foot	Mass Proportion	1.93	0.58	2.13	0.54	2.16	0.34
	Segmental Center of Mass Location	40.50	3.62	40.16	5.40	42.52	4.63
	Radius of Gyration	0.24	0.03	0.25	0.02	0.25	0.02

Tracking Experimental Data

To ensure that the simulations produced kinematics and forces that were similar to those measured experimentally, a feedback linearization algorithm was used to track experimental data (Seth, McPhee, & Pandy, 2004). This algorithm accounts for errors introduced by numerical differentiation by adjusting the accelerations of the system based on the difference between the angular positions and velocities of the model and those that were obtained experimentally. At each time step, these controlled accelerations were used to compute a set of muscle moments about the hip, knee, and ankle joints using inverse dynamics. These muscle moments were then used to compute the angular accelerations which were numerically integrated to obtain the angular velocities and positions at the next time step. The iterative application of this procedure at each time step resulted in a simulation that tracked experimentally obtained angular positions and velocities.

Two Methods to Decompose the Pedal Reaction Force

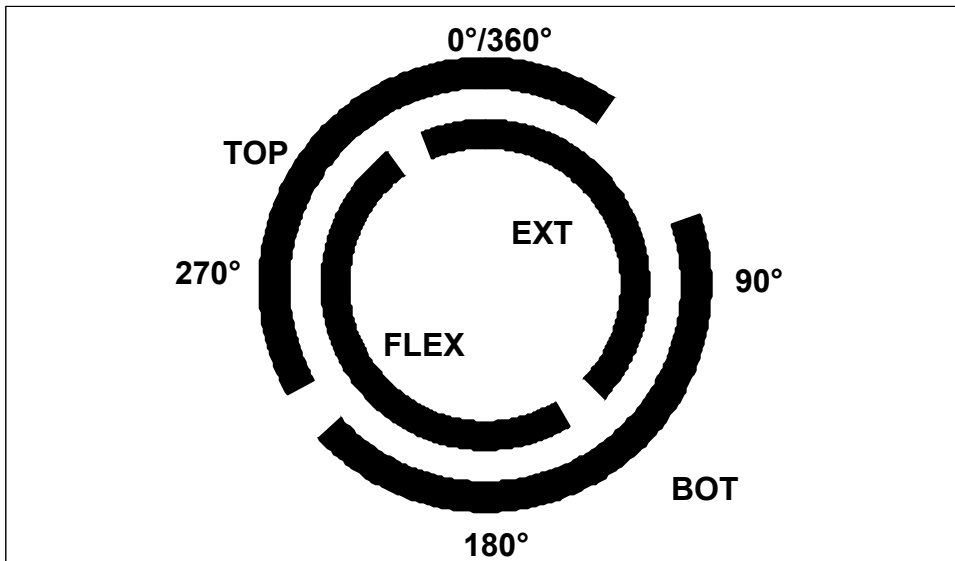
After the tracking solution was found, the ipsilateral pedal reaction force was decomposed into muscular and non-muscular (the sum of gravitational and motion-dependent) components using the PFD and the FDS. In order to match the formulation of the equations of motion presented by Kautz and Hull (1993), the moment arms for intersegmental forces (Appendix E) were decomposed into vertical and horizontal components. Moreover, expressions for the linear accelerations of the segmental centers of mass were computed because these expressions do not directly appear in the formulation of the equations of motion used for the FDS. A detailed description of the PFD can be found in Appendix E.

To decompose the pedal reaction force into muscular and non-muscular components using the FDS, an analytical expression for the resultant force was derived (Kane & Levinson, 1985). The analytical expression of this force can be found in Appendix D. The muscular, gravitational, and motion-dependent components were then found by setting the corresponding parameters (muscle moments, gravity, and angular velocities) associated with the right leg to zero and subtracting the resulting force profile from the total pedal force at each time step. Muscular, gravitational, and motion-dependent force components were also found using the PFD. In both cases, the muscular and non-muscular components acting perpendicular to the crank were found. This component of the pedal reaction force is of interest because it is the only component that accelerates the crank. It is referred to as the tangential crank force (Zajac, Neptune, & Kautz, 2002). Non-muscular force profiles were found by adding the gravitational and motion-dependent components.

Dependent Measures and Statistical Analysis

All force profiles were normalized with respect to the average tangential crank force over the crank cycle to allow for meaningful comparisons between the hypothetical age groups. The normalized forces were then averaged across four different regions of the crank cycle: extensor (EXT), flexor (FLEX), top (TOP), and bottom (BOT) (Neptune, Kautz, & Hull, 1997; Raasch et al., 1997). These regions are of interest because they represent different functional requirements of the nervous system necessary to achieve the goal of the task (Raasch et al., 1997; Raasch & Zajac, 1999). The regions of the crank cycle are illustrated in Figure 2.1. To test the hypothesis that age group differences are dependent on the method being employed, Age x Method MANOVAs with repeated measures were performed for each crank region. Age was the between subject factor and method was the within subject factor. For each MANOVA, the dependent variables were muscular and non-muscular forces averaged across the corresponding region of the crank cycle. If the Age x Method interaction was significant, one-way ANOVAs were performed for each dependent measure and each method. In order to quantify how the effect of age-related changes in anthropometry on the distribution of muscular force application changes throughout the crank cycle, post-hoc t-tests (Student Newman Keuls) were performed for muscular forces if the corresponding one-way ANOVA was significant. The type I error for all statistical tests was set to .05.

Figure 2.1. Regions of the crank cycle. The crank cycle was divided into 4 regions: extensor (EXT, 337°-134°), flexor (FLEX, 149°-327°), top (TOP, 241°-35°), and bottom (BOT, 72°-228°).



RESULTS

The FDS closely tracked the data that were obtained experimentally. Differences between simulated and experimental data were quantified by calculating the relative absolute deviation (RAD, Equation 2.3). For pedal forces, as well as angular positions and velocities, all deviations were smaller than 1%. All tracking results are presented in Appendix F.

$$RAD = 100 \cdot \frac{\frac{1}{n} \left[\sum_{i=1}^n |Y_{\text{exp}_i} - Y_{\text{sim}_i}| \right]}{\text{range}(Y_{\text{exp}})} \% \quad (2.3)$$

where

Y_{exp_i} is the experimentally obtained data profile at the i^{th} sample

Y_{sim_i} is the simulated data profile at the i^{th} sample

n is the number of samples of each profile.

The effect of age-related changes in anthropometry on muscular and non-muscular forces was dependent on the method being employed. In Figures 2.2 and 2.3, the muscular and non-muscular force profiles for all age groups are shown. It can be seen that the differences between force profiles of different age groups are more apparent when the PFD was used, compared to when the FDS was used. For all crank regions, the Method x Age interaction was statistically significant (Table 2.2). Follow up one-way ANOVAs revealed that using the PFD the age effect was significant for all crank regions (see Table 2.3 and Figures 2.4 and 2.5). Using the FDS, the age-effect was only significant during BOT. During EXT, FLEX, and TOP, the age-effect was non-significant (see Figures 2.2, and 2.3 (bottom Figures) and Figures 2.4, and 2.5).

Pairwise comparisons revealed that, anthro-YC's muscular and non-muscular forces differed significantly from those produced by anthro-PA or anthro-OC (Figures 2.2 and 2.3 (top Figures)) only when the PFD was used. During EXT, FLEX, and BOT, anthro-YC produced significantly greater muscular forces when compared to anthro-OC or anthro-PA when the PFD was used. Using this technique during TOP, anthro-YC produced significantly less muscular forces when compared to anthro-OC or anthro-PA.

Table 2.2. Statistical analysis of the Age x Method interactions of the MANOVAs on muscular and non-muscular power profiles during the different crank regions (EXT=extensor, FLEX=flexor, TOP=top, and BOT=bottom).

Crank Region	Wilks' Lambda	F(4,112)	p
EXT	.449	13.79	<.001
FLEX	.318	21.62	<.001
TOP	.497	11.72	<.001
BOT	.588	8.52	<.001

Table 2.3. Statistical analysis of age-related differences in anthropometry on muscular (Mus) and non-muscular (Non-Mus) forces using the pedal force decomposition technique (PFD) and the forward dynamics simulation (FDS). One-way ANOVAs with age being the between subject factor were performed for the extensor (EXT), flexor (FLEX), top (TOP), and bottom (BOT) regions of the crank cycle using each method.

Force (Muscular/ Non-Muscular)	Crank Region	PFD		FDS	
		F(2,57)	p	F(2,57)	p
Mus	EXT	8.28	0.001	0.61	0.548
Mus	FLEX	4.43	0.016	1.15	0.325
Mus	TOP	10.74	<.001	0.97	0.386
Mus	BOT	20.32	<.001	6.61	0.003
Non-Mus	EXT	8.28	0.001	0.94	0.395
Non-Mus	FLEX	4.43	0.016	1.17	0.319
Non-Mus	TOP	10.74	<.001	0.95	0.393
Non-Mus	BOT	20.33	<.001	5.22	0.008

Figure 2.2. Profiles of the muscular component of the pedal reaction force using the pedal force decomposition (PFD) and the forward dynamics simulation (FDS). Mean force profiles are shown for preadolescents (anthro-PA), older children (anthro-OC), and younger children (anthro-YC).

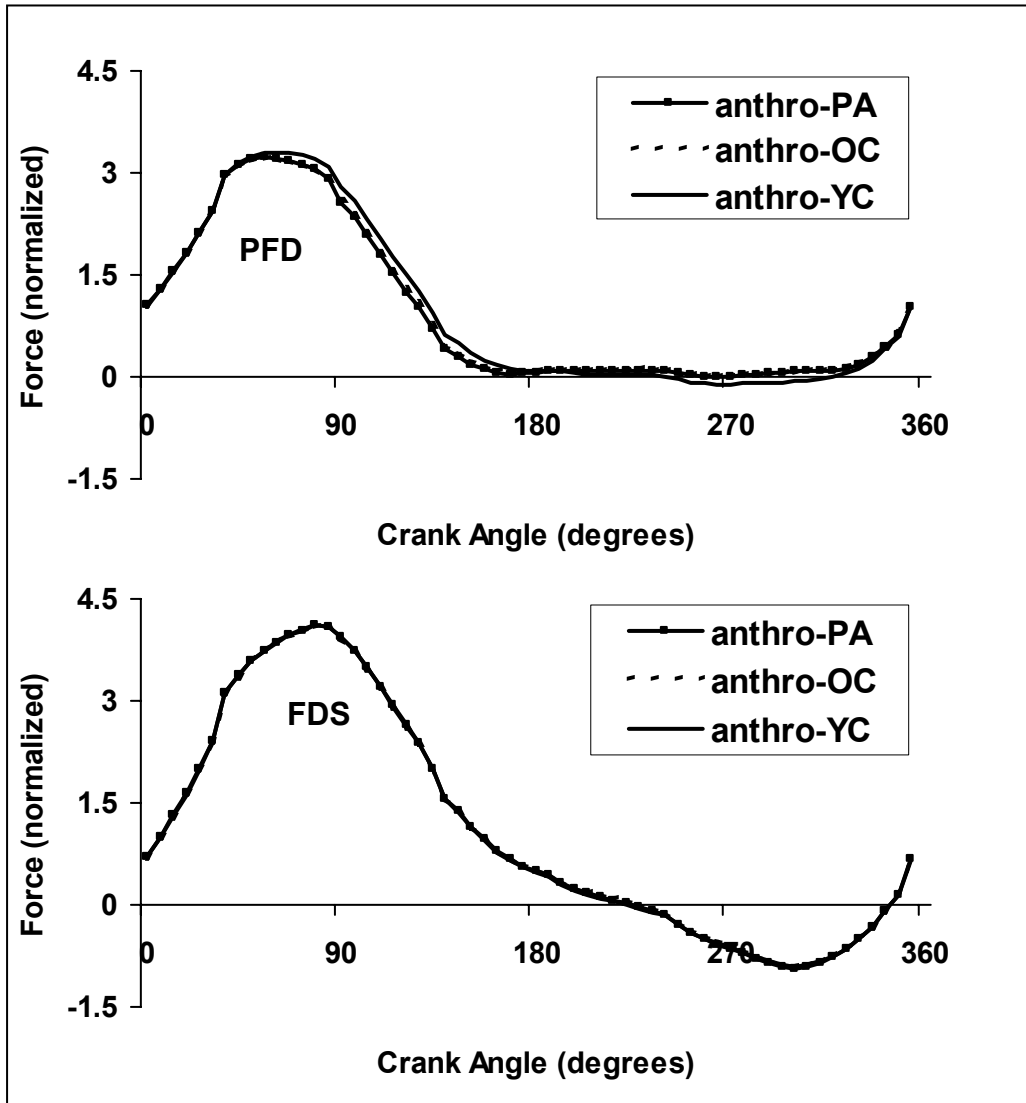


Figure 2.3. Profiles of the non-muscular component of the pedal reaction force using the pedal force decomposition (PFD) and the forward dynamics simulation (FDS). Mean force profiles are shown for preadolescents (anthro-PA), older children (anthro-OC), and younger children (anthro-YC).

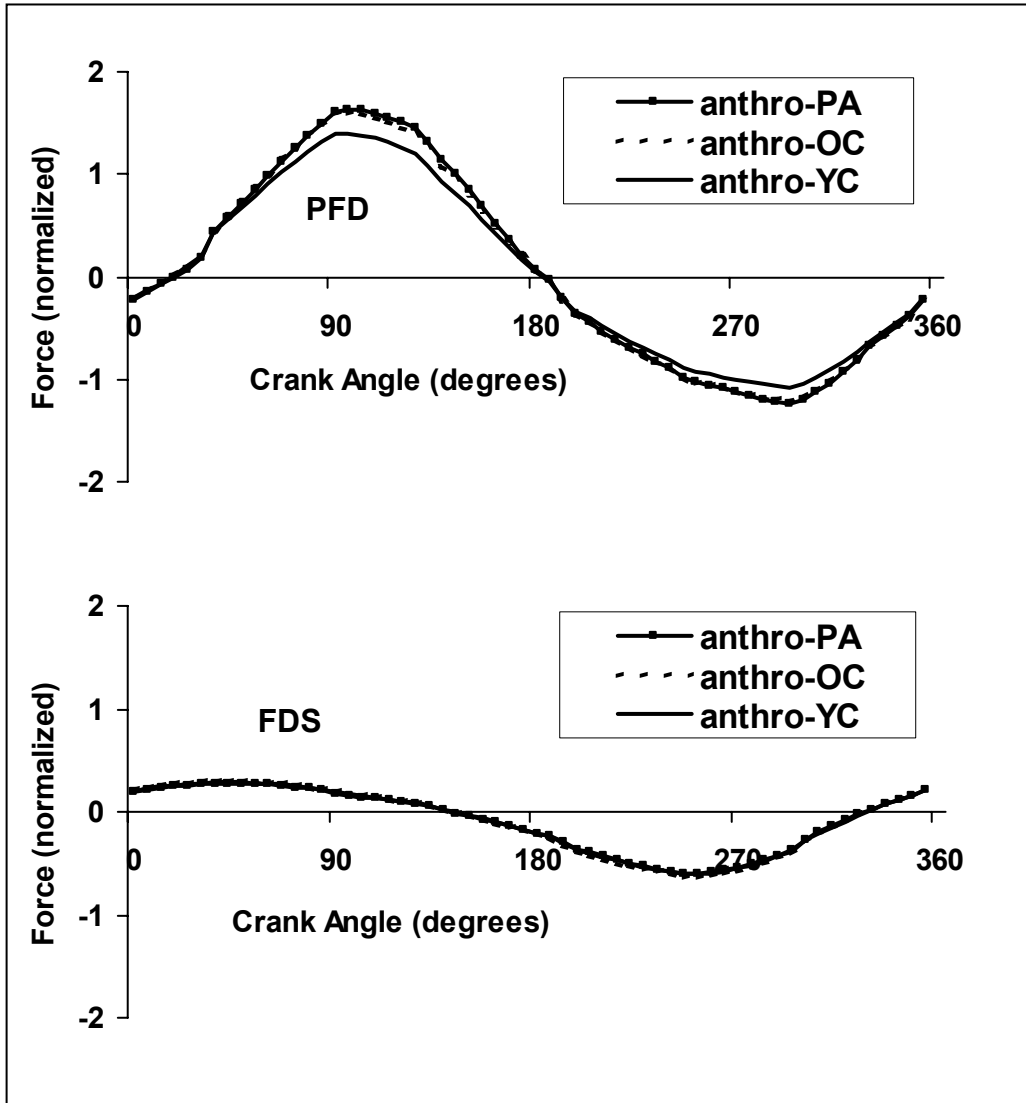


Figure 2.4. Effect of age-related changes in anthropometry on the averaged normalized muscular forces during the extensor (EXT) and flexor (FLEX) regions of the crank cycle. The symbol “*” indicates a statistically significant age effect (anthro-PA=preadolescents, anthro-OC=older children, and anthro-YC=younger children, PFD=pedal force decomposition, FDS=forward dynamics simulation).

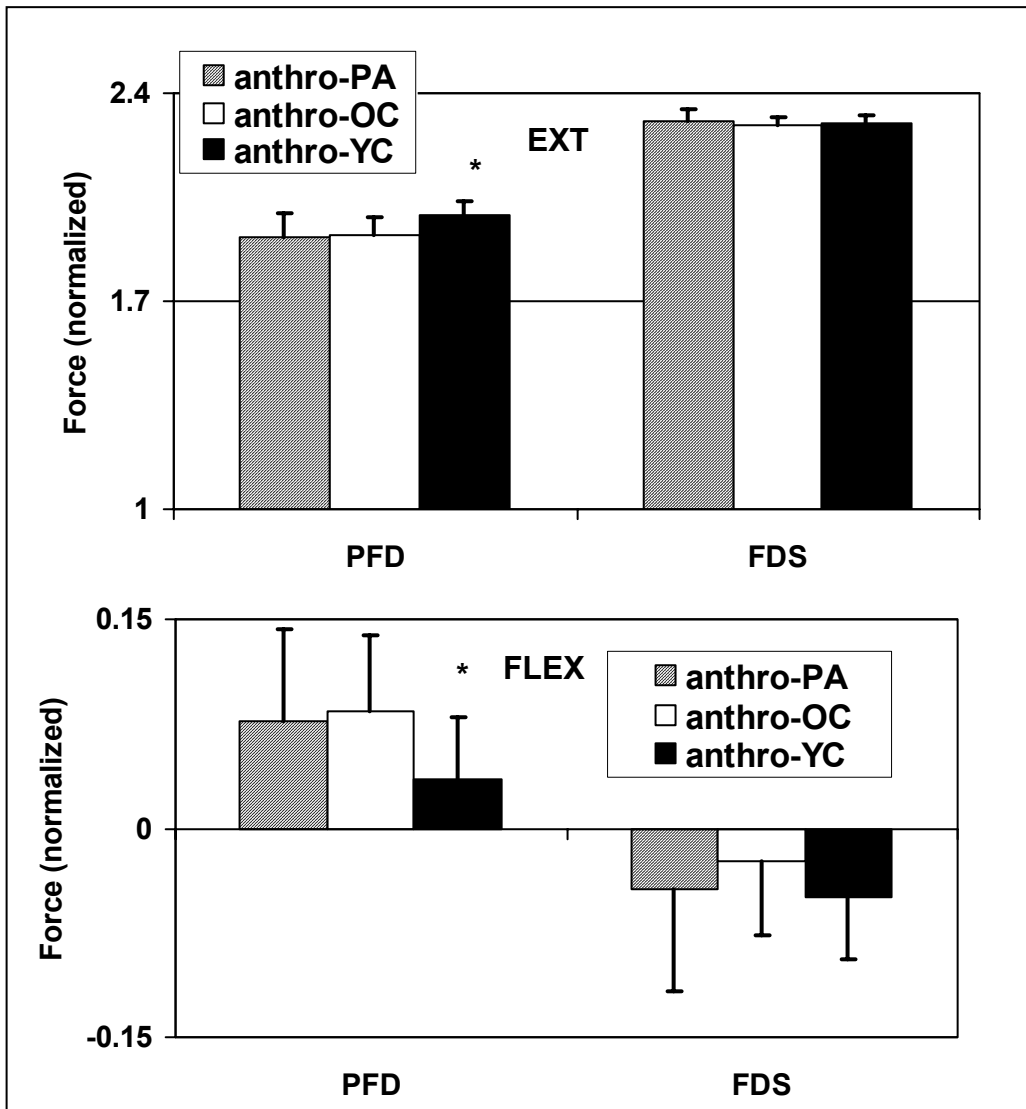
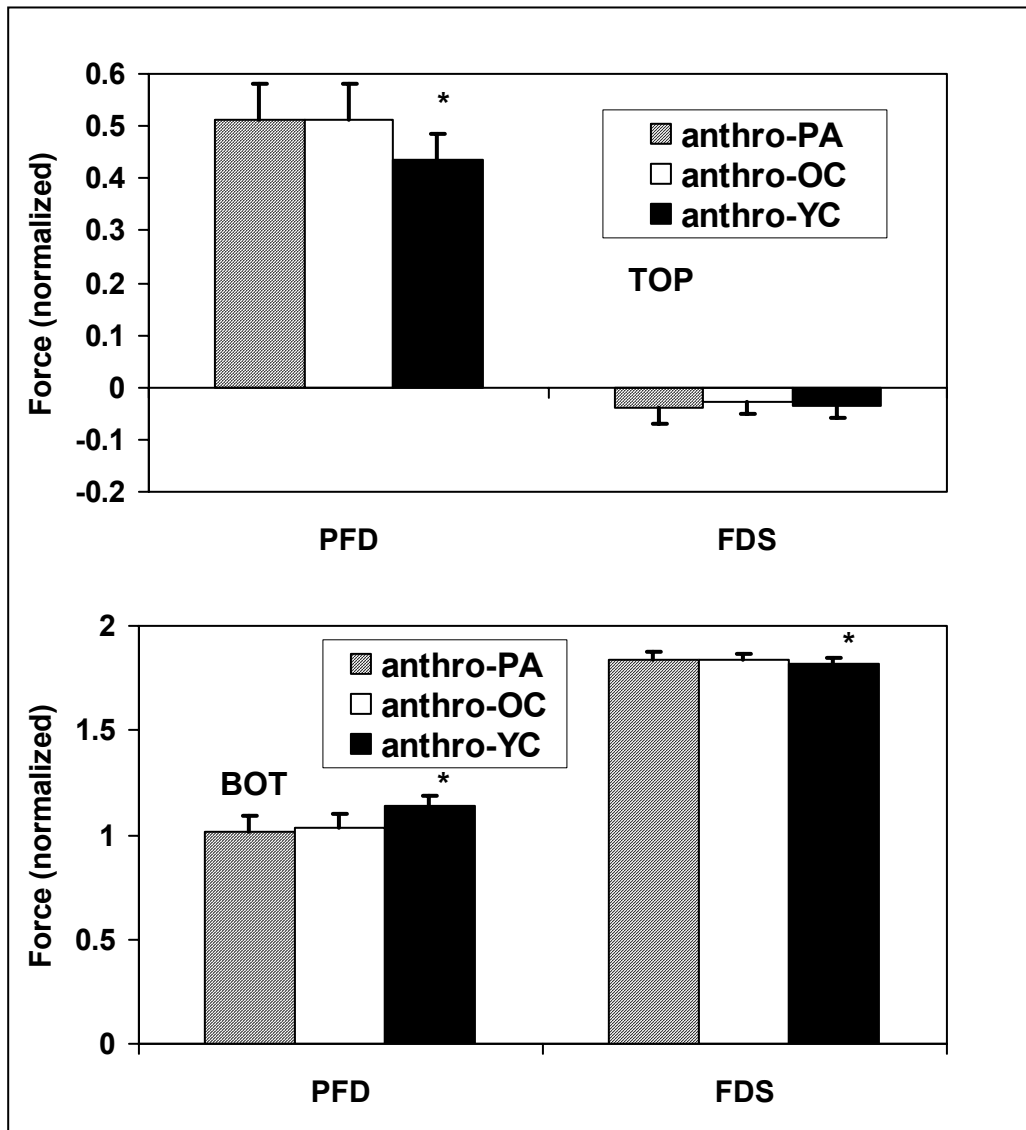


Figure 2.5. Effect of age-related changes in anthropometry on the averaged normalized muscular forces during the top (TOP) and bottom (BOT) regions of the crank cycle. The symbol “*” indicates a statistically significant age effect (anthro-PA=preadolescents, anthro-OC=older children, and anthro-YC=younger children, PFD=pedal force decomposition, FDS=forward dynamics simulation).



DISCUSSION

The purpose of the present investigation was to determine the effect of age-related changes in anthropometry on the application of muscular forces using two different methods. In conformity with the hypothesis we demonstrated that the influence of anthropometry on the force construction of the task depends on the method being employed. Using the PFD, the age differences were more apparent than using the FDS with which only small age-effects were found.

This finding results from the fact that the magnitude of non-muscular forces estimated by the PFD is larger than that estimated by the FDS (Figure 2.3). Changes in anthropometry influence non-muscular forces, and muscular forces have to be adjusted to achieve the desired resultant force. The greater are the non-muscular forces, the greater is the effect of anthropometry on the force construction of the task. As the non-muscular forces were greatest when the using PFD, the effect of differences in anthropometry on the force construction of the task was greater when this technique was used.

During EXT in anthro-YC, the positive non-muscular component was smaller than in anthro-OC and anthro-PA when the PFD was used (Figure 2.3). During this phase, anthro-YC demonstrated a reduction of non-muscular forces by 12% and 13% when compared to anthro-OC and anthro-PA, respectively. Anthro-YC had to compensate for this reduction by increasing muscular forces by 3% and 4% compared to anthro-OC and anthro-PA, respectively. During FLEX, an opposite effect was found. The magnitude of anthro-YC's non-muscular forces (which were negative during this phase) was smaller when compared to anthro-OC and anthro-PA. As a consequence they produced less muscular forces during this phase when compared to anthro-OC and anthro-PA (up to 57%).

Where anthropometry-driven differences in muscular force profiles were apparent when the PFD was used, these differences were small when the FDS was used. Using the FDS, the age-effect was significant only during BOT. However, during this phase, between-group differences in muscular forces were less than 1%. The fact that the statistical test reveals significance was due to the small within-group variability during this phase. We can conclude that the effect of anthropometry on the force construction during pedaling is only apparent when the PFD is used.

The results of the present investigation raise the question why different methods lead to different results when determining the effect of differences in anthropometry on the force construction of the task. Both the PFD and the FDS make inherent assumptions to account for the indeterminacy problem when decomposing the pedal reaction force into muscular and non-muscular components.

When using the PFD, a possible consequence is that muscular or non-muscular forces are erroneously attributed to the pedal reaction force, although they act to accelerate the limbs. When using the FDS, we might attribute muscular or non-muscular forces to limb accelerations although they also contribute to the pedal reaction force. Given the very small non-muscular forces of the FDS, we can speculate that motion-dependent forces contribute to accelerating the limbs rather than to the force directly applied to the pedal. If this were the case, we would expect muscular adjustments to changes in anthropometry to be revealed in muscular contributions to the acceleration of the limbs rather than to the pedal reaction forces. Therefore, an isolated investigation of pedal reaction forces could lead to misleading interpretations. An analysis of the effect of anthropometry on intersegmental dynamics - rather than on the pedal reaction force alone - would allow us to resolve this speculation, because we could quantify muscular contributions to limb accelerations. Intersegmental dynamics have been proven to be

useful in answering questions about muscular coordination in experienced cyclists (Fregly & Zajac, 1996; Neptune, Kautz, & Zajac, 2000; Raasch et al., 1997). Less is known about developmental differences in intersegmental dynamics. The use of this technique will be useful to further investigate the effect of age-related differences in anthropometry on the mechanical construction of the task and should be a subject for future studies.

The results of the present investigation begin to resolve the contradictory findings in the literature. We demonstrated that the effect of age-related differences on the force construction of the task depends on the decomposition technique being employed. Therefore, our data are consistent with those of both Brown (2000) and Korff and Jensen (2004). Brown (2000) found that adding mass to children's limbs alters the force construction of the task using the PFD. Korff and Jensen (2004) found that using the FDS, changes in anthropometry have little effect on the pedal force construction. The results of the present investigation demonstrate that the discrepancy in the findings between these two studies is almost entirely due to the use of different decomposition techniques.

To completely resolve the discrepancy between the two studies and to obtain a conclusive answer to the question of whether differences in anthropometry influence the mechanical construction of the task, two things need to be taken into consideration. First, our results suggest that the investigation of pedal forces in isolation may lead to misleading results. By analyzing muscular and non-muscular contributions to the pedal reaction forces we do not consider the possible effect of age-related differences in anthropometry on muscular contributions to limb accelerations. While an isolated investigation of decomposed pedal reaction forces (i.e., the PFD) has been proven to be useful to illustrate non-muscular influences or muscular efficiency across cadences

(Kautz & Hull, 1993; Neptune & Herzog, 1999), it seems insufficient to determine the effect of age-related differences in anthropometry on the mechanical construction of the task. An analysis of intersegmental dynamics would provide us with a more accurate answer to this question.

Second, the difference in the manipulation of anthropometry between the two studies could have contributed to the discrepancy in results. Where Korff and Jensen (2004) performed mathematical manipulations of anthropometric characteristics, Brown (2000) added mass to children's limbs experimentally. A possible consequence of the experimental manipulation is a loss in control over the kinematics and the resultant forces. Even if age-related differences in the resultant forces and in the kinematics were small, these small differences could be magnified in the decomposed forces. Disadvantages of the theoretical manipulation of anthropometry include the simplifying assumption of constant segmental growth rates and the lack of within-group variability in experimental data. A possible consequence is a discrepancy between statistically significant differences in the decomposed forces and their practical relevance. We showed that using the FDS, between group differences of less than 1% lead to statistical significance, suggesting little practical relevance of the statistical test. The larger between group differences obtained from the PFD (up to 57%) suggest a greater practical relevance of the observed statistical differences. To resolve the issues of experimental control and practical relevance of statistically significant differences, future studies should be conducted to investigate the effect of differences in anthropometry on intersegmental dynamics both experimentally and theoretically.

REFERENCES

- Brown, N. A., & Jensen, J. L. (2003). The development of contact force construction in the dynamic-contact task of cycling. *Journal of Biomechanics*, 36, 1-8.
- Brown, N. A. (2000). *Construction of a dynamic contact task by children: the role of segmental mass and inertia in cycling*. Doctoral dissertation, University of Texas at Austin.
- Centers for Disease Control and Prevention. (2000) *Growth Charts: United States, 2000* [Data file]. Available from Centers for Disease Control and Prevention Web site, <http://www.cdc.gov/growthcharts>
- Fregly, B. J., & Zajac, F. E. (1996). A state-space analysis of mechanical energy generation, absorption, and transfer during pedaling. *Journal of Biomechanics*, 29, 81-90.
- Fregly, B. J., Zajac, F. E., & Dairaghi, C. A. (2000). Bicycle drive system dynamics: theory and experimental validation. *Journal of Biomechanical Engineering*, 122, 446-452.
- Jensen, J. L., & Korff, T. (2004). Adapting to changing task demands: variability in children's response to manipulations of resistance and cadence during pedaling. *Research Quarterly for Exercise and Sport*, 75, 361-369.
- Jensen, J. L., Ulrich, B. D., Thelen, E., Schneider, K., & Zernicke, R. F. (1994). Adaptive dynamics of the leg movement patterns of human infants I. The effects of posture on spontaneous kicking. *Journal of Motor Behavior*, 26, 303-312.
- Jensen, R. K. (1989). Changes in segment inertia proportions between 4 and 20 years. *Journal of Biomechanics*, 22, 529-536.
- Kane, T.R., & Levinson, D.A. (1985). *Dynamics: Theory and Applications*, New York: McGraw-Hill Book Company
- Kautz, S. A., & Hull, M. L. (1993). A theoretical basis for interpreting the force applied to the pedal in cycling. *Journal of Biomechanics*, 26, 155-165.
- Konczak, J., Borutta, M., & Dichgans, J. (1997). The development of goal-directed reaching in infants. II. Learning to produce task-adequate patterns of joint torque. *Experimental Brain Research*, 113, 465-474.

- Korff, T., & Jensen, J. L. (2004). Age-related differences in muscular force application: the effect of segmental growth and its dependence on the force magnitude requirements of the task [Abstract]. *Journal of Sport & Exercise Psychology*, 26(Suppl.), S106-S107.
- Martin, J. C., Farrar, R. P., Wagner, B. M., & Spirduso, W. W., (2000). Maximal power across the lifespan. *Journal of Gerontology: Medical Sciences*, 55A, M311-M316.
- Neptune, R. R., & Herzog, W. (1999). The association between negative muscle work and pedaling rate. *Journal of Biomechanics*, 32, 1021-1026.
- Neptune, R. R., & Hull, M. L. (1995). Accuracy assessment of methods for determining hip movement in seated cycling. *Journal of Biomechanics*, 28, 423-437.
- Neptune, R. R., Kautz, S. A., & Hull, M. L. (1997). The effect of pedaling rate on coordination in cycling. *Journal of Biomechanics*, 30, 1051-1058.
- Neptune, R. R., Kautz, S. A., & Zajac, F. E. (2000). Muscle contributions to specific biomechanical functions do not change in forward versus backward pedaling. *Journal of Biomechanics*, 33, 155-164.
- Raasch, C. C., Zajac, F. E., Ma, B., & Levine, W. S. (1997). Muscle coordination of maximum-speed pedaling. *Journal of Biomechanics*, 30, 595-602.
- Raasch, C. C., & Zajac, F. E. (1999). Locomotor strategy for pedaling: muscle groups and biomechanical functions. *Journal of Neurophysiology*, 82, 515-525.
- Rowland, T. W. (2003). *Children's exercise physiology* (2nd ed.). Champaign, IL: Human Kinetics.
- Seth, A., McPhee, J. J., & Pandy, M. G. (2004). Multi-joint coordination of vertical arm movement. *Applied Bionics and Biomechanics*, 1, 45-56.
- Schneider, K., Zernicke, R. F., Ulrich, B. D., Jensen, J. L., & Thelen, E. (1990). Understanding movement control in infants through the analysis of limb intersegmental dynamics. *Journal of Motor Behavior*, 22, 493-520.
- Zajac, F. E., Neptune, R. R., & Kautz, S. A. (2002). Biomechanics and muscle coordination of human walking. Part I: Introduction to concepts, power transfer, dynamics and simulations. *Gait & Posture*, 16, 215-232.

Chapter 3: Study 2

INTRODUCTION

Motor development during childhood is marked by considerable improvements in motor performance. To understand the underlying mechanisms of these improvements, we need to determine the factors that lead to age-related changes in motor behavior. In this context, the application of muscular forces is of particular interest because it gives us insight into the nervous system's contribution to the construction of the task. While maturation of features of the neuro-motor system often results in improvements in motor behavior, observed age-related differences in muscular force application can be simply a consequence of segmental growth: Differences in body anthropometry (e.g., increases in segmental mass and segment lengths) affect non-muscular (i.e., gravitational and motion-dependent) forces and require muscular adjustments under circumstances where the movement kinematics are identical. The reason for this is that muscular forces must be matched appropriately to non-muscular forces, so that the resultant force (the sum of the muscular and non-muscular forces) complies with the goal of the task.

Anthropometry changes during childhood (Asmussen & Hebøll-Nielsen, 1955; Jensen, 1981, 1986, 1989), thus age-related differences in the application of muscular forces might represent not only neuromaturational changes, but also the functional muscular adjustments that are necessary to account for changing non-muscular forces due to differences in anthropometry (Brown & Jensen, 2003). Segmental masses, segment lengths, segmental moments of inertia, and segmental center of mass locations change in a non-linear fashion during infancy and childhood (Asmussen & Hebøll-Nielsen, 1955; Jensen, 1989; Schneider & Zernicke, 1992; Sun & Jensen, 1994). Jensen (1989) reports that the mass proportion of the thigh increases from 8% to 11% of the total body mass

between 5 and 20 years of age. The segmental center of mass of the shank segment changes to a more proximal position during this time (from 43% to 40% of the total shank length with respect to the knee joint).

Understanding the development of skill and adaptation in children requires knowledge about the effect of anthropometry on the force construction of the task. This is of particular importance if the goal is to attribute observed differences in muscular force application to changes in the biology of the performer. In order to more clearly attribute age-related differences in muscular force application to changes in the biology of the performer, we need to partition those differences that are simply a result of segmental growth. The purpose of this study, then, is twofold. The first purpose was to determine the consequences of age-related differences in anthropometry on the force construction of a motor task. The second purpose was to determine how children adapt skills to fit changing contexts. Thus, we explored the interaction between changing anthropometry and voluntary changes in speed of movement.

Previously, we determined the effect of age-related changes in anthropometry on the muscular component of the pedal reaction force during cycling. We used two different techniques: the pedal force decomposition technique (PFD) described by Kautz and Hull (1993) and a forward dynamics simulation (FDS) (Korff, Study 1). Korff (Study 1) found that changes in anthropometry affect the force construction of the pedaling task (the distribution between the muscular and non-muscular components of the pedal reaction force) only if the PFD is used. Using the FDS, the effect of anthropometry on the force construction of the task was negligible. Due to the limitations of both methods a definitive answer to the question of how anthropometry affects the mechanical construction of the task of pedaling could not be given. It was concluded that a more comprehensive level of analysis, specifically a mechanical energy analysis, is necessary

to determine this effect. Korff (Study 1) speculated that motion-dependent forces could contribute significantly to the acceleration of the limbs of the bicycle rider. If this were the case, we would expect the effect of age-related differences in anthropometry to be revealed in muscular energy that is generated to and absorbed from the limbs rather than in muscular energy that is delivered to the crank directly. Therefore, we hypothesized (a) that the effect of differences in anthropometry on muscular energy delivered to the crank would be non-significant, and (b) that the effect of differences in anthropometry on muscular energy delivered to the limbs would be significant.

In addition to changes in anthropometry, differences in the speed of movement influence non-muscular forces. For a given movement, the motion-dependent forces increase as movement speed increases. The expectation would be that differences in anthropometry have a greater effect on the force distribution between muscular and non-muscular forces at high compared to low movement speeds. This implies that there may be an interactive effect on muscular force application between movement speed and the anthropometry of the performer: The higher the movement speed, the greater the effect of anthropometry on non-muscular forces. As a consequence, greater muscular adjustments would be necessary at high movement speeds if anthropometric characteristics change while the resultant force to be produced is the same. The significance of this effect is critical when age-related differences in muscular force application are interpreted across different movement speeds (Chao, Rabago, Korff, & Jensen, 2002; Korff & Jensen, 2003). At slow movement speeds, the contribution of differences in anthropometry to observed differences in the mechanical construction of the task may be negligible, while it could be significant at high movement speeds. Therefore, we hypothesized that the effect of age-related differences in anthropometry on muscular energy delivered to the limbs and crank would be greater at high compared to low movement speeds.

Quantifying mechanical energy that is delivered to and absorbed from the limbs requires the use of a forward dynamics simulation (FDS) (Fregly & Zajac, 1996). Therefore, the FDS was used as the method of choice in this study. To isolate the effect of non-linear differences in anthropometry on muscular force application, a biomechanical model of the performer was developed. By manipulating the anthropometric parameters of the model, while keeping the kinematics and application of required forces constant, the effect of differences in anthropometry on muscular power production was isolated and possible confounds, such as neuromaturational changes, were eliminated.

METHODS

Forward Dynamics Simulation of Pedaling

A planar model of two-legged pedaling with adult anthropometrics was developed. The positions of the crank axis of rotation and the hip joint were fixed in the inertial reference frame. Each leg was modeled as a 5-bar linkage. Therefore, the model possessed 3 degrees of freedom (right and left thigh angles and crank angle). The foot and shank angles of the right and left legs were constrained to satisfy the configuration constraint equations. The corresponding angular velocities and accelerations were constrained to satisfy the kinematic constraint equations. The equations for the configuration constraints and the kinematic constraints can be found in Appendix D. The model was driven by muscular torques at the hip, ankle, and knee joints, and produced kinematics and forces similar to those created by an experienced cyclist. The bicycle drive dynamics were modeled using an effective resistive load and an effective inertial load (Fregly, Zajac, & Dairaghi, 2000).

Experimental Data

Experimental data from one experienced cyclist were used in this study (height: 167 cm; mass: 61 kg; age: 21 years). During the testing protocol, the participant rode a stationary ergometer at 60 rpm and 120 rpm at a power output of 96 W. Three reflective markers were placed on the pedal. One marker was placed at the center of the pedal, and two markers were aligned with the longitudinal axis of the pedal in the sagittal plane. Markers were also placed on the 2nd metatarsal, the lateral malleolus, the lateral femoral epicondyle, the greater trochanter, and the anterior superior iliac spine (ASIS). The coordinate data were sampled at 60 Hz and low-pass filtered by means of a 2nd order Butterworth filter with zero phase lag. The cut-off frequency was set to 10 Hz. The hip joint center was estimated using the coordinates of the greater trochanter and the ASIS, as described by Neptune and Hull (1995). Joint angles were calculated in two steps. First, the joint centers that satisfied the kinematic constraints of a 5-bar linkage and differed minimally from those obtained experimentally were found. During this gradient-based optimization procedure, the segment lengths were allowed to vary by $\pm 5\%$ of the calculated mean in order to further minimize the difference between the theoretical and experimental joint centers. The absolute angles of the foot, shank, and thigh were then calculated, using these optimal joint positions. These angles were low-pass filtered at 20 Hz using a Butterworth filter with zero phase lag. The corresponding angular velocities and accelerations were obtained by spline fitting and analytical differentiation of the angular positions.

Force data were collected using a custom-designed force pedal with two piezo electric force transducers (Kistler, model 9251AQ01). Force data were sampled at 600 Hz and filtered using a low-pass 4th order Butterworth filter with zero phase lag. The cut-off frequency was set to 20 Hz. The force data were then down-sampled in order to match

the kinematic data. Using the pedal angle obtained from the coordinate data, the forces were transferred from the reference frame of the pedal into the inertial reference frame. For each condition, all of the experimental data were averaged across 5 revolutions.

Tracking Experimental Data

To ensure that the model produced realistic kinematics and kinetics, a feedback linearization algorithm, as described by Seth, McPhee, and Pandy (2004), was employed. This algorithm corrects errors that result from double differentiating the position data by controlling the accelerations based on the error of simulated and experimental positions and velocities, according to Equation 3.1.

$$\mathbf{v}(t) = \ddot{\boldsymbol{\theta}}_{\text{exp}}(t) - 2\boldsymbol{\lambda}[\boldsymbol{\theta}(t) - \boldsymbol{\theta}_{\text{exp}}(t)] - \boldsymbol{\lambda}^2[\dot{\boldsymbol{\theta}}(t) - \dot{\boldsymbol{\theta}}_{\text{exp}}(t)] \quad (3.1)$$

where

$\mathbf{v}(t)$ is a 3x1 vector of the controlled accelerations.

$\boldsymbol{\theta}(t)$ is a 3x1 vector of the angular positions of the model.

$\dot{\boldsymbol{\theta}}(t)$ is a 3x1 vector of the angular velocities of the model.

$\boldsymbol{\theta}_{\text{exp}}(t)$ is a 3x1 vector of the experimentally obtained angular positions.

$\dot{\boldsymbol{\theta}}_{\text{exp}}(t)$ is a 3x1 vector of the experimentally obtained angular velocities.

$\ddot{\boldsymbol{\theta}}_{\text{exp}}(t)$ is a 3x1 vector of the experimentally obtained angular accelerations.

$\boldsymbol{\lambda}$ is a 3x3 diagonal matrix with positive constants λ_1 , λ_2 , and λ_3 on the main diagonal that determine the responsiveness of the controller \mathbf{v} .

The values λ_1 , λ_2 , and λ_3 were 32, 17, and 17, respectively. They were determined using a gradient-based optimization algorithm. The objective of this optimization was to minimize the difference between experimental and simulated angular positions and velocities.

The controlled accelerations, the experimental angular positions and velocities, as well as the reaction forces measured at the pedal, were used to compute the net muscle moments at the ankle, knee, and hip joints, via inverse dynamics at each time step. These joint moments were used to solve the equations of motion for the accelerations, which were then numerically integrated to obtain the states (angular positions and velocities) of the model at the next time step. The iterative application of this procedure at each time step yielded the trajectories of angular positions, velocities, and accelerations, which complied with the kinematic and configuration constraints of the model, and tracked experimentally obtained positions, velocities, and forces.

Modification of Anthropometric Characteristics

Anthropometric characteristics were obtained from Jensen (1989). The anthropometric characteristics of the adult model were scaled to the dimensions of children of three different ages (5, 7.5, and 10 years of age). Based on the adult model, 60 models with children's dimensions were created (20 for each hypothetical age group).

Body mass and the external resistance to be overcome were scaled by the same factor (S_M), because in developmental experiments using pedaling as a task, resistance is commonly scaled with respect to factors that are proportional to mass (Brown & Jensen, 2003; Jensen & Korff, 2004; Martin, Farrar, Wagner, & Spirduso, 2000). The scaling factors S_M for different age groups were chosen to match the body mass of the 50th percentile of children of 5, 7.5, and 10 years of age. These ages were chosen because previous research has shown that during this age-range, considerable improvements in neuromuscular adaptation occur (Chao et al., 2002). The S_M values were determined using the growth charts published by the Centers for Disease Control and Prevention (<http://www.cdc.gov/growthcharts>). The body masses for boys and girls of the relevant ages were determined and averaged. These were determined to be 18 kg, 24 kg, and 32

kg, for 5-, 7.5-, and 10-year-old children, respectively. The scaling factors S_M were found based on these hypothetical masses and the mass of the participant (61 kg).

Segment lengths were scaled using dimensionality theory. Dimensionality theory assumes that the growth rate of a specific anthropometric parameter depends on its Euclidean dimension (Rowland, 2003). In particular, measures of length are one-dimensional, and measures of mass are three-dimensional. If lengths are scaled by a scaling factor S_L and masses are scaled by a scaling factor S_M , the following relationship holds:

$$S_M = S_L^3 \quad (3.2)$$

which is equivalent to

$$S_L = S_M^{(1/3)} \quad (3.3)$$

Therefore, S_L was determined using Equation 3.3. Mass proportions, the segmental center of mass locations, and the radii of gyration were modified according to the regression equations presented by Jensen (1989) and scaled to the dimensions of children of 5, 7.5, and 10 years of age. The differences in the power construction of the anthropometrically modified and the original models reflected the non-linear differences in anthropometry (segmental mass proportions, center of mass locations, radii of gyration, and segment lengths).

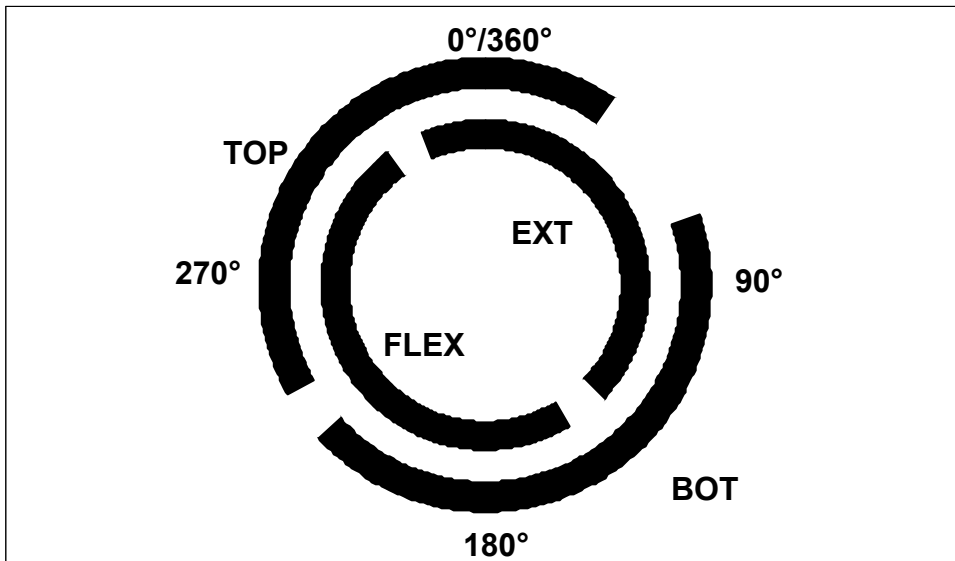
In order to account for within group variability in anthropometry and for measurement errors in anthropometric characteristics (Jensen, 1989), the relative mass proportions, center of mass locations, and radii of gyration were randomly varied within ± 3 times of the standard error reported for each polynomial regression equation (Jensen, 1989) for each hypothetical age group. Based the adult model, we created 20 hypothetical participants in each age group. The hypothetical 5-year-olds are referred to as “anthro-

YC” (representing the anthropometry of younger children), the 7.5-year-olds as “anthro-OC” (representing the anthropometry of older children), and the 10-year-olds as “anthro-PA” (representing the anthropometry of preadolescents). Forward dynamics simulations were run for each hypothetical participant at each cadence (resulting in a total of 120 simulations – 3 age groups, 20 group members, 2 cadences).

Dependent Measures

During each forward dynamics simulation, the following power contributions were determined (Fregly & Zajac, 1996): (a) the power contribution of all the muscles on the ipsilateral side of the body to crank power and (b) the power contribution of all the muscles on the ipsilateral side of the body to the power of the limbs. In order to allow for meaningful comparisons between age groups, all power profiles were normalized by the average muscular crank power over the entire crank cycle. Each normalized power contribution was averaged across four regions of the crank cycle (Neptune, Kautz, & Hull, 1997): (a) extensor (EXT: 337° to 134° of the crank cycle); (b) flexor (FLEX: 149° to 324° of the crank cycle); (c) top (TOP: 241° to 35° of the crank cycle); (d) bottom (BOT: 72° to 228° of the crank cycle). The different regions of the crank cycle are illustrated in Figure 3.1.

Figure 3.1. Regions of the crank cycle. The crank cycle was divided into 4 regions: extensor (EXT, 337°-134°), flexor (FLEX, 149°-327°), top (TOP, 241°-35°), and bottom (BOT, 72°-228°).



Statistical Analysis

Before the statistical analyses of the dependent variables were performed, the validity of the model was verified by determining the difference between the angular positions, velocities, and pedal reaction forces of the forward dynamics simulation and those that were obtained experimentally. The tracking error was quantified by calculating the average absolute deviation between simulated and experimental data profiles expressed as the percentage of the range of the corresponding experimentally obtained data profile (Equation 3.4).

$$Error = 100 \cdot \frac{\frac{1}{n} \left[\sum_{i=1}^n |Y_{exp_i} - Y_{sim_i}| \right]}{range(Y_{exp})} \% \quad (3.4)$$

where

Y_{exp_i} is the experimentally obtained data profile at the i^{th} sample

Y_{sim_i} is the simulated data profile at the i^{th} sample

n is the number of samples of each profile.

The error was quantified for joint angles and angular velocities, as well as the vertical and horizontal components of the pedal reaction force of the ipsilateral side.

Age x Cadence ANOVAs were performed for each region of the crank cycle and each dependent variable. By assessing the main effects for age, we tested the hypotheses relating to age-related differences in muscular power contributions to crank power and limb power. By assessing the Age x Cadence interaction we tested the hypothesis with regard to the dependence of the age effect on movement speed.

If an age main effect was significant, post hoc t-tests (Bonferroni) were performed for the corresponding dependent variable. If the Age x Cadence interaction was

significant, follow up one-way ANOVAs were performed at the corresponding cadence. In case of a follow up ANOVA being significant, post hoc t-tests (Bonferroni) were performed to locate the differences. For all statistical tests, the type I error was set to .05.

RESULTS

Model Verification

The feedback linearization algorithm created a forward dynamics simulation that tracked the experimental data closely. On average, the errors in angular positions and velocities, as well as the horizontal and vertical components of the pedal reaction force were smaller than 1%. For all hypothetical participants, tracking errors were 0.86% and 0.92% at 60 rpm and 120 rpm, respectively. The figures illustrating the differences between experimental and simulated data can be found in Appendix F.

Effect of Differences in Anthropometry on the Muscular Contribution to Crank Power and Limb Power

Age-related differences in anthropometry did not affect the muscular contribution to crank power. During all regions of the crank cycle, the main effect for age on the muscular contribution to crank power was non-significant (Table 3.1). Figures 3.2 and 3.3 illustrate the small effect of anthropometry on the muscular contribution to crank power.

Age-related differences in anthropometry significantly affected the muscular contribution to limb power. During all regions of the crank cycle, the main effect for age on the muscular contribution to limb power was significant (Table 3.1). Post hoc-tests revealed that during EXT and BOT muscular energy absorbed from the limbs increased significantly with an increase in age. During FLEX and TOP, muscular energy delivered to the limbs increased significantly with increasing age. During all regions of the crank cycle, all age groups differed significantly from each other. Figures 3.4 and 3.5 illustrate the significant effect of anthropometry on the muscular contribution to limb power. The figures illustrating all results can be found in Appendix G.

Interactive Effect of Anthropometry and Cadence on Muscular Power Contributions to the Crank and Limbs

For the muscular power contribution to limb power, the effect of age-related changes in anthropometry was dependent on cadence. For all regions of the crank cycle the Age x Cadence interaction was significant (Table 3.2). Follow-up ANOVAs revealed that the age effect was significant at both cadences and during each region of the crank cycle. Post-hoc tests revealed that at each cadence the observed age effects were identical to those observed for the main effect for age. Therefore, we used effect sizes to interpret the difference in the magnitude of the age group differences between cadences. Effect sizes for each dependent variable describing the difference between two age groups were calculated by dividing the difference of group means by the pooled standard deviation. To interpret the effect sizes Cohen's (1988) classification scheme was used. According to Cohen (1988), effect sizes smaller than 0.5 are interpreted as a small effect. Effect sizes greater than 0.5 and smaller than 0.8 are interpreted as a moderate effect. Effect sizes greater than 0.8 are interpreted as a large effect. The analysis of the effect sizes revealed that there was a tendency for the effect sizes to increase with increasing cadence. The mean effect sizes across all age group comparisons and all crank regions were 1.49 and 1.61 at 60 rpm and 120 rpm, respectively. The greatest increases in effect sizes across movement speeds were seen during EXT and during BOT. With increasing cadence, the effect sizes increased by 14% and 55% during EXT and BOT, respectively.

For the muscular power contribution to crank power, the Age x Cadence interaction was non-significant for all of the crank regions analyzed ($p > .21$).

Table 3.1. Statistical analysis on the main effect for age on the muscular contributions to crank power (Mus2Crank) and to limb power (Mus2Limbs). The age effect was assessed during the extensor (EXT), flexor (FLEX), top (TOP), and bottom (BOT) regions of the crank cycle.

Power Contribution	Crank Region	F(2,57)	p
Mus2Crank	EXT	0.52	.60
	FLEX	0.54	.58
	TOP	0.43	.65
	BOT	0.41	.67
Mus2Limbs	EXT	19.00	<.001
	FLEX	34.86	<.001
	TOP	31.58	<.001
	BOT	26.64	<.001

Table 3.2. Statistical analysis on Age x Cadence interaction with regard to the muscular contribution to limb power (Mus2Limbs). The Age x Cadence interaction effect was assessed during the extensor (EXT), flexor (FLEX), top (TOP), and bottom (BOT) regions of the crank cycle.

Power Contribution	Crank Region	F(2,57)	p
Mus2Limbs	EXT	21.23	p<.001
	FLEX	22.42	p<.001
	TOP	19.42	p<.001
	BOT	49.20	p<.001

Figure 3.2. Profiles of the muscular power contribution to crank power for hypothetical preadolescents (anthro-PA), older children (anthro-OC) and younger children (anthro-YC) for 60 rpm (A) and 120 rpm (B). Each region of the crank cycle is abbreviated by its first letter (extensor (E), flexor (F), top (T), and bottom (B)). The numbers 1 and 2 indicate the beginning and the end of a particular region of the crank cycle, respectively (e.g., E1 indicates beginning of the extensor phase, and E2 indicates the end of the extensor phase).

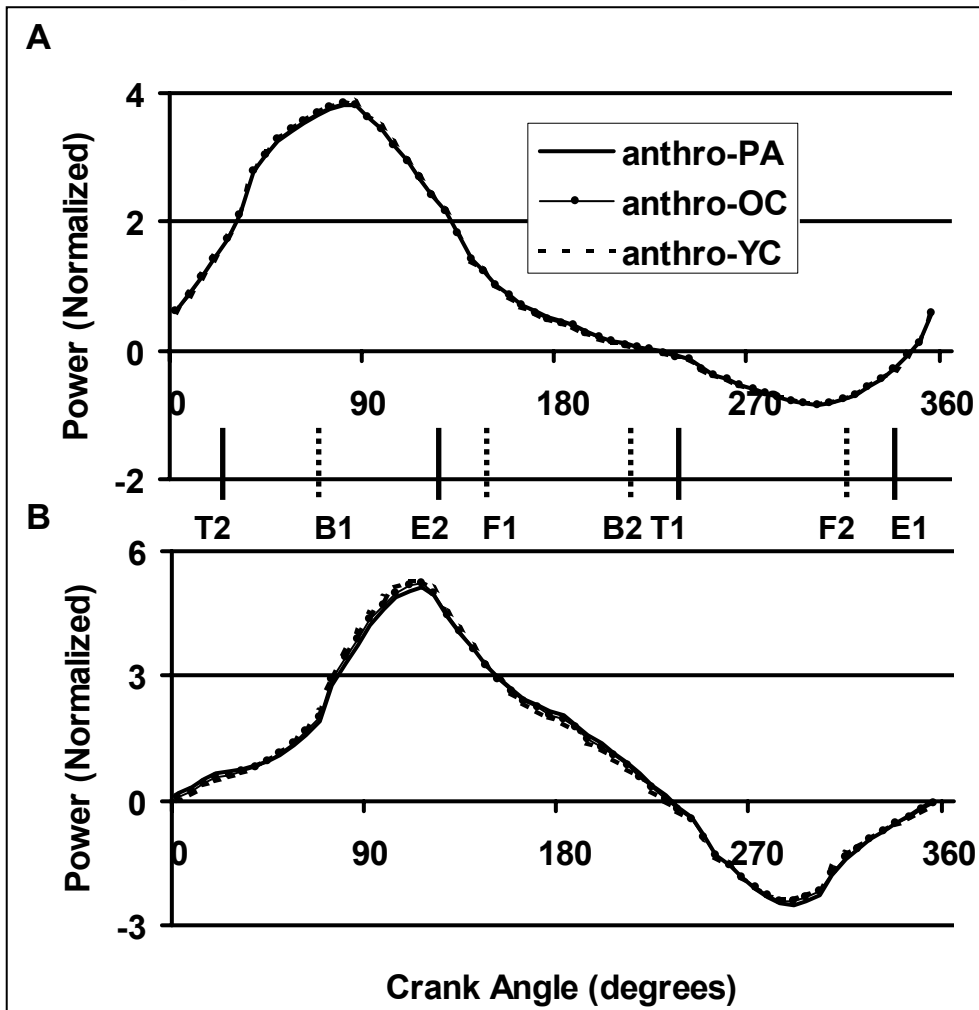


Figure 3.3. Age-group differences in the muscular power contribution to crank power during the extensor phase. Means and standard deviations are shown for hypothetical preadolescents (anthro-PA), older children (anthro-OC) and younger children (anthro-YC) at 60 rpm and 120 rpm. The age effect on the muscular contribution to crank power was non-significant for both cadences.

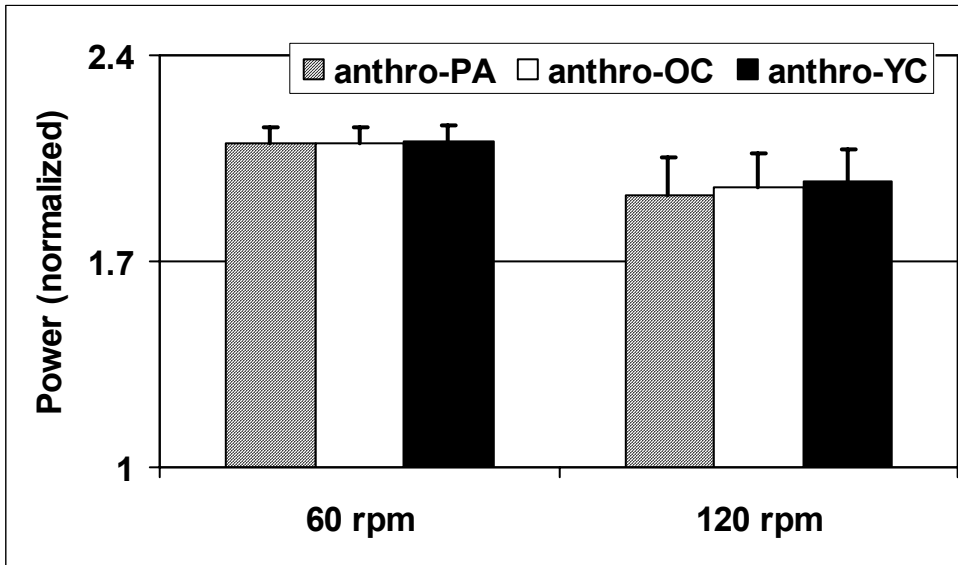


Figure 3.4. Profiles of the muscular power contribution to limb power for hypothetical preadolescents (anthro-PA), older children (anthro-OC) and younger children (anthro-YC) for 60rpm (A) and 120rpm (B). Each region of the crank cycle is abbreviated by its first letter (extensor (E), flexor (F), top (T), and bottom (B). The numbers 1 and 2 indicate the beginning and the end of a particular region of the crank cycle, respectively (e.g., E1 indicates beginning of the extensor phase, and E2 indicates the end of the extensor phase).

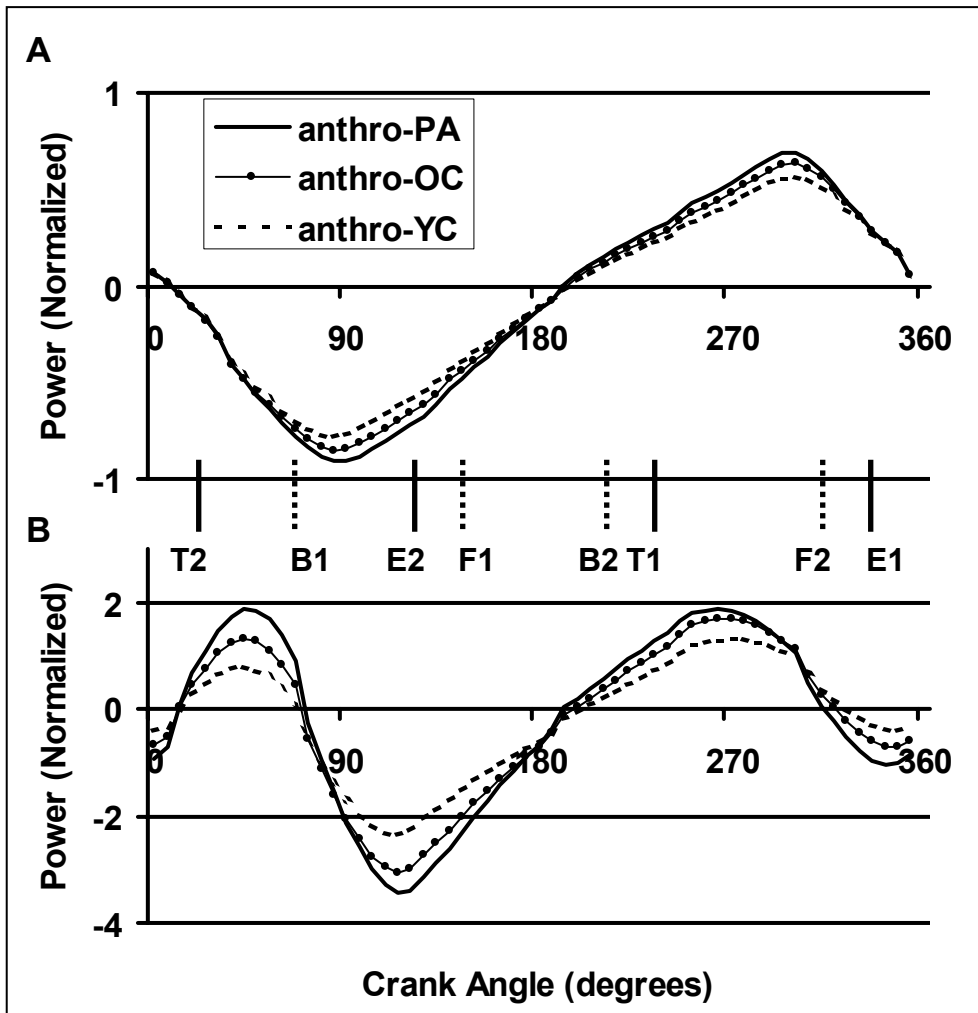


Figure 3.5. Age-group differences in the muscular power contribution to limb power during the extensor phase. Means and standard deviations are shown for hypothetical preadolescents (anthro-PA), older children (anthro-OC) and younger children (anthro-YC) at 60 rpm and 120 rpm. The symbol “*” indicates a significant age effect of the ANOVA at the corresponding cadence.

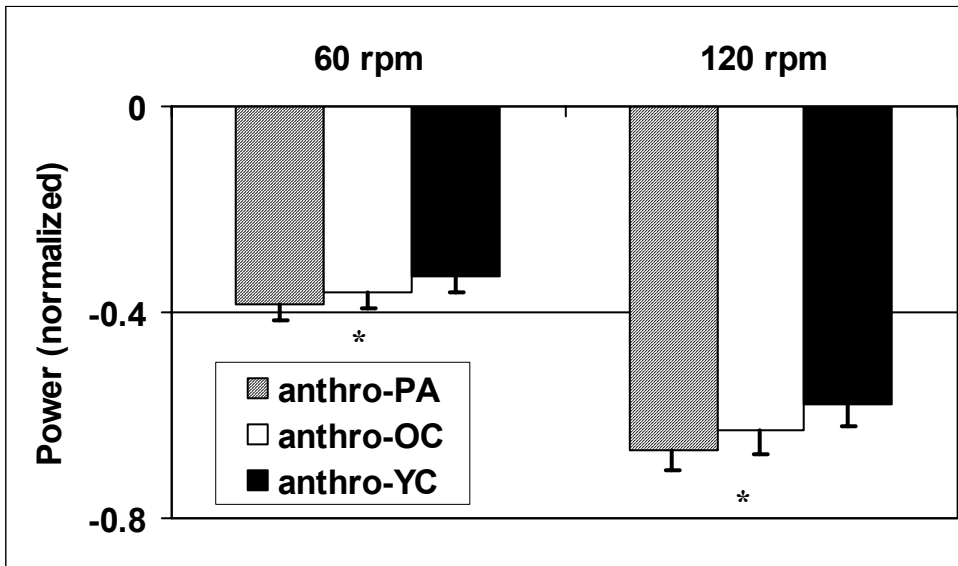


Table 3.3. Effect sizes (ES) and percent differences (% difference) in muscular power contributions to limb power between hypothetical age groups (anthro-YC: younger children, anthro-OC: older children, anthro-PA: preadolescents). Differences are shown for the extensor (EXT), flexor (FLEX), top (TOP), and bottom (BOT) regions of the crank cycle

60 rpm		EXT	FLEX	TOP	BOT
anthro-PA vs. anthro-OC	ES	-0.80	1.31	1.16	-0.73
	% difference	6.75	13.41	9.03	6.79
anthro-PA vs. anthro-YC	ES	-1.84	3.00	2.73	-1.71
	% difference	15.95	32.22	21.87	15.91
anthro-OC vs. anthro-YC	ES	-0.96	1.40	1.35	-0.90
	% difference	7.93	14.23	10.54	7.87
120 rpm		EXT	FLEX	TOP	BOT
anthro-PA vs. anthro-OC	ES	-0.90	1.17	1.04	-1.21
	% difference	6.25	15.94	7.07	9.50
anthro-PA vs. anthro-YC	ES	-2.12	2.71	2.61	-2.63
	% difference	15.09	38.71	17.92	21.32
anthro-OC vs. anthro-YC	ES	-1.08	1.27	1.31	-1.32
	% difference	7.68	16.42	9.20	9.74

DISCUSSION

The results of this investigation demonstrate that changes in anthropometry during childhood result in a need to differently match muscular to non-muscular forces, during a dynamic contact task. The magnitude of this effect increases with increasing movement speed. In conformity with the hypotheses, the effect of anthropometry on the mechanical construction of the task is only apparent in muscular power delivered to and absorbed from the limbs – not in muscular power delivered to the crank. We can conclude that anthropometry does not change the way muscles deliver energy to the crank directly but does change the way muscular energy is transferred to the crank indirectly through energy generation to and energy absorption from the limbs.

The findings of the present investigation resolve contradictory information in the literature. Where Brown (2000) found the effect of anthropometry on the force construction of the task to be significant, Korff and Jensen (2004) found this effect to be negligible. Differences in anthropometry influence non-muscular forces and result in a need to match muscular forces if the resultant force (the sum of muscular and non-muscular forces is to be the same). The greater non-muscular forces are the greater is the effect of anthropometry on the force construction of the task. Korff (Study 1) demonstrated that the differences in findings between Brown (2000) and Korff and Jensen (2004) are partly due to differences in the estimation in non-muscular forces. This difference is the consequence of different methods being employed. Due to the limitations that are present when estimating muscular and non-muscular contributions to the pedal reaction force, it was concluded that a more comprehensive analysis would be necessary to answer the question of how differences in anthropometry influence the mechanical construction of the task. In particular, the small non-muscular contribution to

the pedal reaction force reported by Korff and Jensen (2004) lead to the speculation that non-muscular forces contribute to the acceleration of the limbs, rather than to that of the crank. If this were the case, the effect of age-related differences in anthropometry on the mechanical construction of the task would be revealed in muscular contributions to limb accelerations. The results of the present investigation confirm this speculation as age-related differences in anthropometry affect muscular contributions to limb power. The results thereby confirm results from Brown (2000) who found that adding mass to children's limbs results in a more adult-like construction of the pedal reaction force. The results of the present investigation further findings by Brown (2000) by determining the effect of age-related differences in anthropometry on the mechanical construction of the task more comprehensively. We added detail by differentiating between the effect of anthropometry on the muscular contribution to crank power and the muscular contribution to limb power. The effect of anthropometry was only significant for the muscular contribution to limb power which illustrates that differences in anthropometry affect the indirect transfer of mechanical energy to the crank. These results demonstrate that an analysis of intersegmental dynamics is necessary to fully understand the effect of age-related differences in anthropometry on the interaction between muscular and non-muscular forces.

The results of the present investigation allow us to generalize previous findings with respect to unconstrained non-contact tasks to constrained contact tasks. This generalization is not trivial. On the one hand, one could have expected that anthropometry would not significantly influence the distribution between muscular and non-muscular forces. During contact tasks, greater muscular forces are required when compared to non-contact tasks. For a given movement, non-muscular forces are not affected by the external force requirement which is present during contact tasks.

Therefore, the relative influence of non-muscular forces is smaller during contact tasks when compared to non-contact tasks. Due to the reduced influence of non-muscular forces one could have expected the effect of anthropometry on the distribution between muscular and non-muscular forces to be negligible. In contrast, one could have expected that non-muscular forces would be large enough to elicit a significant effect of differences in anthropometry on the distribution between muscular and non-muscular forces. Support for this hypothesis comes from Schneider et al. (1990) who found non-muscular influences to be significant during kicking. These influences are greater at high compared to low movement speeds. Our results support this second possibility. They thereby allow us to generalize from non-contact tasks to contact tasks in two respects. First, differences in anthropometry result in a need to match muscular to non-muscular forces during both non-contact and contact tasks. Second, this need increases with increasing movement speed.

It is known that children apply muscular forces differently than adults during lower extremity tasks (Brown & Jensen, 2003; Jensen et al., 1994; Schneider et al., 1990). These differences in muscular force application can be due to segmental growth, neuromaturation, or differences in the kinematics of the behavior. In experimental studies, it is often difficult to attribute observed differences to one of these features. In the present study, these limitations were overcome. The influences of neuromaturation and differences in the kinematics of the behavior were eliminated, and differences in muscular force application could be specifically attributed to differences in anthropometry.

From the results of the present investigation, the question about the functional relevance of the observed effects of differences in anthropometry on the mechanical construction of the task arises. The advantage of the theoretical manipulation of

anthropometry which was performed in this study is that all other (possibly confounding) influences on muscular force application were eliminated. The limitation of such a manipulation is that due to the small between subject variability, observed statistical differences may not be functional. However, in spite of the small between subject variability, large between group differences in muscular power contributions to limb power were observed (up to 38% between anthro-PA and anthro-YC, see Table 3.3). In addition, results from Brown (2000) support the physical relevance of the observed differences. Brown (2000) found a significant effect of adding mass to children's limbs on the force construction during cycling. The advantage of Brown's (2000) study design was that the experimental manipulation of anthropometry yielded a more realistic estimate of within group variability. The disadvantage was a lack of control of possibly confounding factors. The results of the present investigation combined with results from Brown (2000) demonstrate that age-related differences in anthropometry result in functionally relevant differences in the mechanical construction of the task of pedaling.

In summary, differences in anthropometry significantly influence the need to match muscular to non-muscular forces which has to be factored in when interpreting age-related differences of muscular force application. In the light of the present results then, caution must be taken when interpreting age-related differences in muscular force application, because differences in anthropometry might be a significant contributor to the differences observed.

REFERENCES

- Asmussen, E., & Heebøll-Nielsen, K. (1955). A dimensional analysis of physical performance and growth in boys. *Journal of Applied Physiology*, 7, 593-603.
- Brown, N. A. (2000). *Construction of a dynamic contact task by children: the role of segmental mass and inertia in cycling*. Doctoral dissertation, University of Texas at Austin.
- Brown, N. A., & Jensen, J. L. (2003). The development of contact force construction in the dynamic-contact task of cycling. *Journal of Biomechanics*, 36, 1-8.
- Centers for Disease Control and Prevention. (2000) *Growth Charts: United States, 2000* [Data file]. Available from Centers for Disease Control and Prevention Web site, <http://www.cdc.gov/growthcharts>
- Chao, P., Rabago, C., Korff, T., & Jensen, J. L. (2002). Muscle activation adaptations in children in response to changes in cycling cadence [Abstract]. *Journal of Sport & Exercise Psychology*, 24(Suppl.), S42-S43.
- Cohen, J. (1988). *Statistical power analysis for the behavioral sciences* (2nd ed.). New Jersey: Lawrence Erlbaum.
- Fregly, B. J., & Zajac, F. E. (1996). A state-space analysis of mechanical energy generation, absorption, and transfer during pedaling. *Journal of Biomechanics*, 29, 81-90.
- Fregly, B. J., Zajac, F. E., & Dairaghi, C. A. (2000). Bicycle drive system dynamics: theory and experimental validation. *Journal of Biomechanical Engineering*, 122, 446-452.
- Hoy, M. G., & Zernicke, R. F. (1986). The role of intersegmental dynamics during rapid limb oscillations. *Journal of Biomechanics*, 19, 867-877.
- Jensen, J. L., Ulrich, B. D., Thelen, E., Schneider, K., & Zernicke, R. F. (1994). Adaptive dynamics of the leg movement patterns of human infants I. The effects of posture on spontaneous kicking. *Journal of Motor Behavior*, 26, 303-312.
- Jensen, J. L., & Korff, T. (2004). Adapting to changing task demands: variability in children's response to manipulations of resistance and cadence during pedaling. *Research Quarterly for Exercise and Sport*, 75, 361-369.
- Jensen, R. K. (1981). The effect of a 12-month growth period on the body moments of inertia of children. *Medicine and Science in Sports and Exercise*, 13, 238-242.

- Jensen, R. K. (1986). Body segment mass, radius and radius of gyration proportions of children. *Journal of Biomechanics*, 19, 359-368.
- Jensen, R. K. (1989). Changes in segment inertia proportions between 4 and 20 years. *Journal of Biomechanics*, 22, 529-536.
- Korff, T., & Jensen, J. L. (2003). Development of adaptation to changing speed requirements in terms of negative muscular work during bicycling [Abstract]. *Research Quarterly for Exercise and Sport*, 74(Suppl.), A32-A33.
- Liu, T., Korff, T., Chao, P., & Jensen, J.L. (2003). Bilateral asymmetry and cycling performance in children. [Abstract]. *Journal of Sport & Exercise Psychology*, 25(Suppl.), S91.
- Martin, J. C., Farrar, R. P., Wagner, B. M., & Spirduso, W. W. (2000). Maximal power across the lifespan. *Journals of Gerontology Series A: Biological Sciences and Medical Sciences*, 55, M311-316.
- Neptune, R. R., & Hull, M. L. (1995). Accuracy assessment of methods for determining hip movement in seated cycling. *Journal of Biomechanics*, 28, 423-437.
- Neptune, R. R., & Kautz, S. A. (2001). Muscle activation and deactivation dynamics: The governing properties in fast cyclical human movement performance? *Exercise and Sport Sciences Reviews*, 29, 76-81.
- Rowland, T. W. (2003). *Children's exercise physiology* (2nd ed.). Champaign, IL: Human Kinetics.
- Schneider, K., & Zernicke, R. F. (1992). Mass, center of mass, and moment of inertia estimates for infant limb segments. *Journal of Biomechanics*, 25, 145-148.
- Schneider, K., Zernicke, R. F., Ulrich, B. D., Jensen, J. L., & Thelen, E. (1990). Understanding movement control in infants through the analysis of limb intersegmental dynamics. *Journal of Motor Behavior*, 22, 493-520.
- Seth, A., McPhee, J.J., & Pandy, M.G. (2004). Multi-joint coordination of vertical arm movement. *Applied Bionics and Biomechanics*, 1, 45-56.
- Sun, H., & Jensen, R. K. (1994). Body segment growth during infancy. *Journal of Biomechanics*, 27, 265-275.

Chapter 4: Study 3

INTRODUCTION

Skillful movement is characterized by a task-appropriate application of muscular forces that results in the desired limb trajectories. Skillfulness in movement is not only defined by the ability to meet the demands of a particular task, but also by the ability to perform the task over a range of task demands. The reason for this is that for many tasks, the context in which they are performed changes constantly, and the neuro-motor system has to respond to those changes. These responses are made by adjusting the muscular forces. A common situation during which such muscular adjustments are made is present when the performer voluntarily changes certain parameters of the task.

The capacity of children for voluntary adaptive skill increases as they grow older. For example, the range of speeds at which children can successfully perform cyclic tasks, such as walking or pedaling, is smaller than that of adults (Jeng, Liao, Lai, & Hou, 1997; Chao, Rabago, Korff, & Jensen, 2002; Liu, Korff, Chao, & Jensen, 2003). Chao et al., (2002), and Liu et al. (2003) demonstrated that while pedaling, children between 4 and 11 years of age are less likely to be successful if movement speed is scaled up to 120 rpm, and this effect is more apparent in younger children compared to older children. In addition to behavioral differences, differences in neuromuscular adaptive responses have also been observed: younger children (less than 7 years of age) are less likely to demonstrate an organized muscle response when creating changes in movement speed than older children or adults (Chao et al., 2002). It is interesting to note that these neuromuscular differences exist even though the task is performed successfully. These results suggest that there is a different developmental schedule for voluntary adaptation

observed at the behavioral level compared to the neuromuscular level: Mature motor behavior does not necessarily represent mature neuromuscular organization.

As children grow older and both their motor behavior and neuromuscular organization improve, one question remains unanswered: How do neuromuscular differences affect (or not affect) the behavioral outcome? From differences in muscle activation patterns or muscular torque profiles alone (Chao et al., 2002), it is difficult to make inferences about their effect on how the goal of the task is achieved. To interpret these differences, we need to know the relationship between the muscular forces or torques and the kinematic outcome that they produce. Thus, the purpose of this study was to determine how age-related differences in voluntary adaptation on a neuromuscular level affect the mechanical construction of the movement outcome. In this investigation pedaling was chosen as the task to be studied because it is well defined: Muscles have to deliver mechanical power to the crank against a constant external resistance to produce a cyclical movement.

The first hypothesis tested was that children would differ from adults in the adjustment of peak muscular joint powers as a response to changes in movement speed: At low and moderate movement speeds, peak muscular joint powers are predicted to be the same in children and adults; at high movement speeds, peak muscular joint powers are predicted to be reduced in children, compared to adults (hypothesis 1). To provide the rationale for this hypothesis, we start with the notion that maximum mechanical power during pedaling is reduced in children, compared to adults (Martin, Farrar, Wagner, & Spirduso, 2000). Mechanical power (i.e., the overall power delivered to the crank) is composed of individual joint powers acting in synergy (Fregly & Zajac, 1996). A possible explanation for the findings of Martin et al. (2000) is that the observed reduction in overall power in children is due to a reduced capacity to produce muscular power at

the individual joints. Knowing that not only maximum power but also maximum movement speed is lower in children than in adults (Chao et al., 2002; Liu et al., 2003), we hypothesized that – in spite of a successful performance of the task – children would demonstrate a reduction in peak muscular joint powers when movement speed approaches their performance limits. Thus, hypothesis 1 was posed to test an Age x Cadence interaction.

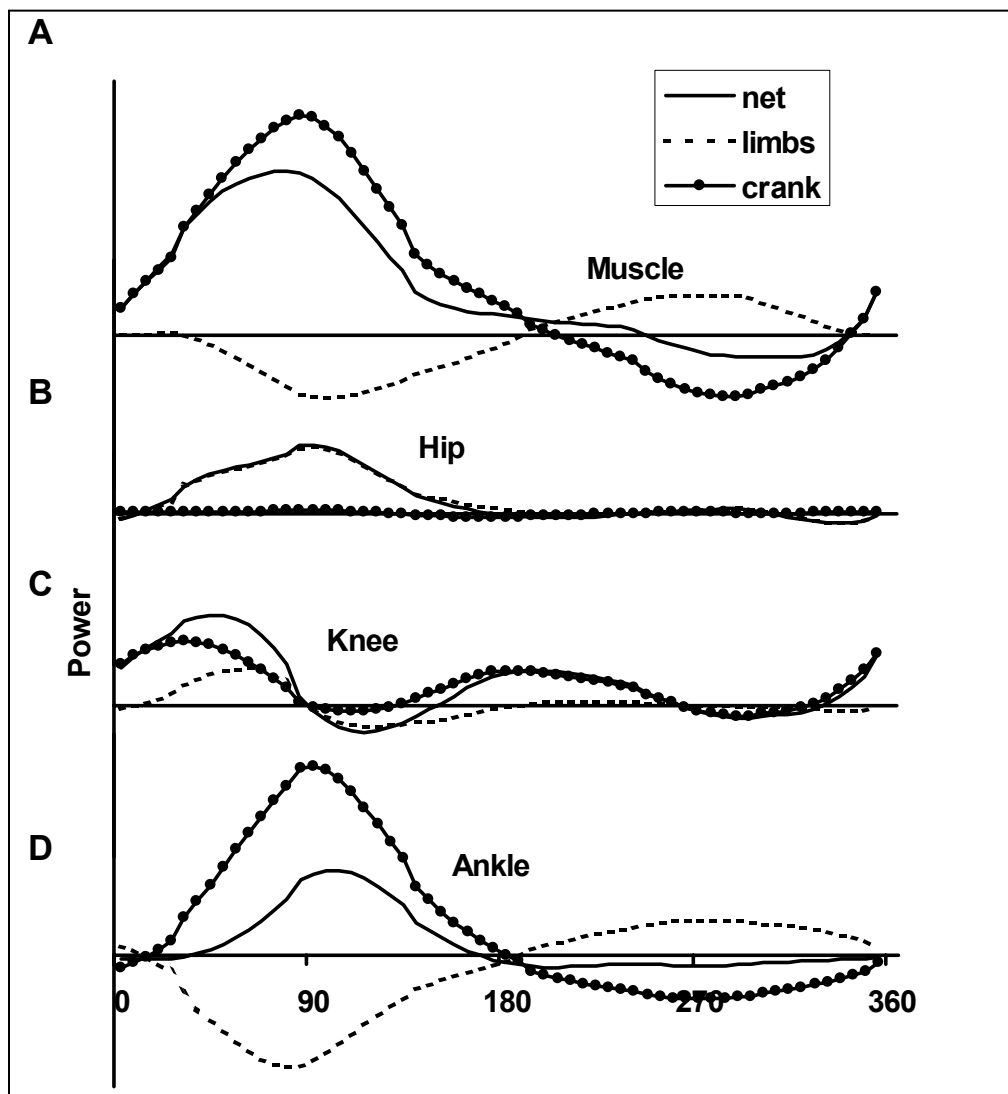
The second hypothesis tested was that as a consequence of the hypothesized reduced peak joint power at high speeds, children would demonstrate a reduction in muscular power production during the extensor phase (the phase of the crank cycle during which most muscular power is produced) (hypothesis 2a). A corollary to this hypothesis is that children would compensate for this reduced power by increasing muscular power during different regions of the crank cycle (hypothesis 2b). Possible regions during which children could increase muscular power include those phases during which the flexor muscles are active and the phases during which the pedal is transitioned through top dead center or bottom dead center of the crank cycle.

Another corollary to hypotheses 2a and 2b is that the age-related differences in muscular power are accompanied by a different mechanical construction of the task. In pedaling, two mechanisms result in muscular power generation to the crank. Mechanical power can be generated by muscles to the crank directly. From the adult literature, we know that in elite cyclists, the knee extensors deliver a large amount of muscular energy to the crank directly (Fregly & Zajac, 1996; Neptune, Kautz, & Zajac, 2000). The second mechanism that is responsible for muscular energy delivery to the crank is an indirect transfer of muscular energy. In adults, the proximal hip extensors deliver muscular energy to the limbs. This energy is absorbed from the limbs by the plantarflexors and transferred to the crank indirectly (Fregly & Zajac, 1996; Neptune et al., 2000). This

interplay between hip extensors and plantarflexors has been described as a muscular synergy between these two muscle groups (Fregly & Zajac, 1996). In Figure 4.1, the mechanical construction of muscular power delivered to the crank for an experienced cyclist is illustrated.

In our developmental context then, the hypothesized reductions in muscular power at high speeds during the power-producing phase could have two possible consequences: (a) a reduction in direct muscular energy generation or (b) a reduction in indirect energy transfer (a weaker inter-muscular synergy). Similarly, the hypothesized compensatory increase in muscular power during different regions of the crank cycle could be due to (a) an increase in direct muscular energy generation or (b) an increase in indirect energy transfer (a stronger inter-muscular synergy). Therefore we hypothesized an age-specific distribution of muscular power delivered to the crank directly and indirectly during the power-producing phase (hypothesis 3a) and during those phases in which children compensate for the reduction in muscular power (hypothesis 3b). On the one hand, one could expect that children use an increased indirect muscular energy transfer to the crank through the muscular synergy between the proximal and distal muscle groups (Neptune et al., 2000). On the other hand one could expect an increased direct muscular energy delivery to the crank. The fact that children's neuromuscular synergies are not fully developed at 10 years of age (Chao et al., 2002; Shumway-Cook & Woollacott, 1985) provides support for this second possibility.

Figure 4.1. Mechanical energy distribution due to all muscles (A), and torques at the hip (B), knee (C), and ankle (D) for an experienced adult cyclist. The net muscular power at each joint is decomposed into power contributions to the crank and the limbs. If the net power of a particular joint is positive, mechanical energy is added to the system. If it is negative, then energy is absorbed. If the crank or limb power contributions are positive, energy is delivered to the crank or the limbs, respectively. If these contributions are negative, energy is absorbed from the crank or the limbs, respectively. The data shown are from an experienced cyclist pedaling at 75 rpm at 96 W. All power profiles are on the same ordinate scale. The data presented were obtained in the Developmental Motor Control Laboratory at the University of Texas at Austin.



METHODS

Experimental Design

Three groups of participants were recruited: a) younger children (YC, $n=11$, 6.0 ± 0.6 years of age); b) older children (OC, $n=8$, 9.4 ± 0.8 years of age); and c) adults (AD, $n=8$, 27.3 ± 2.3 years of age). The inclusion of both YC and OC age groups allowed for a description of age-related changes in muscular force application between the ages of 5 and 10 years of age, a period in which substantial improvements in cycling performance and neuromuscular adaptability occur (Chao, et al., 2002; Liu, et al., 2003; Jensen & Korff, 2004). Separating the age groups into children younger and older than 7 years of age allowed for the testing of age-related changes in muscular force application during a developmental period in which substantial improvements in neuromuscular control are achieved (Shumway-Cook & Woollacott, 1985; Chao, et al., 2002). The adult participants were used as a comparison reference, representing mature performance of the task. This was appropriate because it was our goal to attribute age-related differences in motor behavior to features of the neuro-motor system which can be assumed to be mature at 20 years of age. At the same time, we made sure that observed differences were not confounded by differences in the experience levels between performers.

Through the use of a questionnaire, the number of hours that each participant had ridden a bicycle during the past 5 years was estimated. We conducted a guided interview with the parent and the child. The interview maximized consistency in the interpretability of the questions and the accuracy of the estimate with regard to accumulated cycling experience. All participants had moderate cycling experience. The participants knew how to ride a bicycle, but had not competed or participated in organized rides. All participants had less than 320 hours of cycling experience within the previous 5 years. The mean

values for bicycle riding experience can be seen in Table 4.1. Pearson Product Moment correlations between the number of hours of bicycle-riding experience and each dependent measure (collapsed across all cadences) were performed for each age group. All correlations were statistically non-significant ($p > .05$). It was concluded that in these participants cycling experience did not confound the present analysis.

Table 4.1. Group characteristics of the participants who were included in the final analysis: Means \pm standard deviations are presented for age, predicted peak power, and bicycle riding experience.

	n	Age (years)		Predicted Peak Power (W)	Bicycle Riding experience (hours)
		Range	Mean \pm SD		
Younger Children (YC)	11	5-7	6.0 \pm 0.7	256 \pm 30	80.5 \pm 68.6
Older Children (OC)	8	8-10	9.4 \pm 0.9	392 \pm 137	165.0 \pm 86.2
Adults (AD)	8	25-31	27.3 \pm 2.3	1015 \pm 258	24.1 \pm 30.6

Fitting the Participant to the Bicycle

Using a custom-made crank length adapter, the crank length was adjusted so that it approximated 20% of the participant's leg length. Since the increment of the crank length adapter was 1.5 cm, the maximum deviation between the crank length and 20% of the participant's leg length was 0.75 cm. The seat height was adjusted so that the relative knee angles at top dead center (TDC) and bottom dead center (BDC) were $75^\circ \pm 3^\circ$ and $155^\circ \pm 3^\circ$, respectively. The handlebars were adjusted so that the angle between the trunk and the horizontal axis of the inertial reference frame was 60° . For each participant and each condition, the resistance of the ergometer was set to 10% of predicted instantaneous peak power. Martin et al. (2000) established a regression equation relating lean thigh volume to the instantaneous peak power that participants could generate on an ergometer. Their subjects ranged between 8 and 70 years of age. Even though the equation was not validated for children younger than 8 years of age, it was assumed that younger children have power per muscle mass similar to older children. Therefore it was concluded that for younger children, predicting peak power from lean thigh volume was appropriate. Lean thigh volume was determined using the method described by Martin et al. (2000). The thigh was modeled as two truncated cones. The circumferences at the thigh were measured at the proximal patella, the gluteal furrow, and at mid thigh. The skin-fold thickness was measured on the anterior and posterior sides and subtracted from the measured circumferences. For each cone, the volume was calculated using Equation 4.1.

$$Volume = \frac{\pi h}{3}(r_1^2 + r_1 r_2 + r_2^2) \quad (4.1)$$

where h is the height of the cone

r_1 is the proximal radius of the cone

r_2 is the distal radius of the cone.

The spreadsheet containing the calculations for lean thigh volume can be found in Appendix C.

Procedure

Participants rode a stationary ergometer at 5 different speeds (60, 75, 90, 105, and 120 rpm) at 10% of their predicted peak power. To maximize the children's success rate, a blocked protocol was chosen over a random protocol. Participants started at a cadence of 60 rpm, which was then increased in increments of 15 rpm, up to 120 rpm. Each trial lasted 15 s; the rest periods between trials lasted 20-60 s. The trial length and the rest periods were chosen to maximize performance success (defined as pedaling at the required target cadence), which was most critical in the youngest participants (Liu et al., 2003; Jensen & Korff, 2004). The time span of the rest periods was chosen with the goal of obtaining the participants' full attention, which could result in longer rest periods for the children. For children, rest periods were extended to up to 5 minutes, if requested by the child. Visual and auditory feedback were given via a cycling computer and a metronome, in order to maximize the probability that the participants were pedaling at the required target cadence. During testing, the performance of the participants was monitored. If a participant did not hit the target cadence during a particular condition, he/she was allowed to repeat this condition after the regular testing protocol had been completed.

Data Collection, Treatment, and Equipment

Experimental data were collected with the goal to describe a biomechanical model of pedaling. The segments of each lower limb combined with the crank were modeled as

5-bar linkages (Fregly & Zajac, 1996). Thus, this model consisted of two 5-bar linkages. Kinematic data were collected at 60 Hz, using a 5-camera Vicon 250 system (Oxford Metrics, UK). Pedal forces were collected at 600 Hz by means of a custom-made pedal with two tri-axial piezoelectric force sensors (Kistler, model 9251AQ01). Kinematic data and force data were low-pass filtered with no phase lag at cutoff frequencies of 10 Hz and 20 Hz respectively, using Butterworth filters.

Experimental joint centers were estimated from kinematic data. The center of the ankle joint was estimated from the coordinates of a marker placed on the lateral malleolus. The center of the knee joint was estimated from the coordinates of a marker placed on the lateral femoral epicondyle. The hip joint center was estimated from the coordinates of markers placed on the greater trochanter and the anterior superior iliac spine using a method described by Neptune and Hull (1995). Experimental angles were found through the use of a gradient-based optimization algorithm (`fminsearch`, Mathworks Inc., MI). This optimization algorithm found the joint positions that complied with the configuration constraints of the 5-bar linkage and differed minimally from the experimentally estimated joint centers. In the optimization procedure, the segment lengths were also optimized to further reduce this difference. The segment lengths were allowed to deviate up to 5% of the calculated mean. Based on these optimal joint positions and segment lengths, the angular positions were calculated. These positions were low-pass filtered at 20 Hz, using a Butterworth filter with zero phase lag. Angular velocities and accelerations were obtained by fitting the position data to cubic splines and analytical differentiation.

The analyzed revolutions were chosen based on two inclusion criteria: First, they had to be within ± 5 rpm of the target cadence. Second, the power produced by the ipsilateral leg had to be greater than 42.5% and smaller than 57.5% of the total power

output. Ideally, the power produced by the ipsilateral leg would be 50% of the total power output. However, bilateral asymmetry leads to deviations from this ratio. The consequence is that the ipsilateral leg delivers more or less than 50% of the total power to the crank. To avoid a confounding effect on the dependent variables, a limit of acceptable bilateral asymmetry was defined. A sensitivity analysis with regard to this limit of acceptable bilateral asymmetry was performed (see results section of this chapter).

Depending on how many revolutions within a trial met the inclusion criteria, the kinematic and force data of up to 5 revolutions were averaged resulting in one representative revolution per participant and condition. This average revolution was then used for a forward dynamics simulation. For a total of 6 trials (5 in the YC group and 1 in the OC group), there were no revolutions that met the inclusion criteria. For 1 OC and 2 YC, no revolutions met the inclusion criteria at 105 rpm. This was also the case for 2 YC at 60 rpm, and 1 YC at 120 rpm. These trials were eliminated from further analysis. The values for the dependent measures for these 6 trials were replaced by the group mean for the statistical analysis. Therefore, the minimum numbers of values contributing to a group mean of any dependent measure were 9 in the YC group. In the OC group, 7 values contributed to the group mean at 105 rpm, where 8 values contributed to the group means under the remaining conditions.

Forward Dynamics Simulation

A planar model of two-legged cycling actuated by muscle torques about the hip, knee, and ankle joints was developed (Fregly & Zajac, 1996). The positions of the hip and the crank center of rotation were constrained to be fixed in space, and therefore the model consisted of two 5-bar linkages and possessed 3 degrees of freedom. The crank angle and the right and left hip angles were used as the independent degrees of freedom. The shank and foot angles and angular velocities were constrained to satisfy the

kinematic constraint equations. The bicycle drive dynamics were modeled using an effective rotational resistive load and an effective rotational inertial load (Fregly, Zajac, & Dairaghi, 2000).

All anthropometric parameters of the model were modified for each individual participant. The experimentally obtained values for body mass and segmental lengths were used. Segmental mass proportions, the center of mass locations, and moments of inertia were estimated using the regression equations presented by Jensen (1989). A feedback linearization algorithm (Seth, McPhee, & Pandy, 2004) was used to find the tracking solution that resulted in the minimization of the differences between simulated and experimental data for each participant. A forward dynamics simulation was performed for each participant at each of the 5 cadences.

Dependent Variables

Muscular power contributions were calculated by decomposing the total power of the entire system. For the described model, the total power of the entire system can be described using Equation 4.1 (Kane & Levinson, 1985; Fregly & Zajac, 1996).

$$P = [M(\theta)\ddot{\theta} - V(\theta, \dot{\theta}) - G(\theta)]^T \cdot \dot{\theta} \quad (4.1)$$

where

the scalar P is the total power of the system

M is the 3x3 mass matrix of the system

θ is a 3x1 vector of angular positions

$\dot{\theta}$ is a 3x1 vector of angular velocities

$\ddot{\theta}$ is a 3x1 vector of angular accelerations

V is a 3x1 vector containing expressions that depend on angular velocities (centripetal and Coriolis forces)

G is a 3x1 vector containing expressions that depend on gravity

\cdot represents the dot product operation for two vectors

The total power of the system was decomposed into muscular and non-muscular components. First, the muscular contribution to the angular accelerations was found by setting to zero the contributions of gravitational, centripetal, and frictional forces to the angular accelerations. The muscular contribution to the total power of the system was found by setting V and G to zero in Equation 4.1. Using an analogous method, the muscular power contributions were further decomposed into the individual contributions of ankle, knee, and hip torques, which yielded the net power produced by each joint torque. These individual muscular power contributions were decomposed into the contributions to the power of the crank (crank power) and the power of the bicycle rider's limbs (limb power). The muscular contribution (ipsilateral muscular crank power) and the contribution of individual muscular joint powers to the mechanical power of the crank were found by setting the masses and moments of inertia of the feet, shanks, and thighs to zero. The muscular contribution and the contribution of individual muscular joint powers to limb power were found by setting the mass of the crank to zero. All power profiles were normalized with respect to the average power transferred to the crank over the entire crank cycle by all muscles of the ipsilateral limb, in order to allow for meaningful comparisons between participants.

Regarding the hypothesis that at high speeds, peak muscular joint power would be lower in children compared to adults (hypothesis 1), the normalized peak powers at each joint were calculated. To test this hypothesis, for each muscular net joint power, Age x Cadence ANOVAs were performed for peak muscular power at the hip, knee, and ankle joints.

In order to test hypotheses 2 and 3, the crank cycle was divided into four phases, extensor (EXT), flexor (FLEX), top (TOP), and bottom (BOT). These phases were defined according to Neptune, Kautz, and Hull (1997). EXT and FLEX were defined from 337° to 134° and 149° to 324° of the crank cycle, respectively. TOP and BOT were defined from 241° to 35° and 72° to 228° of the crank cycle, respectively.

To test the hypothesis that at high movement speeds, children would demonstrate a reduction in net muscular power during the extensor phase (hypothesis 2a), the normalized net muscular power was averaged across EXT, and an Age x Cadence ANOVA was performed. Regarding the hypothesis that children would compensate for the reduced net muscular power during EXT by producing more power during different regions of the crank cycle (hypothesis 2b), the normalized net muscular power was averaged across FLEX, TOP, and BOT. For each phase, an Age x Cadence ANOVA on net muscular power profiles were performed. In the remainder of this chapter, the phase during which children compensate for the reduced muscular power production during the extensor phase will be referred to as the compensatory phase.

To test the hypothesis that at high movement speeds the amount of direct or indirect delivery of muscular energy to the crank during the EXT would be lower in children than in adults (hypothesis 3a), the following power contributions were averaged across EXT: a) the direct contribution of knee power to crank power; b) the contribution of ankle power to limb power; and c) the contribution of hip power to limb power. Age x Cadence ANOVAs were performed for each of these power contributions. Regarding the hypothesis that at high movement speeds children would demonstrate a different muscular synergy during the compensatory phases when compared to adults (hypothesis 3b), Age x Cadence ANOVAs were performed for each of these power contributions during the compensatory phase.

When the sphericity-assumption of an ANOVA was violated (Huynh-Feldt's $\epsilon < 0.75$), the multivariate method (Wilks' Lambda) was used (Schutz & Gessaroli, 1987). In the case where Huynh-Feldt's $\epsilon > 0.75$, the univariate method was used and the degrees of freedom were adjusted accordingly. In cases where the Age x Cadence interaction of an ANOVA was significant, follow up one-way ANOVAs with age being the between subject factor were performed on each cadence level for the corresponding dependent measure. Effect sizes (ES) were used to describe and interpret pairwise comparisons (Cohen, 1988). The type I error for all statistical analyses was .05.

RESULTS

Tracking Results

Before the statistical analyses were performed the tracking error was quantified by calculating the differences between the simulated and experimental data. This was done for angular positions, angular velocities and for horizontal and vertical force profiles. For each pair (simulated and experimental) of data profiles we calculated the relative absolute deviation (RAD – equation 4.2).

$$RAD = 100 \cdot \frac{\frac{1}{n} \left[\sum_{i=1}^n |Y_{exp_i} - Y_{sim_i}| \right]}{range(Y_{exp})} \% \quad (4.2)$$

where

Y_{exp_i} is the experimentally obtained data profile at the i^{th} sample

Y_{sim_i} is the simulated data profile at the i^{th} sample

n is the number of samples for each profile

Averaged across all trials within each group, the tracking errors were 0.97% for each age group. The tracking errors for all participants and all conditions can be found in Appendix J.

Sensitivity Analysis for Bilateral Asymmetry

Before the data were analyzed, a sensitivity analysis was performed to quantify the effect of the acceptable limits of bilateral asymmetry on the dependent variables. For this sensitivity analysis, the trial with the greatest accepted bilateral asymmetry – observed in a member of the YC group at 60 rpm – was chosen. For this trial, the reaction forces at the pedal were scaled so that the power produced by the ipsilateral leg was 50%, 42.5%, and 57.5% of the external power output. The deviations of the dependent

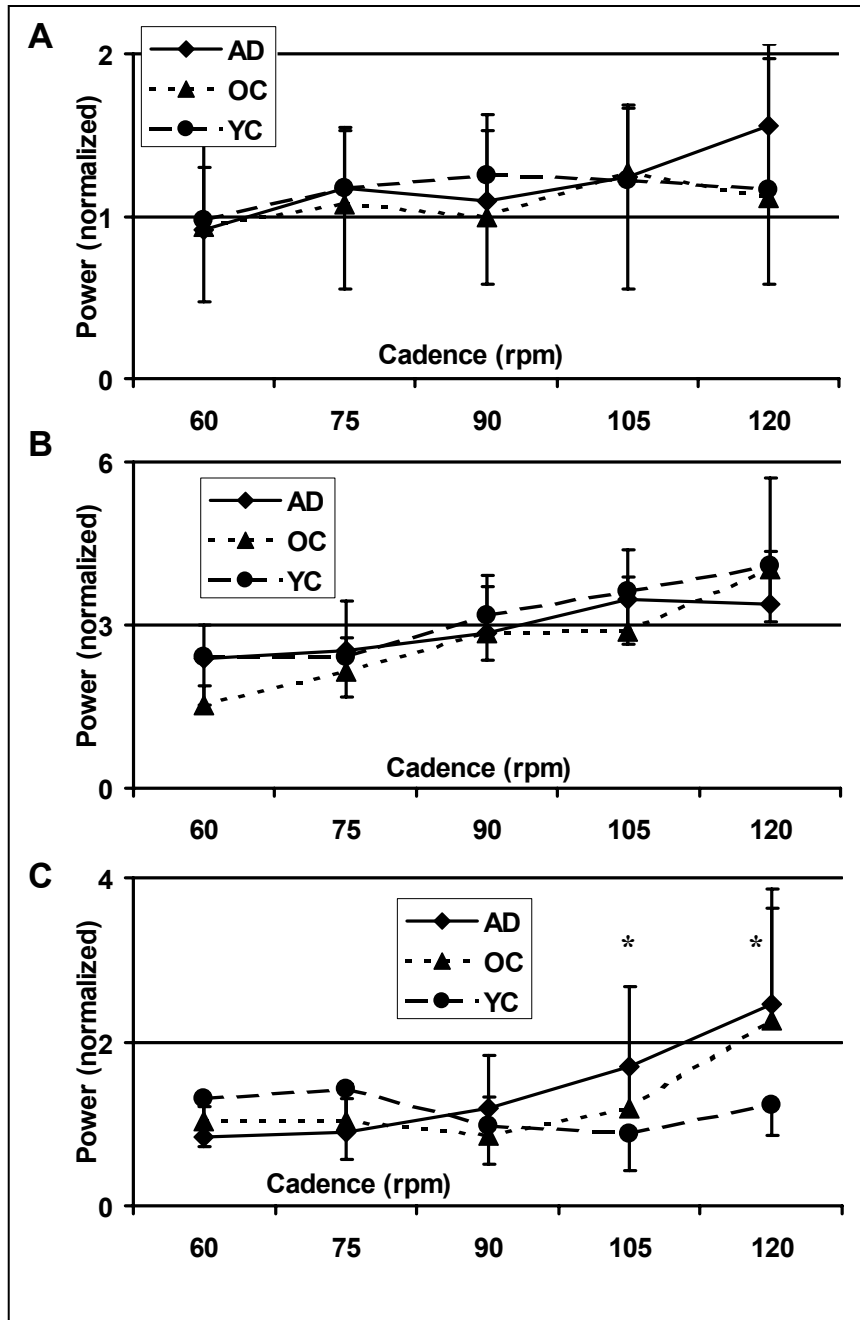
measures at the 42.5% and 57.5% conditions from those at the 50% condition were always smaller than 50% of one standard deviation of the mean in the AD group for the corresponding dependent variables. Therefore, the range of permitted bilateral asymmetry was considered acceptable and did not confound the analysis. The standard deviation of the AD group was chosen as a reference because in this group, the inter-subject variability was smallest for most of the dependent variables. Therefore, this standard can be considered conservative which emphasizes the negligibility of the possible confound of bilateral asymmetry in this study. The details on this sensitivity analysis are given in Appendix H.

Peak Power – Hypothesis 1

Peak power at the hip joint was dependent on age and cadence. The hypothesized Age x Cadence interaction for peak power was significant (Wilks' Lambda=.441, $F(8,42)=2.65$, $p=.019$). Follow up ANOVAs revealed that the effect of age on peak muscular power at the hip joint was significant at 105 rpm and 120 rpm. The analysis of the effect sizes revealed that the Age x Cadence interaction for peak muscular power at the hip joint was most apparent for those comparisons that included the YC group. The increase in cadence resulted in a reversal of the observed differences in peak power at the hip joint (Figure 4.2C). At the slow movement speeds, YC's peak hip joint power was greater than in OC and AD. The effect sizes describing the differences between YC and AD and YC and OC at these cadences were large and moderate, respectively (see Table II in Appendix I). At the higher movement speeds (105 rpm and 120 rpm), YC produced less peak power at the hip joint when compared to OC and AD (Figure 4.2C). The effect sizes for these comparisons were moderate or large, but positive indicating that peak hip joint power was greater in AD and OC when compared to YC. At the ankle and knee joints, the Age x Cadence interactions and the main effects for age were non-significant

($F(8,96)=0.75$, $p=.640$ for the ankle joint; $F(8,96)=1.42$, $p=.220$ for the knee joint)
(Figures 4.2A and 4.2B).

Figure 4.2. Effect of cadence on peak power at the ankle (A), knee (B), and hip (C) joints. The symbol “*” indicates a significant age-effect at the corresponding cadence. Means and standard deviations are plotted for adults (AD), older children (OC), and younger children (YC).



Net Muscular Power – Hypotheses 2a and 2b

Hypothesis 2a – net muscular power during EXT

Age-related differences in net muscular power production during EXT were dependent on cadence. The hypothesized Age x Cadence interaction was significant (Wilks' Lambda=.413, $F(8,42)=2.92$, $p=.011$). Follow up ANOVAs revealed that at all cadences, the age effect was statistically significant (see Figures 4.3 and 4.4). At all cadences the effect sizes describing the difference in net muscular power during EXT between AD and YC were large, indicating that AD produced more muscular power during EXT than YC (Table I2 – Appendix I). At all cadences below 120 rpm, the effect sizes describing the difference between YC and OC were moderate or small. Only at 120 rpm was the effect size large, indicating that at this cadence OC produced significantly more muscular power than YC during EXT. The effect sizes comparing AD and OC were large at all cadences below 120 rpm, indicating that AD produced significantly more muscular power than OC. Interestingly, at 120 rpm the effect size describing the difference between AD and OC was small, indicating a similar muscular power production during EXT for these two groups. All effect sizes describing the age group differences in muscular power during EXT can be found in Table I2 in Appendix I.

Hypothesis 2b – net muscular power during FLEX, TOP, and BOT

The Age x Cadence interactions for net muscular power were significant during TOP and BOT (Wilks' Lambda=.405, $F(8,42)=3.00$, $p=.009$ for TOP and Wilks' Lambda=.478, $F(8,42)=2.34$, $p=.035$ for BOT). However, only during TOP did children produce significantly greater net muscular power than AD (see Figures 4.3 and 4.5). As a result, TOP was considered the compensatory phase, during which children compensated for the reduced power production during EXT. During TOP, the age effect was

significant only at high movement speeds (90 rpm, 105 rpm, and 120 rpm, see Figure 4.5). The effect sizes describing differences between YC and AD as well as OC and AD at these cadences were large (Table I3 – Appendix I). This indicated that at high movement speeds, children produced more net muscular power during TOP when compared to adults. The effect sizes describing the differences between YC and OC were small or moderate at all cadences.

Figure 4.3. Net muscular power for adults (AD), older children (OC), and younger children (YC) at 5 different cadences. The data for each age group are averaged across participants.

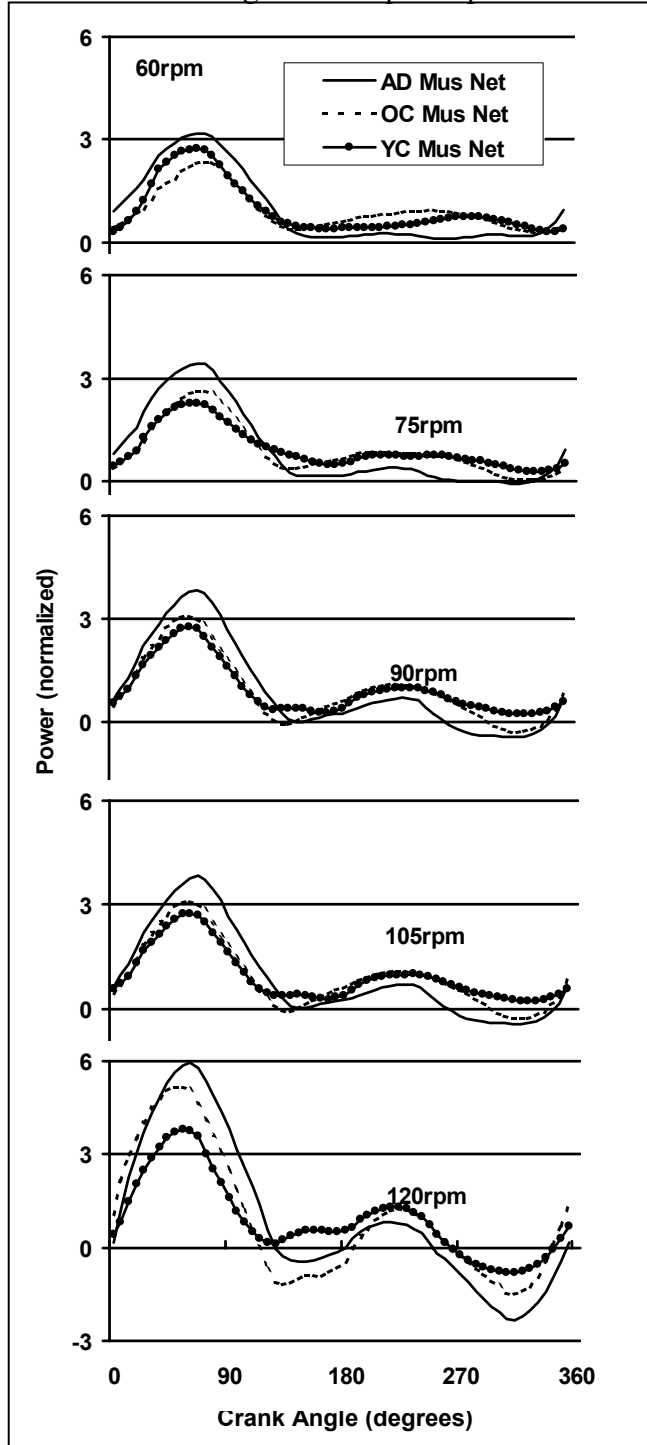


Figure 4.4. Effect of age and cadence on net muscular power during the extensor phase (EXT). The age-effect was statistically significant (“*”) at all cadences. Means and standard deviations are plotted for adults (AD), older children (OC), and younger children (YC).

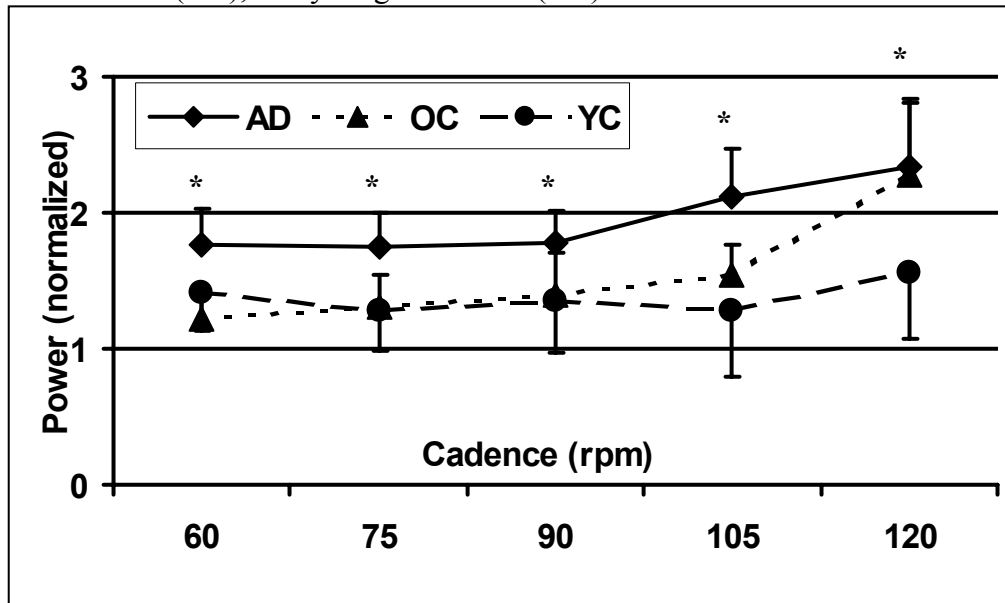
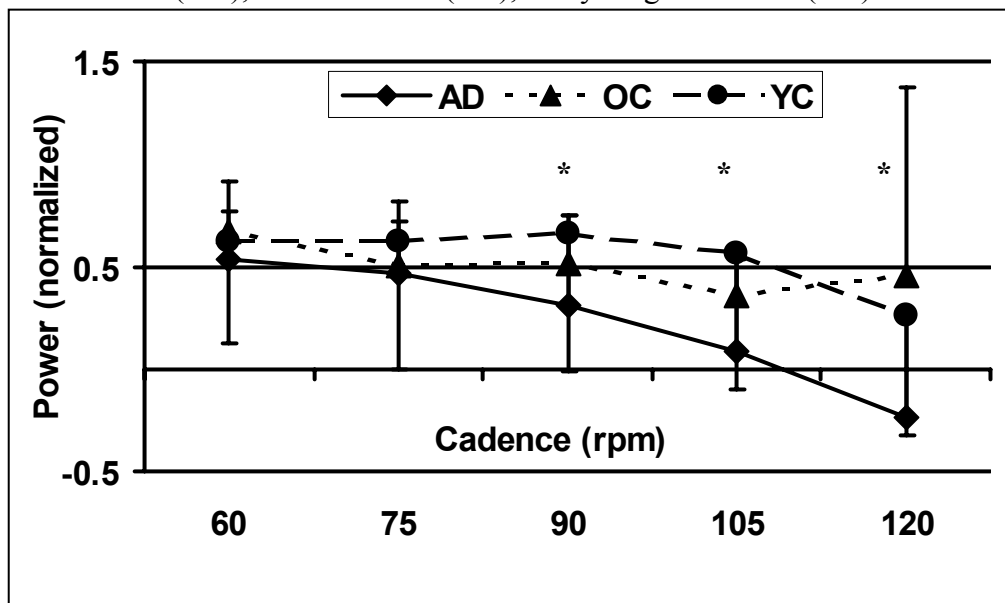


Figure 4.5. Effect of age and cadence on net muscular power during the top phase (TOP). The symbol “*” indicates a significant age-effect at the corresponding cadence. Means and standard deviations are plotted for adults (AD), older children (OC), and younger children (YC).



Muscular Synergy – Hypotheses 3a and 3b

Hypothesis 3a – muscular synergy during EXT

Age-related differences in the hip power contribution to limb power during EXT were dependent on movement speed (Wilks' Lambda=.470, $F(8,42)=2.40$, $p=.031$). Follow up ANOVAs revealed that during EXT, the age effect for the hip power contribution to limb power was only significant at 105 rpm. The effect sizes revealed that there was a cadence dependent reversal in the differences between children and adults. At slow movement speeds (60 rpm and 75 rpm), children's hip power contributions to limb power were slightly greater than those of adults (see Figures 4.6 and 4.12). The effect sizes describing these differences were small ($ES < 0.43$). At higher movement speeds (90 rpm, 105 rpm, and 120 rpm), adults' hip power contributions to limb power were greater when compared to children. This effect was most apparent for the AD-YC comparison. The effect sizes describing the differences between these groups were moderate and large at these cadences ($0.71 < ES < 1.39$). The effect sizes describing the OC-AD comparison were moderate or small ($0.33 < ES < 0.54$). This indicates that during EXT, adults delivered more energy generated at the hip joint to the limbs only at high movement speeds, and that this effect was most pronounced when AD were compared to YC. It is interesting to note that during EXT at high movement speeds (105 rpm and 120 rpm), the hip power contribution to limb power was negative in YC (see Figures 4.6 and 4.12). For OC, the hip power contribution to limb power was negative only at 120 rpm. The negative values imply that during EXT at the high movement speeds, children's hip muscles absorbed energy from the limbs (rather than delivering it to the limbs).

The effect of age on muscular power absorbed from the limbs (and transferred to the crank) by the ankle torque was dependent on cadence (Wilks' Lambda=.481,

$F(8,42)=2.32$, $p=.037$). Follow up ANOVAs revealed that the age effect was significant only at 105 rpm. In spite of this significant Age x Cadence interaction during EXT, the age group differences were largely independent of cadence during this phase of the crank cycle (see Figures 4.7 and 4.13). At all cadences, the ankle power contribution to limb power was greater in adults when compared to children. The effect sizes describing the differences between children and adults were moderate or large at all cadences ($0.56 < ES < 1.89$), the only two exceptions being the AD-OC and AD-YC comparisons at 75 rpm ($ES=0.19$ and $ES=0.45$), see Table I4, Appendix I). The effect sizes describing the difference between YC and OC were small or moderate at all cadences ($ES < 0.62$).

The Age x Cadence interaction for the direct knee power contribution to crank power during EXT failed statistical significance (Wilks' Lambda=.557, $F(8,42)=1.78$, $p=.118$) (see Figures 4.8 and 4.14).

Figure 4.6. Effect of age and cadence on the hip power contribution to limb power during the extensor phase (EXT). The symbol “*” indicates a significant age-effect at the corresponding cadence. Means and standard deviations are plotted for adults (AD), older children (OC), and younger children (YC).

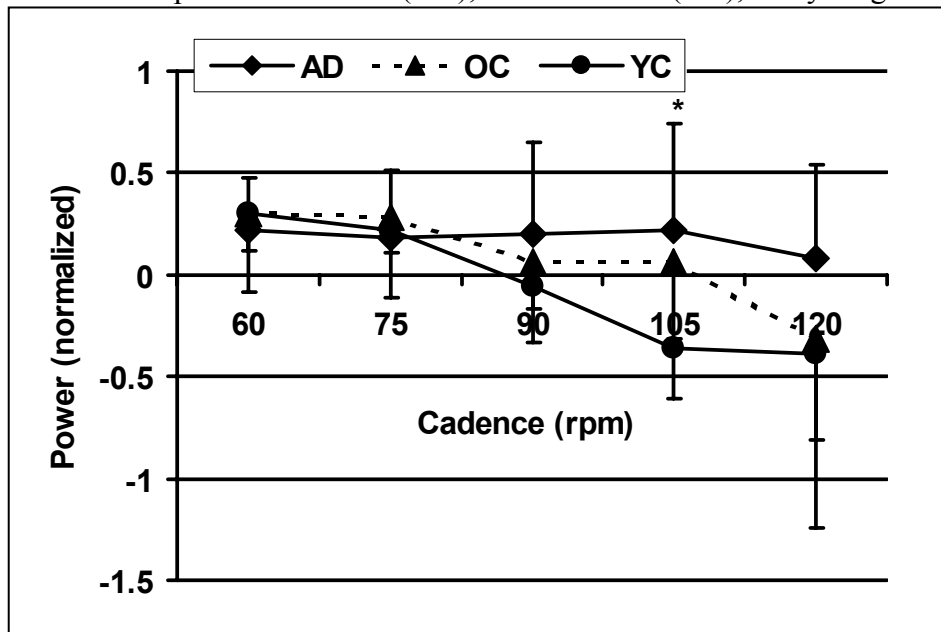


Figure 4.7. Effect of age and cadence on the ankle power contribution to limb power during the extensor phase (EXT). The negative numbers indicate that energy is absorbed from the limbs and transferred to the crank. The symbol “*” indicates a significant age-effect at the corresponding cadence. Means and standard deviations are plotted for adults (AD), older children (OC), and younger children (YC).

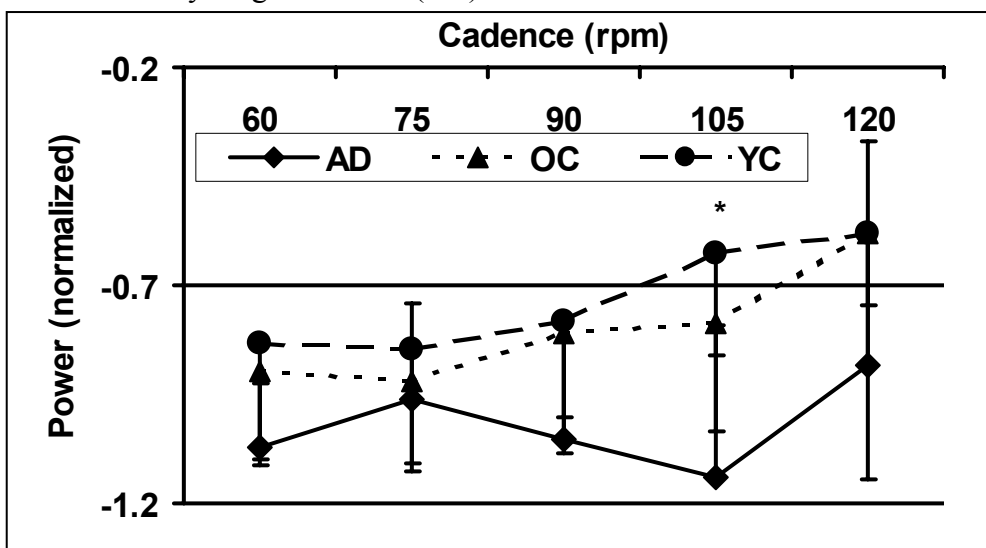
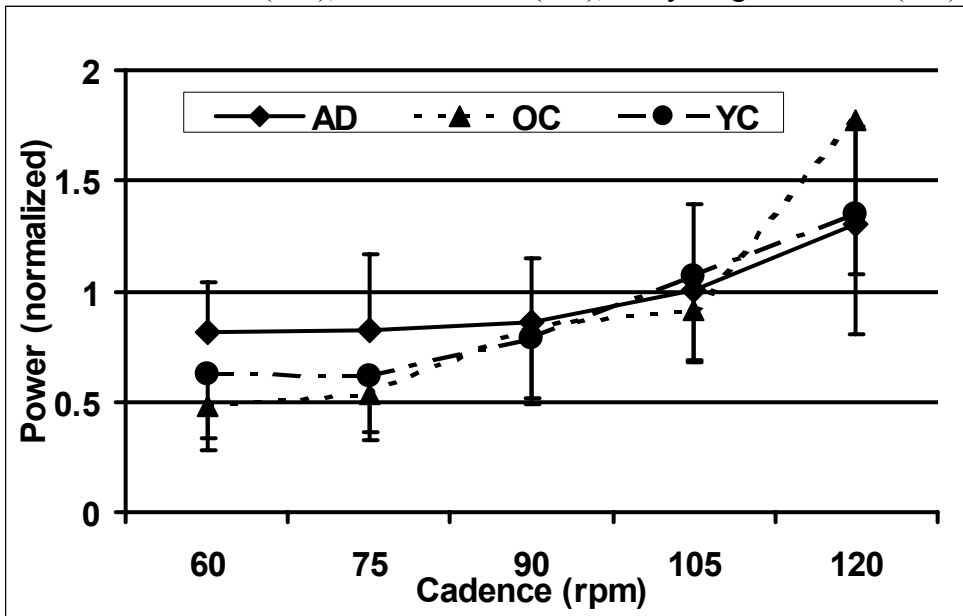


Figure 4.8. Effect of age and cadence on the knee power contribution to crank power during the extensor phase (EXT). The Age x Cadence interaction was statistically non-significant. Means and standard deviations are plotted for adults (AD), older children (OC), and younger children (YC).



Hypothesis 3b – muscular synergy during the compensatory phase

Children compensated for the reduced muscular power production at high movement speeds during EXT by increasing the knee power contribution to crank power during the compensatory phase (TOP) (see Figures 4.11 and 4.14). For the hip and ankle power contributions to limb power during TOP, the Age x Cadence interactions failed statistical significance (Wilks' Lambda=.640, $F(8,42)=1.31$, $p=.264$ for the hip and Wilks' Lambda=.565, $F(8,42)=1.73$, $p=.119$ for the ankle). Figures 4.9 and 4.10 show the effect of age and cadence on the hip power contribution to limb power and the ankle power contribution to limb power, respectively during TOP.

During TOP, age group differences in the direct contribution of knee joint power to crank power were dependent on cadence (Wilks' Lambda=.392, $F(8,42)=3.14$, $p=.007$). Follow up ANOVAs revealed that the age effect was significant at the three fastest cadences (90 rpm, 105 rpm, and 120 rpm). At these cadences, the effect sizes describing the differences between adults and children were large ($ES>1.71$), indicating that children's knee power contribution to crank power was significantly greater than that of adults (see Figures 4.11 and 4.14). The effect sizes describing the difference between OC and YC were small at all cadences ($ES<0.38$, see Table I5, Appendix I).

Figure 4.9. Effect of age and cadence on the hip power contribution to limb power during the top phase (TOP). The Age x Cadence interaction was statistically non-significant. Means and standard deviations are plotted for adults (AD), older children (OC), and younger children (YC).

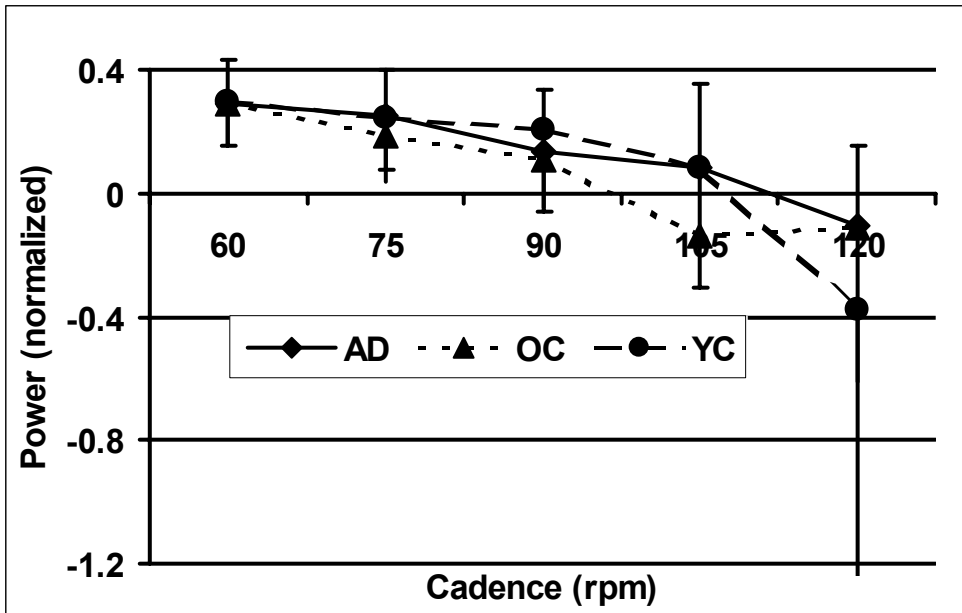


Figure 4.10. Effect of age and cadence on the ankle power contribution to limb power during the top phase (TOP). The Age x Cadence interaction was statistically non-significant. Means and standard deviations are plotted for adults (AD), older children (OC), and younger children (YC).

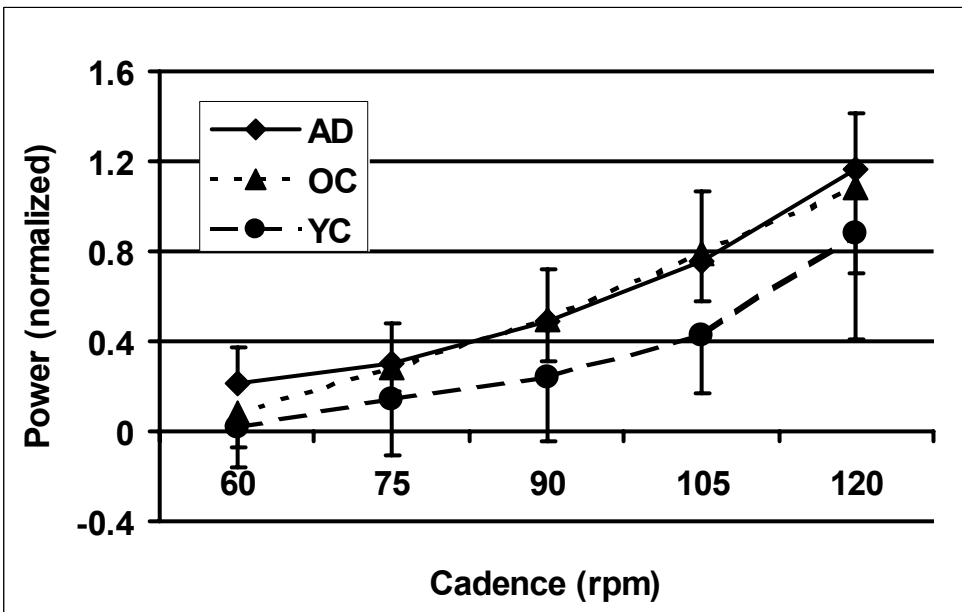


Figure 4.11. Effect of age and cadence on the knee power contribution to crank power during the top phase (TOP). The symbol “*” indicates a significant age-effect at the corresponding cadences. Means and standard deviations are plotted for adults (AD), older children (OC), and younger children (YC).

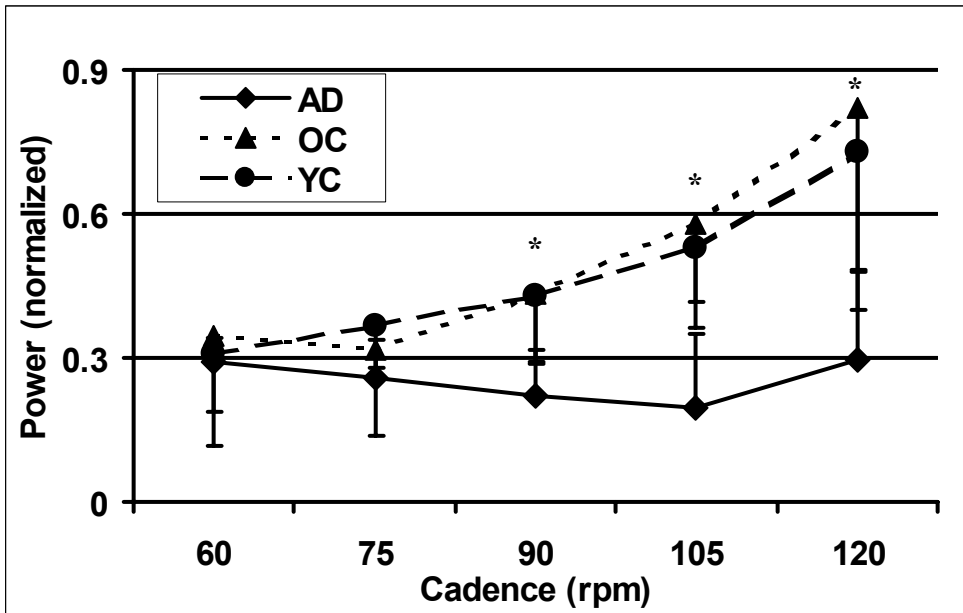


Figure 4.12. Contribution of hip power to limb power for adults (AD), older children (OC), and younger children (YC) at 5 different cadences. The data for each age group are averaged across participants.

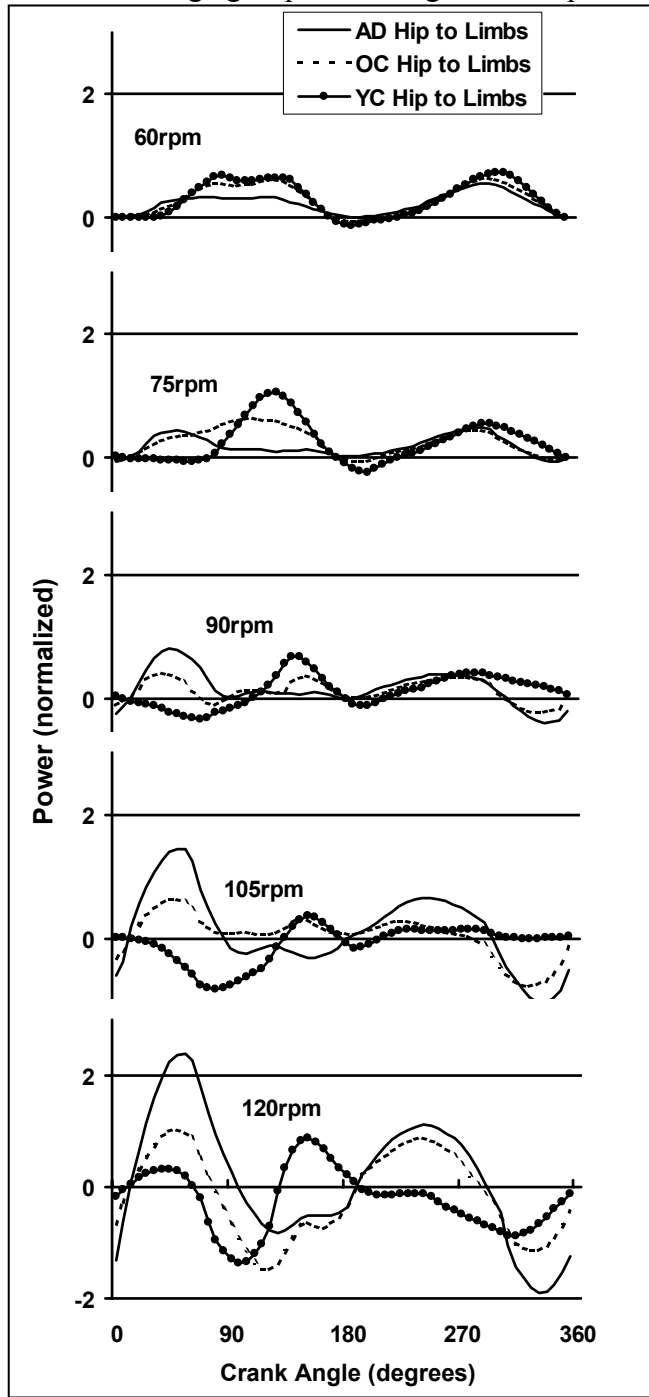


Figure 4.13. Ankle power contribution to limb power for adults (AD), older children (OC), and younger children (YC) at 5 different cadences. The data for each age group are averaged across participants.

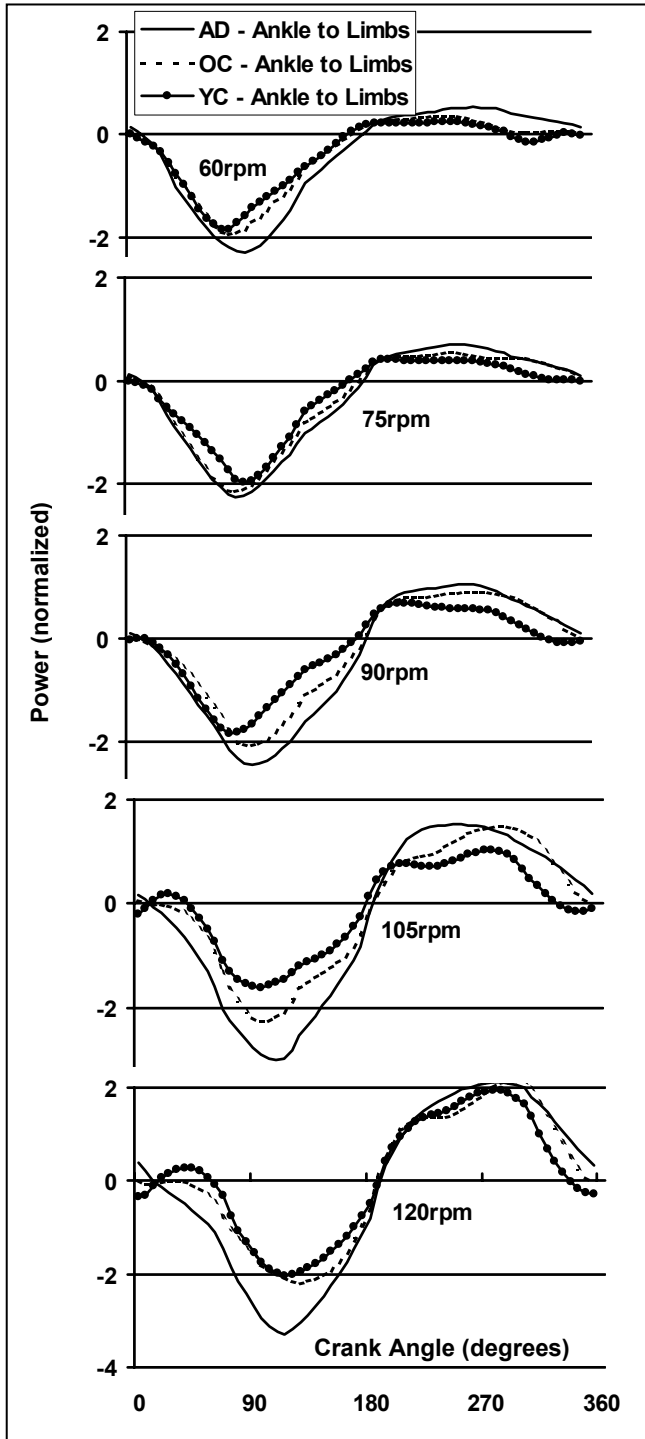
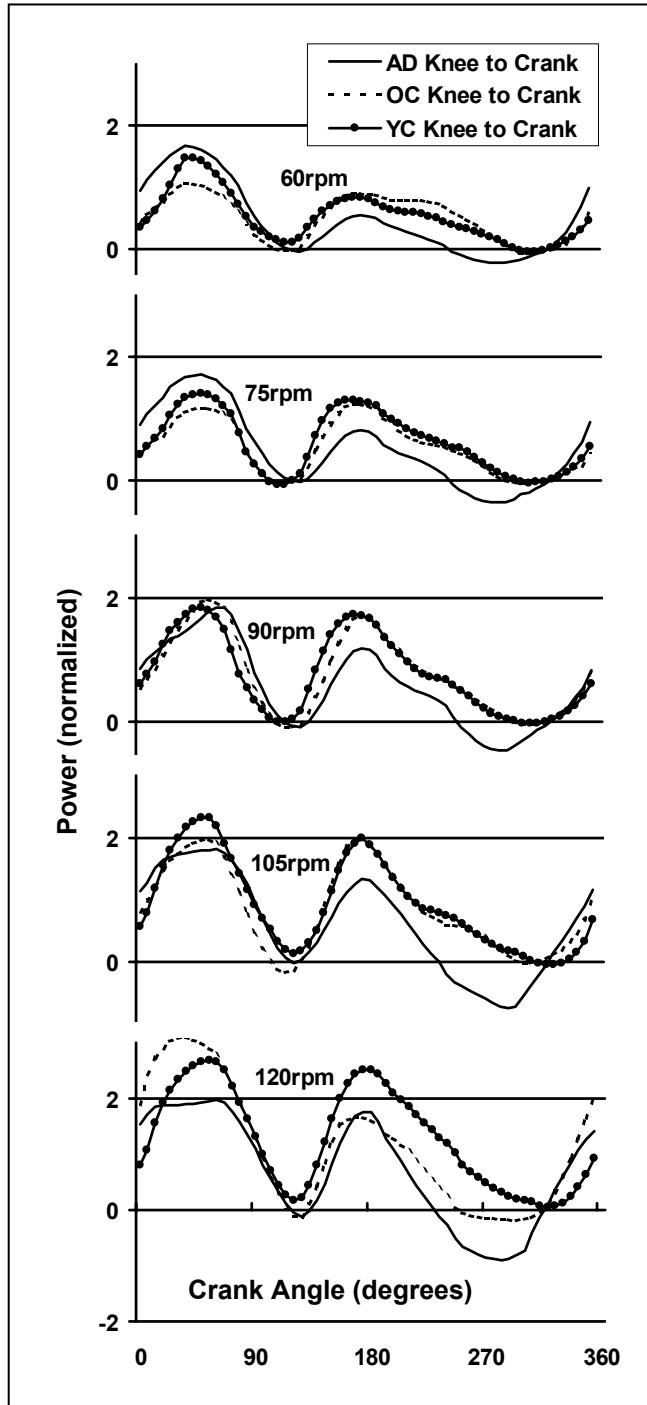


Figure 4.14. Direct knee power contribution to crank power for adults (AD), older children (OC), and younger children (YC) at 5 different cadences. The data for each age group are averaged across participants.

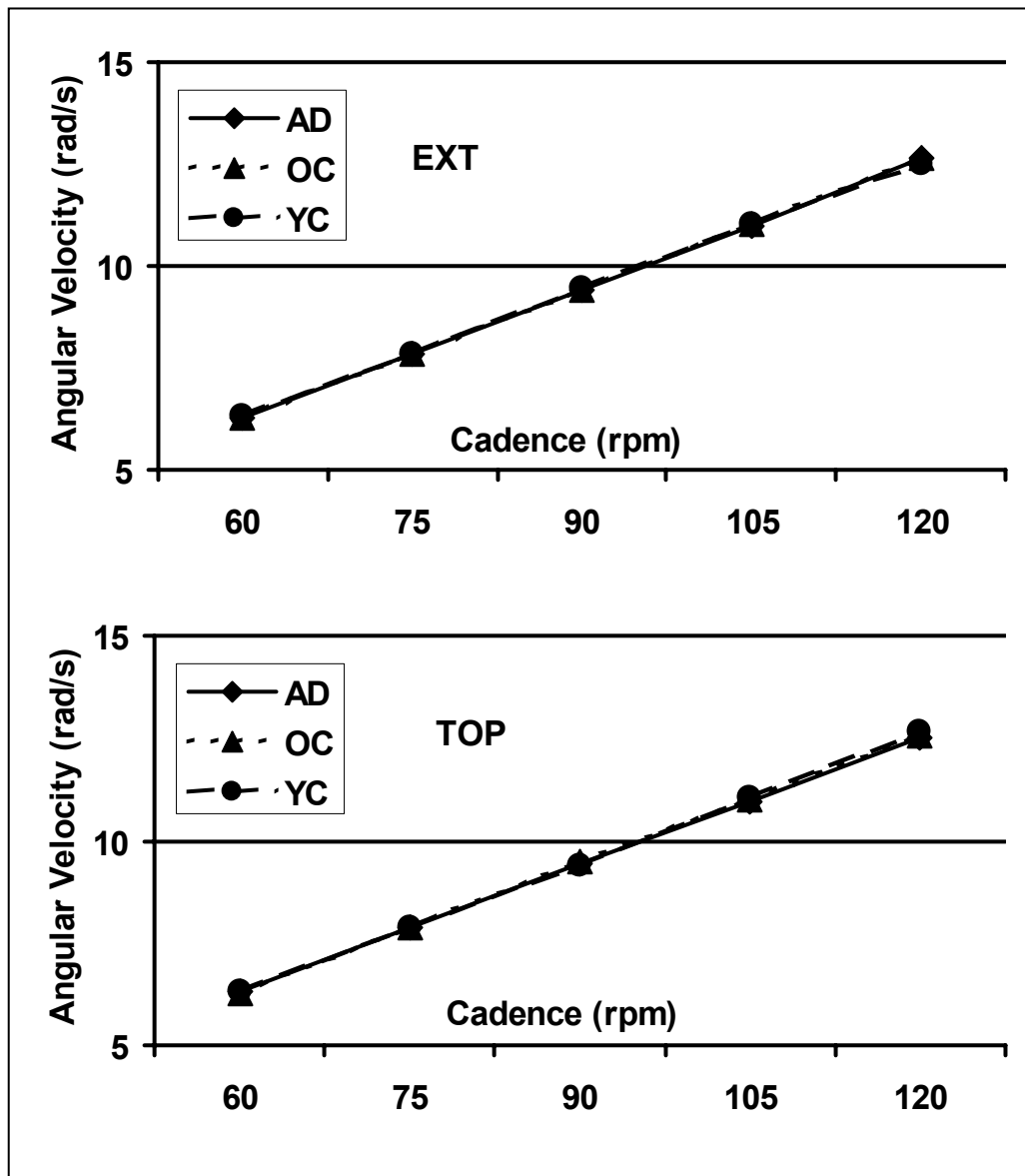


Crank Angular Velocity Profiles

In an additional analysis, we tested whether the observed differences in muscular power production were accompanied by behavioral differences. It is important to distinguish between age-related differences in adaptability on a behavioral and neuromuscular level, because adaptability on these two levels may occur on different developmental schedules (Chao et al., 2002; Jensen & Korff, 2004). In order to test whether the observed differences in muscular power production resulted in a different movement pattern, we performed Age x Cadence ANOVAs on crank angular velocities during EXT and TOP.

No age-related differences in crank angular velocities were found. During both, EXT and TOP, the main effects for age were non-significant ($F(2,24)=0.381$, $p=.687$ for EXT and $F(2,24)=1.451$, $p=.254$ for TOP) (see Figure 4.15). The Age x Cadence interactions also failed statistical significance (Wilks' Lambda=.734, $F(8,42)=0.876$, $p=.544$ for EXT and Wilks' Lambda=.648, $F(8,42)=1.269$, $p=.285$ for TOP) (see Figure 4.15). It was concluded that the observed neuromuscular differences between age groups were not accompanied by behavioral differences.

Figure 4.15. Effect of age and cadence on the crank angular velocities during the extensor (EXT) top (TOP) regions. Means and standard deviations are plotted for adults (AD), older children (OC), and younger children (YC).



DISCUSSION

The results of the present investigation demonstrate that the neuromuscular mechanism which children use to voluntarily adapt to changes in movement speed is different compared to adults. At high movement speeds, children demonstrated reduced muscular joint powers at the hip joint which led to a weaker muscular synergy during the power-producing phase. Children compensated by delivering more muscular energy directly to the crank in the phase during which the pedal is propelled through top dead center.

The first hypothesis was posed to test if at high movement speeds, children, compared to adults, would produce less maximum muscular power at the ankle, knee and hip joints. This hypothesized relationship was only present at the hip joint indicating a joint dependence of this effect. In conformity with hypotheses 2a and 3a, the reduction in peak muscular joint powers was accompanied by a reduction in net muscular power during the extensor phase and a weaker synergy between hip extensors and plantarflexors. Hypotheses 2b and 3b were posed to determine how children would compensate for the reduced muscular power production during the extensor phase. As hypothesized, children demonstrated an increase in muscular power production during the phase in which the pedal is propelled through top dead center by using their knee extensors to deliver more muscular energy directly to the crank.

The age-related differences in the mechanical construction of the pedaling task were most apparent in the younger children. They demonstrated a weaker synergy between hip extensors and plantarflexors at high movement speeds during the power-producing phase than older children or adults. It is important to note that in YC, energy was *absorbed from* (and not delivered to) the limbs by the hip extensors at high

movement speeds. In these children, the hip extensor-plantarflexor synergy was completely missing during this phase, and they did not take any advantage of this synergy to facilitate energy delivery to the crank at high movement speeds.

As the averaged normalized muscular power across the crank cycle was equal for all participants, children needed to compensate for the reduced muscular power production during the extensor phase by an increased muscular power production during a different region of the crank cycle. Children demonstrated an increase in muscular power production during the phase in which the pedal is propelled through top dead center. This increase in muscular power was achieved by more direct muscular energy delivery by the knee extensors to the crank. We can conclude that at high movement speeds, children compensated for their lack of inter-muscular coordination (weaker inter-muscular synergy) by an increase in direct muscular energy delivery. The fact that this compensation occurred in the phase during which the pedal is transitioned through top dead center, suggests that during this phase children's knee extensors produced larger forces that are directed horizontally. As there is some evidence that control over the extensor muscles is acquired earlier during childhood than control over flexor muscles (Roncesvalles, Woollacott, Brown, & Jensen 2004; Yang, Stephens, & Vishram, 1998), a greater extensor control may be the reason for children compensating during TOP and not during BOT or FLEX (during which more flexor activity would be required). This compensatory strategy may be energetically more expensive. Bearing in mind that during TOP the knee joint is almost fully flexed (and therefore the vasti muscles are lengthened), it is possible that this force production occurred on the descending (and therefore an unfavorable) section of the force length curve of the vasti muscles. Assuming that during the extensor phase (during which children produce less power) the vasti fiber lengths are

on a more favorable section on the force length curve, the children's compensatory strategy may result in increased energy expenditure and therefore less efficiency.

Although our results suggest that children compensated for reduced muscular power production during EXT by increasing direct muscular power contributions to crank power, it cannot be fully ruled out that indirect energy transfer was also used as a compensatory mechanism. Although no age-related differences in the ankle power contribution to limb power were found during TOP, it is possible that differences in the contributions of individual muscles exist. Neptune et al. (2000) demonstrated that during TOP, the plantarflexors and dorsiflexors are co-active and have opposite effects. While the dorsiflexors absorb energy from the limbs, the plantarflexors deliver energy to the limbs. This mechanism cannot be revealed in an analysis of net muscular power at the ankle which is a limitation of the torque driven model.

The findings of the present investigation have important implications for teachers, coaches, and therapists, because they suggest that it is a lack of intermuscular coordination rather than muscular power production per se that limits the range of movement speeds at which children can perform the task successfully. A limitation to this speculation is the fact that we analyzed only successful trials. Therefore, it is possible that children *chose* to construct the task differently at high movement speeds. However, previous research has shown that 120 rpm is close to children's performance limits (Chao et al., 2002; Liu et al., 2003), and we can assume that scaling up the task close to this limit would reduce the number of possible solutions of the task sufficiently to evoke the observed behavior.

The results of this investigation confirm and extend previous findings about differences in voluntary adaptive skill performance between children younger and older than 7 years of age. In older children, the hip power contribution to limb power was

significantly greater than in younger children during EXT. On the other hand the YC-OC differences with respect ankle power contributions to limb power were comparatively small. Together, these findings suggest that in older children the energy delivered by the hip extensors to the limbs was not yet fully used for synergistic energy generation to the crank. We can speculate that an adult-like synergy begins to emerge between 6 and 9 years of age, bearing in mind that we found no hip extensor-plantarflexor synergy in YC at high speeds. This stands in agreement with previous findings that there are significant changes in the neuromuscular synergies between the ages of 6 and 9 years of age (Chao et al., 2002). Chao et al. (2002) demonstrated that children older than 7 years of age are more likely to show an organized response in terms of muscle activation patterns in response to cadence changes in pedaling than children younger than 7 years of age. Both age groups had the same level of bicycle riding experience, thus the observed differences were age-related and not experience-related. The results of the present investigation confirm these results and extend them by an explicit attribution of the observed differences between younger and older children to age-related differences in the strength of the synergy between hip extensors and plantarflexors. This is an important step toward understanding the mechanisms that lead to previously observed differences in muscle activation patterns between 4 and 10 years of age (Chao et al., 2002).

The results of the present investigation also allow for a generalization from the emergence of the reactive adaptive capacities to the voluntary adaptive capacities in children. Where in this investigation participants were asked to change voluntarily a parameter (movement speed) of the task (pedaling), reactive adaptation is necessary when an external influence is imposed on the system. Shumway-Cook and Woollacott (1985), as well as Sundermier, Woollacott, Roncesvalles, and Jensen, (2001), demonstrated significant differences in muscular synergies between children younger and older than 7

years of age in response to externally imposed balance perturbations. Our findings that voluntary adaptations improve at 7 years of age are therefore in agreement with those on reactive adaptations. The results of the present investigation in combination with those of Shumway-Cook and Woollacott (1985) and Sundermier et al., (2001) suggest that muscular synergies for both reactive and voluntary adaptations change considerably at around 7 years of age.

The fact that the greatest differences in muscular power production were seen at the hip joint allows us to make another interesting link to a study which investigated the reactive capacity for children to adapt. Roncesvalles et al. (2004) demonstrated that as a response to balance perturbations, 9-year-old children demonstrate greater muscular activity and flexor torques at the hip than 5-year-old children. This increased hip flexor activity was accompanied by a greater success rate. The results of the present investigation hint at the generalizability of the relationship between muscular force production at the hip and performance success from reactive to voluntary adaptations and their development during childhood. Even though not specifically tested, it can be speculated that the observed reduction in muscular power generation at the hip and the weaker hip extensor-plantarflexor synergy is a possible contributor to the reduced rate of children's success at high movement speeds (Chao et al., 2002). However, the data do not provide incontrovertible support for this speculation, because only successful revolutions were analyzed.

Another possible source for the weaker synergy between hip extensors and plantarflexors is the children's inability to sufficiently stiffen the ankle joint to allow for an efficient transfer of muscular energy from the limbs to the crank. However, the fact that no age-related differences in peak power at the ankle joint were found suggests that children were able to generate sufficient muscular power at the ankle joint, even at high

movement speeds. A limitation to this conclusion is that differences in the degree of co-contraction of plantarflexors and dorsiflexors could also contribute to age-related differences in ankle joint stiffness. Future research should be aimed at investigating the reduced hip extensor-plantarflexor synergy on a muscular level and at specifically attributing this reduced synergy to children's failure in performance at high movement speeds.

Finally, the results of the present investigation extend our knowledge about the relationship between adaptation on a behavioral and a neuromuscular level. Jensen and Korff (2004) investigated children's response to voluntary changes in movement speed in terms of kinematic variability. Their results indicate that at moderate and moderately high speeds (60 rpm-100 rpm), children between 4 and 14 years of age adapt in an adult-like fashion. The results of the present investigation confirm these results by demonstrating that age-related differences in muscular power and its mechanical construction are small or non-existent at 60 rpm and 75 rpm. In addition, these results extend the findings by Jensen and Korff (2004) in two ways: First, the range of tested speeds was greater in the present investigation. Pedaling at 120 rpm is close to the performance limit of younger children. The fact that the greatest age-related differences were found at the highest movement speeds allows us to conclude that an adult-like adaptation to changes in movement speed is only possible if children pedal well below their performance limits. Second, the level of analysis included kinetic variables making possible inferences about neuromuscular synergies, where Jensen and Korff (2004) investigated adaptability on a behavioral level (i.e., in terms of kinematics). It is of particular significance that children adapt in an adult-like fashion on a behavioral level when asked to pedal at 100 rpm (Jensen & Korff, 2004), whereas in the present investigation large differences in the neuromuscular synergy are seen at similar cadences (i.e., 90 rpm and 105 rpm). By

showing that age-related differences in muscular power production are not accompanied by differences in the behavior (crank angular velocity) we demonstrated that the analysis on a behavioral level does not necessarily reveal neuromuscular mechanisms that lead to differences (or similarities) in movement behavior and adaptation. This notion has implications for teachers, coaches, and therapists, who are most often limited to an analysis of observable behavior.

In summary, the results of this study revealed age-related differences in voluntary adaptive skill in terms of muscular power production. At high movement speeds, maximum muscular power at the hip joint was reduced in children when compared to adults. During the extensor phase, a reduction in indirect energy transfer was observed in children when compared to adults. Children compensated for this by delivering more muscular energy directly to the crank during the phase that transitions the pedal through top dead center. These results suggest that it is the ability to efficiently take advantage of the transfer of segmental energy (the strength of the muscular synergy) that leads to age-related differences in voluntary adaptation, rather than a reduction in muscular power generation per se. Children compensated for the lack of inter-muscular coordination by direct muscular energy delivery to the crank using their knee extensors which is possibly energetically more costly. The results extend our knowledge by describing children's capacity to adapt over a broad range of task demands and by attributing observed overall differences to a specific muscular synergy. These findings are important because they increase our knowledge about factors that lead to age-related improvement in adaptive skills and give us hints about possible factors that limit the range of task demands to which children can adapt. Future research should be aimed at using this information to determine the factors that lead to performance failure at high movement speeds, and to further illuminate the source of the observed differences. In particular, it is of interest to

ascertain why younger children demonstrate a reduction in hip joint power. Possible explanations are differences in muscle-intrinsic properties (Asai & Aoki, 1996; Lexell, Sjoström, Nordlund, & Taylor, 1992) or in recruitment strategies (Gibbs, Harrison, & Stevens, 1997). It is also of interest how children's knee extensors compensate for the reduced power production at the hip joint. One could speculate that children use the power producing monoarticular vasti muscles rather than the bi-articular rectus femoris which is responsible for fine-tuning the movement (Jacobs & van Ingen Schenau, 1992; Neptune et al., 2000). Musculo-skeletal modeling techniques will be helpful in answering these questions.

REFERENCES

- Asai, H., & Aoki, J. (1996). Force development of dynamic and static contractions in children and adults. *International Journal of Sports Medicine*, 17, 170-174.
- Chao, P., Rabago, C., Korff, T., & Jensen, J. L. (2002). Muscle activation adaptations in children in response to changes in cycling cadence [Abstract]. *Journal of Sport & Exercise Psychology*, 24(Suppl.), S42-S43.
- Fregly, B. J., & Zajac, F. E. (1996). A state-space analysis of mechanical energy generation, absorption, and transfer during pedaling. *Journal of Biomechanics*, 29, 81-90.
- Fregly, B. J., Zajac, F. E., & Dairaghi, C. A. (2000). Bicycle drive system dynamics: theory and experimental validation. *Journal of Biomechanical Engineering*, 122, 446-452.
- Gibbs, J., Harrison, L. M., & Stephens, J. A. (1997). Cross-correlation analysis of motor unit activity recorded from two separate thumb muscles during development in man. *Journal of Physiology*, 499, 255-266.
- Jacobs, R., & van Ingen Schenau, G. J. (1992). Control of an external force in leg extensions in humans. *Journal of Physiology*, 457, 611-626.
- Jeng, S. F., Liao, H. F., Lai, J. S., & Hou, J. W. (1997). Optimization of walking in children. *Medicine and Science in Sports and Exercise*, 29, 370-376.
- Jensen, J. L., & Korff, T. (2004). Adapting to changing task demands: variability in children's response to manipulations of resistance and cadence during pedaling. *Research Quarterly for Exercise and Sport*, 75, 361-369.
- Jensen, R. K. (1989). Changes in segment inertia proportions between 4 and 20 years. *Journal of Biomechanics*, 22, 529-536.
- Kane, T. R., & Levinson, D. A. (1985). *Dynamics: Theory and Applications*, McGraw-Hill Book Company: New York.
- Lexell, J., Sjoström, M., Nordlund, A. S., & Taylor, C. C. (1992). Growth and development of human muscle: A quantitative morphological study of whole vastus lateralis from childhood to adult age. *Muscle & Nerve*, 15, 404-409.
- Liu, T., Korff, T., Chao, P., & Jensen, J.L. (2003). Bilateral asymmetry and cycling performance in children. [Abstract]. *Journal of Sport & Exercise Psychology*, 25(Suppl.), S91.

- Martin, J. C., Farrar, R. P., Wagner, B. M., & Spirduso, W. W., (2000). Maximal power across the lifespan. *Journal of Gerontology: Medical Sciences*, 55A, M311-M316.
- Neptune, R. R., & Hull, M. L. (1995). Accuracy assessment of methods for determining hip movement in seated cycling. *Journal of Biomechanics*, 28, 423-437.
- Neptune, R. R., & Herzog, W. (1999). The association between negative muscle work and pedaling rate. *Journal of Biomechanics*, 32, 1021-1026.
- Neptune, R. R., Kautz, S. A., & Zajac, F. E. (2000). Muscle contributions to specific biomechanical functions do not change in forward versus backward pedaling. *Journal of Biomechanics*, 33, 155-164.
- Raasch, C. C., Zajac, F. E., Ma, B., & Levine, W. S. (1997). Muscle coordination of maximum-speed pedaling. *Journal of Biomechanics*, 30, 595-602.
- Roncesvalles, M. N., Woollacott, M. H., Brown, N., & Jensen, J. L. (2004). An emerging postural response: is control of the hip possible in the newly walking child? *Journal of Motor Behavior*, 36, 147-159.
- Seth, A., McPhee, J.J., & Pandy, M.G. (2004). Multi-joint coordination of vertical arm movement. *Applied Bionics and Biomechanics*, 1, 45-56.
- Shumway-Cook, A., & Woollacott, M. H. (1985). The growth of stability: Postural control from a developmental perspective. *Journal of Motor Behavior*, 17, 131-147.
- Sundermier, L., Woollacott, M. H., Roncesvalles, N., & Jensen, J. L. (2001). The development of balance control in children: comparisons of EMG and kinetic variables and chronological and developmental groupings. *Experimental Brain Research*, 136, 340-350.
- Yang, J. F., Stephens, M. J., & Vishram, R. (1998). Infant stepping: a method to study the sensory control of human walking. *Journal of Physiology*, 507, 927-937.

Chapter 5: General Discussion

During childhood, various factors result in changes in motor behavior. On an end effector level, these changes can be revealed in differences in the application of muscular forces which give us information about the nervous system's contribution to the task (Winter & Eng, 1995). To allow for a valid interpretation of age-related differences in muscular force application, two methodological prerequisites must be assumed:

1. The method used to estimate muscular forces must be accurate – bearing in mind that muscular forces cannot be measured directly.
2. Age-related differences in muscular force application must not be confounded by factors other than those to which observed differences are to be attributed.

The goal of this dissertation was to differentiate between the effects of growth and physical maturation on the application of muscular forces. Three studies were performed. The first study was an investigation of how the use of different methods can lead to different answers to a developmental question. The results of this study revealed that an analysis of intersegmental dynamics is necessary to fully understand the effect of growth on muscular force application. Therefore such an analysis was chosen for Studies 2 and 3. Studies 2 and 3 were designed to differentiate between the influences of growth and maturation of the neuro-motor system on children's adaptability in terms of muscular power production. Distinguishing between these two factors is important because the interpretation of observed age-related differences in muscular force application might be different, depending on their source. If the sources are differences in anthropometry, differences in muscular force application might be interpreted as functional. The fact that anthropometry influences non-muscular forces can result in a need to match muscular to non-muscular forces in a different fashion if the resultant force to be produced has to be

the same. On the other hand, age-related differences in muscular force application may be interpreted as immature if these differences can be specifically attributed to maturing features of the neuro-motor system.

In Study 2, we found that age-related differences in anthropometry have a significant effect on the indirect transfer of muscular energy to the crank. These results increase our understanding about the interaction of muscular and non-muscular influences during a dynamic contact task. The goal of Study 3 was to determine age-related differences in voluntary adaptive skill. The results indicated that a reduction in muscular power generation in children at high movement speeds results in a different adaptive strategy. It was demonstrated that in children, at high movement speeds, a reduction in muscular power production results in a different muscular synergy that is used to deliver energy to the crank during pedaling. These results extend our understanding about the acquisition of voluntary adaptive skill and the relationship between the development of adaptability on a neuromuscular level and on a behavioral level which has important implications for teachers, coaches, and therapists.

The main question that arises from the results of this dissertation is: What are the sources of the observed reduction of muscular power production in children? One might speculate that age-related differences in the muscle-intrinsic properties or in motor unit recruitment are possible contributors to the observed differences. We know that certain muscle-intrinsic properties such as fiber type distribution (Lexell, Sjostrom, Nordlund, & Taylor, 1992), the force velocity-relationship (Asai & Aoki, 1996), electromechanical delay (Lin, Brown, & Walsh, 1994; Asai & Aoki, 1996), or muscle-tendon compliance (Lin, Brown, & Walsh, 1997) are different in children when compared to adults. As results of Study 3 indicate that age-related differences in muscular power production are most apparent at the hip joint, it is of particular interest how differences in the muscle-

intrinsic properties of the hip extensors influence muscular power production and the mechanical construction of the cycling task. To specifically test the hypothesis that differences in muscle-intrinsic properties contribute to age-related differences in muscular power production, a biomechanical model that includes individual muscles (Raasch et al., 1997; Neptune & Hull, 1998) could be used.

In this context, it is important to mention a limitation of the present analysis. The model used in this dissertation was driven by muscular torques – not muscular forces. This implies that at each joint, only one torque representing the forces of all muscles that span that joint actuated the forward dynamics simulation. Where this type of analysis is useful to quantify overall muscular contributions to the mechanical constructions of the task, it does not capture contributions of individual muscles that span the same joint. As a consequence, certain mechanisms such as co-contraction or the distribution of synergistic muscular contributions cannot be quantified. However, the analysis on a torque level gives us first hints about possible mechanisms of muscular power production and muscular synergies on an individual muscle level. It must also be noted that there are two major methodological limitations associated with implementing such muscle models in developmental research. First, the use of muscle models requires detailed information about the muscle-intrinsic properties of the performer such as tendon stiffness, activation and deactivation times, maximum isometric force, or optimal fiber lengths. Where we have some information about what these quantities are in adults (Delp, et al., 1990), little is known about how they change during childhood (though we know they *do* change). Therefore, future research should be aimed at quantifying the change of muscle-intrinsic properties in children. The second limitation associated with implementing muscle models in developmental research is that they are computationally expensive. Children are typically more variable in their motor performance when compared to adults (Clark,

Whitall, & Phillips, 1988; Jensen & Korff, 2004). Therefore, larger sample sizes are needed to obtain a given level of statistical power. Note that in this dissertation, a total of about 300 torque-driven simulations were performed. Performing an equivalent number of forward dynamics simulations that are driven by individual muscular forces would require a great deal of computation time because of the increased number of possible mathematical solutions. Therefore, future research should also be aimed at estimating muscular forces more efficiently.

Another possible source of the observed differences in muscular power production is an age-related difference in the recruitment of motor units. One could speculate that adults recruit motor units more efficiently to take advantage of the synergy of hip extensors and plantarflexors in order to deliver muscular energy to the crank during pedaling. As the recruitment of motor units is not only a function of age (Gibbs, Harrison, & Stephens, 1997) but also a function of practice (Bernardi, Solomonow, Nguyen, Smith, & Baratta, 1996), it is possible that the observed age-related differences in muscular power production would be reduced if children were given the opportunity to practice the task. In the present investigations, cycling experience was held constant in order to isolate the *age-related* differences in muscular power production. In Study 2, the experimental manipulations were manipulations of model anthropometrics and therefore all other factors (including experience) were held constant. In Study 3, all participants' prior bicycle-riding experience was within certain boundaries and comparable across age groups. To specifically test the hypothesis that different strategies of motor unit recruitment lead to the observed differences in muscular power production, a longitudinal study during which the child is accumulating experience of the cycling task could be conducted. During such a study, care should be taken that this repeated exposure to the task does not result in physiological adaptations of muscle-intrinsic properties so that

differences in muscular power production that occur over time can be specifically attributed to improvements in motor unit recruitment.

In summary, we have conducted a sequence of studies in which age-related differences in adaptability in terms of muscular synergies were determined and attributed to differences in muscular power production. Two studies were performed to assure the validity of this attribution. First, a suitable method to estimate muscular forces was determined. Second, the possible confound of differences in anthropometry was quantified. The results of the investigations increase our knowledge about the factors that lead to age-related improvement in adaptive skill and give us hints about the factors that are limiting children's performance ranges. The results of this dissertation have practical implications for teachers, coaches, and therapists and are important prerequisites for future research which should be aimed at identifying the source of the observed differences and specifically at determining the factors that limit children's performance.

Appendix A: Consent Forms

CONSENT FORM- ADULT

THE DEVELOPMENT OF LOWER LIMB FORCE CONTROL DURING CYCLING

You are invited to participate in a study investigating the control of leg movements during stationary cycling. My name is Tom Korff and I am a graduate student at The University of Texas at Austin, Department of Kinesiology & Health Education. I am undertaking this study under the direct supervision of Jody L. Jensen, Ph.D. In this study, I hope to learn more about how children develop the ability to control movement of their legs during various stages of their growth and development. We are also studying adults and their ability to control the movement of their legs so a comparison can be made to the performance and ability of children during the same cycling task.

If you decide to participate, I will ask you to perform stationary cycling at different pedaling speeds and different workloads. These speeds and workloads are similar to those experienced during normal cycling outdoors. The stationary bike you will ride is very stable and it is extremely unlikely that you could fall. The bike is also adjustable such that for your height, the bike can be made comfortable for you to pedal. Testing should take no longer than one and a half hours, including the time it takes to familiarize you with the laboratory and to prepare for the cycling activity.

To prepare for the collection of data, we will place reflective markers on your legs. These markers will go on your foot, ankle, and the outside of the knee and hip joints. Double-sided tape will keep these in place. It is also possible that we will record the activity of your muscles. In this case, sensors will be positioned on your legs. The sensors are attached with tape. The type of sensors we use are very common in this type of research and no problems have been reported following their use. The markers and sensors will not limit your movement. You will be able to pedal freely and comfortably. Pedaling will be constant for periods of 1 to 5 minutes, but well below your maximal effort. In total, you will pedal the bicycle for about 10-20 minutes.

While you pedal, special cameras will record the action of your lower limb. Only the reflective markers will be seen by these special cameras and you can in no way be identified from the camera images. Neither your name nor any personal information will be stored with the camera records. We will also record you with a video camera while you are riding the bike. The video recording might identify you as a subject. The video may be used for educational purposes (such as training students or making class presentations) or research purposes (pictures or videos shown at professional conferences or used – without identifying information – in research publications).

An identification code will be used for all participants. Any information that is obtained in connection with this study and that can be identified with you will remain confidential and will be disclosed only with your permission. There will be no direct benefit to you following your participation in this study. Your assistance through participation will help us to better understand how movement abilities develop and are controlled by our bodies.

Your decision whether or not to participate will not affect your association with The University of Texas at Austin. If you decide not to participate, you are free to withdraw your approval for participation at any time without penalty.

You are making a decision as to whether you will or will not to participate. Your signature indicates that you have read the information provided above and have decided to participate. You may withdraw at any time after you have signed this form should you choose to discontinue your involvement in this study.

In the unlikely event of injury as a result of your participation in this study, no treatment will be provided, and no payment can be provided in the event of a medical problem. Basic first aid will be provided at the time of injury and you will be encouraged to consult your physician.

If you have any questions after reading this form, please contact Dr. Jody L. Jensen (512-232-2685) or myself (Tom Korff at 512-232-2686). If you have additional questions later, we will be happy to answer them.

A copy of this form will be provided for your records.

Signature of Participant

Date

Signature of Investigator

Date

CONSENT FORM – CHILD OLDER THAN 7 YEARS OF AGE

THE DEVELOPMENT OF LOWER LIMB FORCE CONTROL DURING CYCLING

Your child is invited to participate in a study investigating the control of leg movements during stationary cycling. My name is Tom Korff and I am a graduate student at The University of Texas at Austin, Department of Kinesiology & Health Education. I am undertaking this study under the direct supervision of Jody L. Jensen, Ph.D. In this study, I hope to learn more about how children develop the ability to control movement of their legs during various stages of their growth and development. We are also studying adults and their ability to control the movement of their legs so a comparison can be made to the performance and ability of children during the same cycling task.

If you decide to allow your child to participate, I will ask him or her to perform stationary cycling at different pedaling speeds and different workloads. These speeds and workloads are similar to those experienced during normal cycling outdoors. The stationary bike your child will ride is very stable and it is extremely unlikely that he or she could fall. The bike is also adjustable such that for your child's height, the bike can be made comfortable for him or her to pedal. Simply, we can adjust the seat and handle bar position to suit your child. Testing should take no longer than one and a half hours, including the time it takes to familiarize your child with the laboratory and to prepare for the cycling activity.

To prepare for the collection of data, we will place reflective markers on your child's legs. These markers will go on his or her foot, ankle, and the outside of the knee and hip joints. Double-sided tape will keep these in place. It is also possible that we will record the activity of your child's muscles. In this case, sensors will be positioned on your child's legs. The sensors are attached with tape. The type of sensors we use are very common in this type of research and no problems have been reported following their use. The markers and sensors will not limit your child's movement. Your child will be able to pedal freely and comfortably. Pedaling will be constant for periods of 1 to 5 minutes, but well below your child's maximal effort. In total, your child will pedal the bicycle for about 10-20 minutes.

While your child pedals, special cameras will record the action of his or her lower limb. Only the reflective markers will be seen by these special cameras and he or she can in no way be identified from the camera images. Neither your child's name nor any personal information will be stored with the camera records. We will also record your child with a video camera while he or she is riding the bike. The video recording might identify your child as a subject. The video may be used for educational purposes (such as training students or making class presentations) or research purposes (pictures or videos shown at professional conferences or used – without identifying information – in research publications).

An identification code will be used for all participants. Any information that is obtained in connection with this study and that can be identified with you will remain confidential and will be disclosed only with your permission. There will be no direct benefit to you or your child following your participation in this study. Your child's assistance through participation will help us to better understand how movement abilities develop and are controlled by our bodies.

Your decision whether or not to allow your child to participate will not affect your association, or the association of your child, with The University of Texas at Austin. If you decide your child should not participate, you are free to withdraw your approval for participation at any time without penalty.

You are making a decision as to whether your child will or will not to participate. Your signature indicates that you have read the information provided above and have decided to give permission for your child to participate. Your child may withdraw, and you may withdraw your permission at any time after you have signed this form should you choose to discontinue his or her involvement in this study.

In the unlikely event of injury as a result of your child's participation in this study, no treatment will be provided, and no payment can be provided in the event of a medical problem. Basic first aid will be provided at the time of injury and you will be encouraged to consult your physician.

If you have any questions after reading this form, please contact Dr. Jody L. Jensen (512-232-2685) or myself (Tom Korff at 512-232-2686). If you have additional questions later, we will be happy to answer them.

A copy of this form will be provided for your records.

Signature of Parent/Guardian

Date

Signature of Participant

Date

Signature of Investigator

Date

CONSENT FORM – CHILD YOUNGER THAN 7 YEARS OF AGE

THE DEVELOPMENT OF LOWER LIMB FORCE CONTROL DURING CYCLING

Your child is invited to participate in a study investigating the control of leg movements during stationary cycling. My name is Tom Korff and I am a graduate student at The University of Texas at Austin, Department of Kinesiology & Health Education. I am undertaking this study under the direct supervision of Jody L. Jensen, Ph.D. In this study, I hope to learn more about how children develop the ability to control movement of their legs during various stages of their growth and development. We are also studying adults and their ability to control the movement of their legs so a comparison can be made to the performance and ability of children during the same cycling task.

If you decide to allow your child to participate, I will ask him or her to perform stationary cycling at different pedaling speeds and different workloads. These speeds and workloads are similar to those experienced during normal cycling outdoors. The stationary bike your child will ride is very stable and it is extremely unlikely that he or she could fall. The bike is also adjustable such that for your child's height, the bike can be made comfortable for him or her to pedal. Simply, we can adjust the seat and handle bar position to suit your child. Testing should take no longer than one and a half hours, including the time it takes to familiarize your child with the laboratory and to prepare for the cycling activity.

To prepare for the collection of data, we will place reflective markers on your child's legs. These markers will go on his or her foot, ankle, and the outside of the knee and hip joints. Double-sided tape will keep these in place. It is also possible that we will record the activity of your child's muscles. In this case, sensors will be positioned on your child's legs. The sensors are attached with tape. The type of sensors we use are very common in this type of research and no problems have been reported following their use. The markers and sensors will not limit your child's movement. Your child will be able to pedal freely and comfortably. Pedaling will be constant for periods of 1 to 5 minutes, but well below your child's maximal effort. In total, your child will pedal the bicycle for about 10-20 minutes.

While your child pedals, special cameras will record the action of his or her lower limb. Only the reflective markers will be seen by these special cameras and he or she can in no way be identified from the camera images. Neither your child's name nor any personal information will be stored with the camera records. We will also record your child with a video camera while he or she is riding the bike. The video recording might identify your child as a subject. The video may be used for educational purposes (such as training students or making class presentations) or research purposes (pictures or videos shown at professional conferences or used – without identifying information – in research publications).

An identification code will be used for all participants. Any information that is obtained in connection with this study and that can be identified with you will remain confidential and will be disclosed only with your permission. There will be no direct benefit to you or your child following your participation in this study. Your child's assistance through participation will help us to better understand how movement abilities develop and are controlled by our bodies.

Your decision whether or not to allow your child to participate will not affect your association, or the association of your child, with The University of Texas at Austin. If you decide your child should not participate, you are free to withdraw your approval for participation at any time without penalty.

You are making a decision as to whether your child will or will not to participate. Your signature indicates that you have read the information provided above and have decided to give permission for your child to participate. Your child may withdraw, and you may withdraw your permission at any time after you have signed this form should you choose to discontinue his or her involvement in this study.

In the unlikely event of injury as a result of your child's participation in this study, no treatment will be provided, and no payment can be provided in the event of a medical problem. Basic first aid will be provided at the time of injury and you will be encouraged to consult your physician.

If you have any questions after reading this form, please contact Dr. Jody L. Jensen (512-232-2685) or myself (Tom Korff at 512-232-2686). If you have additional questions later, we will be happy to answer them.

A copy of this form will be provided for your records.

Signature of Parent/Guardian

Date

Signature of Investigator

Date

Appendix B: Bicycle-Riding Questionnaires

ACTIVITY QUESTIONNAIRE BIKING– ADULT

Subject ID _____

At what age did you start riding a bike? _____

Did you ride your bike to get around when you were a child (e.g. Did you ride your bike to school/friends?) Please explain.

Do you own a bike? _____

How often have you ridden a bike in the past five years?

Activity	Number of Years	Months / Year	Weeks / Month	Days / Week	Hours / Day	TOTAL HOURS
e.g.	2	6	4 (all)	2	1.5	144
Biking						
Stationary Biking						

If you do not ride a bike on a regular basis, please provide specific information on how often and how many hours you have ridden a bike within the past 5 years.

If there are other things about your cycling history that you think are worth mentioning, please write them down here.

ACTIVITY QUESTIONNAIRE BIKING– CHILD

Subject ID _____

At what age did your child start riding a bike? _____

Does your child ride a bike to get around (e.g. Does your child ride his/her bike to school/friends?) Please explain.

Does your child own a bike? _____

How often has your child ridden a bike in the past five years?

Activity	Number of Years	Months / Year	Weeks / Month	Days / Week	Hours / Day	TOTAL HOURS
e.g.	2	6	4 (all)	2	1.5	144
Biking						

If your child does not ride a bike on a regular basis, please provide specific information on how often and how many hours your child has ridden a bike within the past 5 years.

If there are other things about your child's cycling history that you think are worth mentioning, please write them down here.

Appendix C: Subject Information

SUBJECT INFORMATION SHEET

Date: _____

Study: _____

Subject Name: _____

Subject ID: _____

Subject Address: _____

Sex (m/f): _____

Subject Phone: _____

Date of Birth: _____

Parent/Guardian: _____

Date of Birth: _____

Chronological Age (in days): _____

Height (cm): _____

Leg length (cm): _____

Weight (kg): _____

Bike height: _____

Knee angle at TDC: _____

Knee angle at BDC: _____

Trunk angle: _____

PI: _____

Lab Assistants & Assignments

Notes

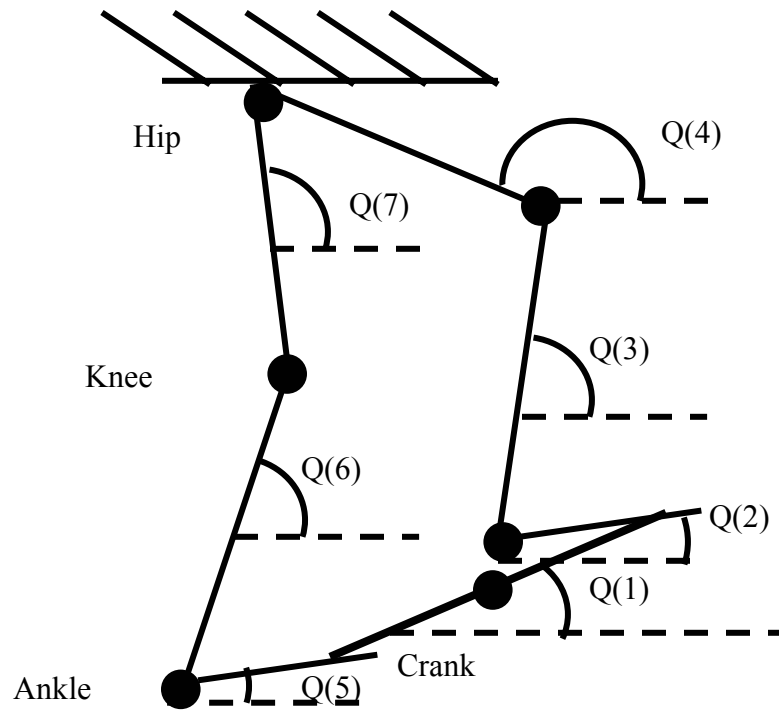
SPREADSHEET FOR ESTIMATING PEAK POWER

Subject ID			
Thigh Length 1 - proximal	=D2/2	thigh length	
Thigh Length 2 - distal	=D2/2		
Circumferences		Lean limb circumferences	
C1 (gluteal furrow)		LC1	=B5-B15*PI()
C2 (mid thigh)		LC2	=B6-B22*PI()
C3 (proximal patella)		LC3	=B7-B29*PI()
Skin fold thickness		Lean limb diameters	
gluteal furrow front 1		LD1	=D5/PI()
gluteal furrow front 2		LD2	=D6/PI()
gluteal furrow front 3		LD3	=D7/PI()
gluteal furrow back 1		Radius	
gluteal furrow back 2		R1	=D9/2
gluteal furrow back 3		R2	=D10/2
average gluteal furrow	=AVERAGE(B9:B14)	R3	=D11/2
mid thigh front 1		Heights	
mid thigh front 2		height1(proximal)	=SQRT((B2)^2-(D14-D13)^2)
mid thigh front 3		height2 (distal)	=SQRT((B3)^2-(D15-D14)^2)
mid thigh back 1		Volumes	
mid thigh back 2		Cone1 (proximal)	=(PI()*D17/3)* (D13^2+D14*D13+D14^2)
mid thigh back 3		Cone2 (distal)	=(PI()*D18/3)* (D14^2+D14*D15+D15^2)
average mid thigh	=AVERAGE(B16:B21)	Sum	=(D20+D21)/1000
proximal patella front 1		Pmax	=(215.96*D22+48.53)
proximal patella front 2			
proximal patella front 3			
proximal patella back 1			
proximal patella back 2			
proximal patella back 3			
average proximal patella	=AVERAGE(B23:B28)		

Crank length (0.2 x leg length)						
Crank length used						
	Value on ergometer scale					
		60 RPM	75 RPM	90 RPM	105 RPM	120 RPM
5% Pmax	=0.05*D23	=0.0345*B42	=B42*0.0276	=B42*0.023	=B42*0.0197	=B42*0.0172
10% Pmax	=0.1*D23	=0.0345*B43	=B43*0.0276	=B43*0.023	=B43*0.0197	=B43*0.0172
15% Pmax	=0.15*D23	=0.0345*B44	=B44*0.0276	=B44*0.023	=B44*0.0197	=B44*0.0172
20% Pmax	=0.2*D23	=0.0345*B45	=B45*0.0276	=B45*0.023	=B45*0.0197	=B45*0.0172
25% Pmax	=0.25*D23	=0.0345*B46	=B46*0.0276	=B46*0.023	=B46*0.0197	=B46*0.0172
Foot length (heel - longest toe)						
Shank length (lateral malleolus - lateral knee joint line)						
Thigh length (lateral knee joint line - greater trochanter)						
Leg length (floor - greater trochanter)						
Standing ASIS height (floor - ASIS)						
Anterior thigh length (patella - ASIS)						
Standing gluteal fold height (gluteal fold - floor)						
Mid calf (mid belly of Gastrocnemius)						

Appendix D: Pedaling Model

Figure D1. Planar model of 2-legged pedaling. The configuration is described by 7 angles. All angles are defined with respect to the horizontal axis of the inertial reference frame. Positive angles are defined counterclockwise.



Nomenclature

Q(1)	Crank Angle
Q(2)	Right Foot Angle
Q(3)	Right Shank Angle
Q(4)	Right Thigh Angle
Q(5)	Left Foot Angle
Q(6)	Left Shank Angle
Q(7)	Left Thigh Angle
U(1)	Crank Angular Velocity
U(2)	Right Foot Angular Velocity
U(3)	Right Shank Angular Velocity
U(4)	Right Thigh Angular Velocity
U(5)	Left Foot Angular Velocity
U(6)	Left Shank Angular Velocity
U(7)	Left Thigh Angular Velocity
Ud(1)	Crank Angular Acceleration
Ud(2)	Right Foot Angular Acceleration
Ud(3)	Right Shank Angular Acceleration
Ud(4)	Right Thigh Angular Acceleration
Ud(5)	Left Foot Angular Acceleration
Ud(6)	Left Shank Angular Acceleration
Ud(7)	Left Thigh Angular Acceleration
CL	Crank Length
RFL	Right Foot Length
RTL	Right Thigh Length
RSL	Right Shank Length
LFL	Left Foot Length
LTS	Left Shank Length
LTL	Left Thigh Length
SL	Seat Length (fixed distance between the hip joint and the crank axis of rotation)
SA	Seat Angle (angle of the line connecting the hip joint and the crank axis of rotation with respect to the inertial horizontal axis)
RRF	Distance between the COM of the right foot and the right ankle joint
RRS	Distance between the COM of the right shank and the right knee joint
RRT	Distance between the COM of the right thigh and the hip joint
RLF	Distance between the COM of the left foot and the left ankle joint
RLS	Distance between the COM of the left shank and the left knee joint
RLT	Distance between the COM of the left thigh and the hip joint
MRF	Mass of the right foot
MRS	Mass of the right shank
MRT	Mass of the right thigh
MLF	Mass of the left foot
MLS	Mass of the left shank
MLT	Mass of the left thigh

IRF	Moment of inertia of the right foot
IRS	Moment of inertia of the right shank
IRT	Moment of inertia of the right thigh
ILF	Moment of inertia of the left foot
ILS	Moment of inertia of the left shank
ILT	Moment of inertia of the left thigh
ICR	Effective rotational inertia about the crank axis of rotation
M(1)	Muscle moment about the right ankle joint
M(2)	Muscle moment about the right knee joint
M(3)	Muscle moment about the right hip joint
M(4)	Muscle moment about the left ankle joint
M(5)	Muscle moment about the left knee joint
M(6)	Muscle moment about the left hip joint
FP(1)	Horizontal component of the pedal reaction force
FP(2)	Vertical component of the pedal reaction force
EXT	Effective rotational torque due to frictional forces

Kinematic Constraint Equations

Due to the hip joint and the crank axis of rotation being fixed in space, the model is kinematically constrained in terms of angular positions, velocities and accelerations.

Angular Positions

$$\begin{aligned} SL * \cos(SA) + RFL * \cos(Q(2)) - CL * \cos(Q(1)) - RSL * \cos(Q(3)) - RTL * \cos(Q(4)) &= 0 \\ SL * \cos(SA) + LFL * \cos(Q(5)) + CL * \cos(Q(1)) - LSL * \cos(Q(6)) - LTL * \cos(Q(7)) &= 0 \end{aligned}$$

Angular Velocities

$$\begin{aligned} U(2) &= (CL * \sin(Q(1)-Q(3)) * U(1) - RTL * \sin(Q(3)-Q(4)) * U(4)) / (RFL * \sin(Q(2)-Q(3))) \\ U(3) &= (CL * \sin(Q(1)-Q(2)) * U(1) - RTL * \sin(Q(2)-Q(4)) * U(4)) / (RSL * \sin(Q(2)-Q(3))) \\ U(5) &= -(CL * \sin(Q(1)-Q(6)) * U(1) + LTL * \sin(Q(6)-Q(7)) * U(7)) / (LFL * \sin(Q(5)-Q(6))) \\ U(6) &= -(CL * \sin(Q(1)-Q(5)) * U(1) + LTL * \sin(Q(5)-Q(7)) * U(7)) / (LSL * \sin(Q(5)-Q(6))) \end{aligned}$$

Angular Accelerations

$$\begin{aligned} Ud(2) &= (RSL * U(3)^2 + CL * \cos(Q(1)-Q(3)) * U(1)^2 + RTL * \cos(Q(3)-Q(4)) * U(4)^2 + CL * \sin(Q(1)-Q(3)) * Ud(1) - RTL * \sin(Q(3)-Q(4)) * Ud(4)) / (RFL * \sin(Q(2)-Q(3))) - \cos(Q(2)-Q(3)) * U(2)^2 / \sin(Q(2)-Q(3)) \\ Ud(3) &= \cos(Q(2)-Q(3)) * U(3)^2 / \sin(Q(2)-Q(3)) + (CL * \cos(Q(1)-Q(2)) * U(1)^2 + RTL * \cos(Q(2)-Q(4)) * U(4)^2 + CL * \sin(Q(1)-Q(2)) * Ud(1) - RFL * U(2)^2 - RTL * \sin(Q(2)-Q(4)) * Ud(4)) / (RSL * \sin(Q(2)-Q(3))) \\ Ud(5) &= (LSL * U(6)^2 + LTL * \cos(Q(6)-Q(7)) * U(7)^2 - CL * \cos(Q(1)-Q(6)) * U(1)^2 - CL * \sin(Q(1)-Q(6)) * Ud(1) - LTL * \sin(Q(6)-Q(7)) * Ud(7)) / (LFL * \sin(Q(5)-Q(6))) - \cos(Q(5)-Q(6)) * U(5)^2 / \sin(Q(5)-Q(6)) \\ Ud(6) &= \cos(Q(5)-Q(6)) * U(6)^2 / \sin(Q(5)-Q(6)) + (LTL * \cos(Q(5)-Q(7)) * U(7)^2 - LFL * U(5)^2 - CL * \cos(Q(1)-Q(5)) * U(1)^2 - CL * \sin(Q(1)-Q(5)) * Ud(1) - LTL * \sin(Q(5)-Q(7)) * Ud(7)) / (LSL * \sin(Q(5)-Q(6))) \end{aligned}$$

Analytical expressions for the horizontal and vertical components of the pedal reaction force

Horizontal Component

$$\begin{aligned}
 FP(1) = & ((MRF*RRF*RTL^2*\cos(Q(4))*\cos(Q(2)-Q(4))- \\
 & RFL*(IRT+MRF*RTL^2+MRS*RTL^2+MRT*RRT^2)*\cos(Q(2)))*(M(2)+G* \\
 & MRF*RSL*\cos(Q(3))+G*MRS*RRS*\cos(Q(3))+MRF*RRF*RSL*\cos(Q(2)- \\
 & Q(3))*Ud(2)-M(1)-MRS*RRS*RTL*\sin(Q(3)-Q(4))*U(4)^2- \\
 & MRF*RSL*(RRF*\sin(Q(2)-Q(3))*U(2)^2+RTL*\sin(Q(3)-Q(4))*U(4)^2- \\
 & (IRS+MRF*RSL^2+MRS*RRS^2)*Ud(3))- \\
 & (RTL^2*(MRF*RSL+MRS*RRS)*\cos(Q(4))*\cos(Q(3)-Q(4))- \\
 & RSL*(IRT+MRF*RTL^2+MRS*RTL^2+MRT*RRT^2)*\cos(Q(3)))*(G*MRF*R \\
 & RF*\cos(Q(2))+(IRF+MRF*RRF^2)*Ud(2)-M(1)-MRF*RRF*(RSL*\sin(Q(2)- \\
 & Q(3))*U(3)^2+RTL*\sin(Q(2)-Q(4))*U(4)^2)-MRF*RRF*RSL*\cos(Q(2)- \\
 & Q(3))*Ud(3))-RTL*(MRF*RRF*RSL*\cos(Q(3))*\cos(Q(2)-Q(4))- \\
 & RFL*(MRF*RSL+MRS*RRS)*\cos(Q(2))*\cos(Q(3)- \\
 & Q(4)))*(M(3)+G*MRF*RTL*\cos(Q(4))+G*MRS*RTL*\cos(Q(4))+G*MRT*RR \\
 & T*\cos(Q(4))+RTL*(MRS*RRS*\sin(Q(3)-Q(4))*U(3)^2-MRF*(RRF*\sin(Q(2)- \\
 & Q(4))*U(2)^2-RSL*\sin(Q(3)-Q(4))*U(3)^2))+MRF*RRF*RTL*\cos(Q(2)- \\
 & Q(4))*Ud(2)-M(2)-RTL*(MRF*RSL+MRS*RRS)*\cos(Q(3)-Q(4))*Ud(3)))/ \\
 & (RTL^2*\sin(Q(4))*(MRF*RRF*RSL*\cos(Q(3))*\cos(Q(2)-Q(4))- \\
 & RFL*(MRF*RSL+MRS*RRS)*\cos(Q(2))*\cos(Q(3)-Q(4)))- \\
 & RFL*RSL*(IRT+MRF*RTL^2+MRS*RTL^2+MRT*RRT^2)*\sin(Q(2)-Q(3))- \\
 & RTL^2*\cos(Q(4))*(MRF*RRF*RSL*\sin(Q(3))*\cos(Q(2)-Q(4))- \\
 & RFL*(MRF*RSL+MRS*RRS)*\sin(Q(2))*\cos(Q(3)-Q(4))))
 \end{aligned}$$

Vertical Component

$$\begin{aligned} FP(2) = & ((MRF*RRF*RTL^2*\sin(Q(4))*\cos(Q(2)-Q(4))- \\ & RFL*(IRT+MRF*RTL^2+MRS*RTL^2+MRT*RRT^2)*\sin(Q(2)))*(M(2)+G*M \\ & RF*RSL*\cos(Q(3))+G*MRS*RRS*\cos(Q(3))+MRF*RRF*RSL*\cos(Q(2)- \\ & Q(3))*Ud(2)-M(1)-MRS*RRS*RTL*\sin(Q(3)-Q(4))*U(4)^2- \\ & MRF*RSL*(RRF*\sin(Q(2)-Q(3))*U(2)^2+RTL*\sin(Q(3)-Q(4))*U(4)^2- \\ & (IRS+MRF*RSL^2+MRS*RRS^2)*Ud(3))- \\ & (RTL^2*(MRF*RSL+MRS*RRS)*\sin(Q(4))*\cos(Q(3)-Q(4))- \\ & RSL*(IRT+MRF*RTL^2+MRS*RTL^2+MRT*RRT^2)*\sin(Q(3)))*(G*MRF*R \\ & RF*\cos(Q(2))+(IRF+MRF*RRF^2)*Ud(2)-M(1)-MRF*RRF*(RSL*\sin(Q(2)- \\ & Q(3))*U(3)^2+RTL*\sin(Q(2)-Q(4))*U(4)^2)-MRF*RRF*RSL*\cos(Q(2)- \\ & Q(3))*Ud(3))-RTL*(MRF*RRF*RSL*\sin(Q(3))*\cos(Q(2)-Q(4))- \\ & RFL*(MRF*RSL+MRS*RRS)*\sin(Q(2))*\cos(Q(3)- \\ & Q(4)))*(M(3)+G*MRF*RTL*\cos(Q(4))+G*MRS*RTL*\cos(Q(4))+G*MRT*RR \\ & T*\cos(Q(4))+RTL*(MRS*RRS*\sin(Q(3)-Q(4))*U(3)^2-MRF*(RRF*\sin(Q(2)- \\ & Q(4))*U(2)^2-RSL*\sin(Q(3)-Q(4))*U(3)^2))+MRF*RRF*RTL*\cos(Q(2)- \\ & Q(4))*Ud(2)-M(2)-RTL*(MRF*RSL+MRS*RRS)*\cos(Q(3)- \\ & Q(4))*Ud(3))/RTL^2*\sin(Q(4))*(MRF*RRF*RSL*\cos(Q(3))*\cos(Q(2)-Q(4))- \\ & RFL*(MRF*RSL+MRS*RRS)*\cos(Q(2))*\cos(Q(3)-Q(4)))- \\ & RFL*RSL*(IRT+MRF*RTL^2+MRS*RTL^2+MRT*RRT^2)*\sin(Q(2)-Q(3))- \\ & RTL^2*\cos(Q(4))*(MRF*RRF*RSL*\sin(Q(3))*\cos(Q(2)-Q(4))- \\ & RFL*(MRF*RSL+MRS*RRS)*\sin(Q(2))*\cos(Q(3)-Q(4)))) \end{aligned}$$

Decomposition of mechanical power

The equations of motion of the mechanical system can be described by the equation D1.

$$M(\ddot{\theta}) = T(\theta, \dot{\theta}) \quad (D1)$$

where

M is a the 3 x 3 mass matrix of the system

T is a 3 x 1 vector containing all torques due to external, gravitational, and motion-dependent forces. For the model of bike riding, M and T are of the following forms:

$$M = \begin{bmatrix} M(1,1) & M(1,2) & M(1,3) \\ M(2,1) & M(2,2) & M(2,3) \\ M(3,1) & M(3,2) & M(3,3) \end{bmatrix}$$

$$T = \begin{bmatrix} T(1,1) \\ T(1,2) \\ T(1,3) \end{bmatrix}$$

where

$$\begin{aligned} M(1,1) = & (ICR + CL^2 * \sin(Q(1) - Q(6)) * (ILF * \sin(Q(1) - Q(6)) / (LFL * \sin(Q(5) - Q(6))) - \\ & MLF * RLF * (\sin(Q(1) - Q(5)) / \tan(Q(5) - Q(6)) - RLF * \sin(Q(1) - Q(6)) / (LFL * \sin(Q(5) - \\ & Q(6)))) / (LFL * \sin(Q(5) - Q(6))) + CL^2 * \sin(Q(1) - \\ & Q(5)) * ((ILS + MLS * RLS^2) * \sin(Q(1) - Q(5)) / (LSL * \sin(Q(5) - \\ & Q(6))) + LSL * MLF * (\sin(Q(1) - Q(5)) / \sin(Q(5) - Q(6)) - RLF * \sin(Q(1) - \\ & Q(6)) / (LFL * \tan(Q(5) - Q(6)))) / (LSL * \sin(Q(5) - Q(6))) + CL^2 * \sin(Q(1) - \\ & Q(3)) * (IRF * \sin(Q(1) - Q(3)) / (RFL * \sin(Q(2) - Q(3))) - MRF * RRF * (\sin(Q(1) - \\ & Q(2)) / \tan(Q(2) - Q(3)) - RRF * \sin(Q(1) - Q(3)) / (RFL * \sin(Q(2) - Q(3)))) - \\ & MCR * RFL * (\cos(Q(1) - Q(2)) + \sin(Q(1) - Q(2)) / \tan(Q(2) - Q(3)) - \sin(Q(1) - \\ & Q(3)) / \sin(Q(2) - Q(3))) / (RFL * \sin(Q(2) - Q(3))) + CL^2 * \sin(Q(1) - \\ & Q(2)) * ((IRS + MRS * RRS^2) * \sin(Q(1) - Q(2)) / (RSL * \sin(Q(2) - \\ & Q(3))) + MRF * RSL * (\sin(Q(1) - Q(2)) / \sin(Q(2) - Q(3)) - RRF * \sin(Q(1) - \\ & Q(3)) / (RFL * \tan(Q(2) - Q(3)))) + MCR * RSL * (\cos(Q(1) - Q(3)) + \sin(Q(1) - \\ & Q(2)) / \sin(Q(2) - Q(3)) - \sin(Q(1) - Q(3)) / \tan(Q(2) - Q(3))) / (RSL * \sin(Q(2) - Q(3)))); \end{aligned}$$

$$M(1,2) = -CL*RTL*(\sin(Q(1)-Q(3))*(\text{IRF}*\sin(Q(3)-Q(4))/(\text{RFL}*\sin(Q(2)-Q(3))))- \\ \text{MCR}*\text{RFL}*(\sin(Q(2)-Q(4))/\tan(Q(2)-Q(3))-\cos(Q(2)-Q(4))-\sin(Q(3)- \\ Q(4))/\sin(Q(2)-Q(3)))-\text{MRF}*\text{RRF}*(\sin(Q(2)-Q(4))/\tan(Q(2)-Q(3))-\cos(Q(2)- \\ Q(4))-\text{RRF}*\sin(Q(3)-Q(4))/(\text{RFL}*\sin(Q(2)-Q(3)))))/(\text{RFL}*\sin(Q(2)-Q(3)))- \\ \text{MCR}*(\cos(Q(1)-Q(4))-(\sin(Q(2)-Q(4))*\cos(Q(1)-Q(3))-\sin(Q(3)-Q(4))*\cos(\\ Q(1)-Q(2)))/\sin(Q(2)-Q(3)))-\sin(Q(1)-Q(2))*(\text{MRS}*\text{RRS}*(\cos(Q(3)-Q(4))- \\ \text{RRS}*\sin(Q(2)-Q(4))/(\text{RSL}*\sin(Q(2)-Q(3))))-\text{IRS}*\sin(Q(2)-Q(4))/(\text{RSL}*\sin(Q(2)- \\ Q(3)))-\text{MCR}*\text{RSL}*(\sin(Q(2)-Q(4))/\sin(Q(2)-Q(3))-\cos(Q(3)-Q(4))-\sin(Q(3)- \\ Q(4))/\tan(Q(2)-Q(3)))-\text{MRF}*\text{RSL}*(\sin(Q(2)-Q(4))/\sin(Q(2)-Q(3))-\cos(Q(3)- \\ Q(4))-\text{RRF}*\sin(Q(3)-Q(4))/(\text{RFL}*\tan(Q(2)-Q(3)))))/(\text{RSL}*\sin(Q(2)-Q(3))));$$

$$M(1,3) = + CL*(\sin(Q(1)-Q(6))*(\text{ILF}*\text{LTL}*\sin(Q(6)-Q(7))/(\text{LFL}*\sin(Q(5)-Q(6))))- \\ \text{MLF}*\text{RLF}*(\text{LTL}*\sin(Q(5)-Q(7))/\tan(Q(5)-Q(6))-\text{RTL}*\cos(Q(5)-Q(7))- \\ \text{LTL}*\text{RLF}*\sin(Q(6)-Q(7))/(\text{LFL}*\sin(Q(5)-Q(6)))))/(\text{LFL}*\sin(Q(5)-Q(6)))-\sin(\\ Q(1)-Q(5))*(\text{MLS}*\text{RLS}*(\text{RTL}*\cos(Q(6)-Q(7))-\text{LTL}*\text{RLS}*\sin(Q(5)- \\ Q(7))/(\text{LSL}*\sin(Q(5)-Q(6))))-\text{ILS}*\text{LTL}*\sin(Q(5)-Q(7))/(\text{LSL}*\sin(Q(5)-Q(6)))- \\ \text{LSL}*\text{MLF}*(\text{LTL}*\sin(Q(5)-Q(7))/\sin(Q(5)-Q(6))-\text{RTL}*\cos(Q(6)-Q(7))- \\ \text{LTL}*\text{RLF}*\sin(Q(6)-Q(7))/(\text{LFL}*\tan(Q(5)-Q(6)))))/(\text{LSL}*\sin(Q(5)-Q(6))));$$

$$M(2,1) = - CL*RTL*(\sin(Q(3)-Q(4))*(\text{IRF}*\sin(Q(1)-Q(3))/(\text{RFL}*\sin(Q(2)-Q(3))))- \\ \text{MRF}*\text{RRF}*(\sin(Q(1)-Q(2))/\tan(Q(2)-Q(3))-\text{RRF}*\sin(Q(1)-Q(3))/(\text{RFL}*\sin(Q(2)- \\ Q(3)))))-\text{MCR}*\text{RFL}*(\cos(Q(1)-Q(2))+\sin(Q(1)-Q(2))/\tan(Q(2)-Q(3))-\sin(Q(1)- \\ Q(3))/\sin(Q(2)-Q(3)))/(\text{RFL}*\sin(Q(2)-Q(3)))-\text{MCR}*(\cos(Q(1)-Q(4))+(\sin(Q(1)- \\ Q(2))*\cos(Q(3)-Q(4))-\sin(Q(1)-Q(3))*\cos(Q(2)-Q(4)))/\sin(Q(2)-Q(3)))- \\ \text{MRF}*(\sin(Q(1)-Q(2))*\cos(Q(3)-Q(4))/\sin(Q(2)-Q(3))-\text{RRF}*\sin(Q(1)- \\ Q(3))*\cos(Q(2)-Q(4))/(\text{RFL}*\sin(Q(2)-Q(3))))-(\text{MRS}*\text{RRS}*\sin(Q(1)- \\ Q(2))*\cos(Q(3)-Q(4))-\sin(Q(2)-Q(4))*((\text{IRS}+\text{MRS}*\text{RRS}^2)*\sin(Q(1)- \\ Q(2))/(\text{RSL}*\sin(Q(2)-Q(3)))+\text{MRF}*\text{RSL}*(\sin(Q(1)-Q(2))/\sin(Q(2)-Q(3))- \\ \text{RRF}*\sin(Q(1)-Q(3))/(\text{RFL}*\tan(Q(2)-Q(3))))+\text{MCR}*\text{RSL}*(\cos(Q(1)- \\ Q(3))+\sin(Q(1)-Q(2))/\sin(Q(2)-Q(3))-\sin(Q(1)-Q(3))/\tan(Q(2)- \\ Q(3)))))/(\text{RSL}*\sin(Q(2)-Q(3))));$$

$$M(2,2) = +(\text{IRT} + \text{MRT}*\text{RRT}^2 + \text{RTL}^2*\sin(Q(3)-Q(4))*(\text{IRF}*\sin(Q(3)- \\ Q(4))/(\text{RFL}*\sin(Q(2)-Q(3)))-\text{MCR}*\text{RFL}*(\sin(Q(2)-Q(4))/\tan(Q(2)-Q(3))- \\ \cos(Q(2)-Q(4))-\sin(Q(3)-Q(4))/\sin(Q(2)-Q(3)))-\text{MRF}*\text{RRF}*(\sin(Q(2)-Q(4))/ \\ \tan(Q(2)-Q(3))-\cos(Q(2)-Q(4))-\text{RRF}*\sin(Q(3)-Q(4))/(\text{RFL}*\sin(Q(2)- \\ Q(3)))))/(\text{RFL}*\sin(Q(2)-Q(3)))-\text{MRS}*\text{RTL}^2*(-1+\text{RRS}*\sin(Q(2)- \\ Q(4))*\cos(Q(3)-Q(4))/(\text{RSL}*\sin(Q(2)-Q(3))))-\text{MRF}*\text{RTL}^2*(-1+\sin(Q(2)- \\ Q(4))*\cos(Q(3)-Q(4))/\sin(Q(2)-Q(3))-\text{RRF}*\sin(Q(3)-Q(4))*\cos(Q(2)-Q(4))/(\text{RFL} \\ *\sin(Q(2)-Q(3))))-\text{RTL}^2*\sin(Q(2)-Q(4))*(\text{MRS}*\text{RRS}*(\cos(Q(3)-Q(4))- \\ \text{RRS}*\sin(Q(2)-Q(4))/(\text{RSL}*\sin(Q(2)-Q(3))))-\text{IRS}*\sin(Q(2)-Q(4))/(\text{RSL}*\sin(Q(2)- \\ Q(3)))-\text{MCR}*\text{RSL}*(\sin(Q(2)-Q(4))/\sin(Q(2)-Q(3))-\cos(Q(3)-Q(4))-\sin(Q(3)- \\ Q(4))/\tan(Q(2)-Q(3)))-\text{MRF}*\text{RSL}*(\sin(Q(2)-Q(4))/\sin(Q(2)-Q(3))-\cos(Q(3)- \\ Q(4))-\text{RRF}*\sin(Q(3)-Q(4))/(\text{RFL}*\tan(Q(2)-Q(3)))))/(\text{RSL}*\sin(Q(2)-Q(3))));$$

$$M(2,3)=0;$$

$$M(3,1)= \quad + \quad CL*(LTL*\sin(Q(6)-Q(7))*(ILF*\sin(Q(1)-Q(6))/(LFL*\sin(Q(5)-Q(6)))-MLF*RLF*(\sin(Q(1)-Q(5))/\tan(Q(5)-Q(6))-RLF*\sin(Q(1)-Q(6))/(LFL*\sin(Q(5)-Q(6))))/(LFL*\sin(Q(5)-Q(6)))-MLF*RTL*(\sin(Q(1)-Q(5))*\cos(Q(6)-Q(7))/\sin(Q(5)-Q(6))-RLF*\sin(Q(1)-Q(6))*\cos(Q(5)-Q(7))/(LFL*\sin(Q(5)-Q(6)))-MLS*RLS*RTL*\sin(Q(1)-Q(5))*\cos(Q(6)-Q(7))-LTL*\sin(Q(5)-Q(7))*((ILS+MLS*RLS^2)*\sin(Q(1)-Q(5))/(LSL*\sin(Q(5)-Q(6)))+LSL*MLF*(\sin(Q(1)-Q(5))/\sin(Q(5)-Q(6))-RLF*\sin(Q(1)-Q(6))/(LFL*\tan(Q(5)-Q(6))))/(LSL*\sin(Q(5)-Q(6))));$$

$$M(3,2)=0;$$

$$M(3,3)=+(ILT+MLT*RLT^2+MLS*RTL*(RTL-LTL*RLS*\sin(Q(5)-Q(7))*\cos(Q(6)-Q(7))/(LSL*\sin(Q(5)-Q(6)))+LTL*\sin(Q(6)-Q(7))*(ILF*LTL*\sin(Q(6)-Q(7)))/(LFL*\sin(Q(5)-Q(6)))-MLF*RLF*(LTL*\sin(Q(5)-Q(7))/\tan(Q(5)-Q(6))-RTL*\cos(Q(5)-Q(7))-LTL*RLF*\sin(Q(6)-Q(7))/(LFL*\sin(Q(5)-Q(6))))/(LFL*\sin(Q(5)-Q(6)))-MLF*RTL*(LTL*\sin(Q(5)-Q(7))*\cos(Q(6)-Q(7))/\sin(Q(5)-Q(6))-RTL-LTL*RLF*\sin(Q(6)-Q(7))*\cos(Q(5)-Q(7))/(LFL*\sin(Q(5)-Q(6)))-LTL*\sin(Q(5)-Q(7))*(MLS*RLS*(RTL*\cos(Q(6)-Q(7))-LTL*RLS*\sin(Q(5)-Q(7))/(LSL*\sin(Q(5)-Q(6))))-ILS*LTL*\sin(Q(5)-Q(7))/(LSL*\sin(Q(5)-Q(6)))-LSL*MLF*(LTL*\sin(Q(5)-Q(7))/\sin(Q(5)-Q(6))-RTL*\cos(Q(6)-Q(7))-LTL*RLF*\sin(Q(6)-Q(7))/(LFL*\tan(Q(5)-Q(6))))/(LSL*\sin(Q(5)-Q(6))));$$

$$T(1,1)= \quad EXT \quad + \quad CL*M(1)*\sin(Q(1)-Q(3))/(RFL*\sin(Q(2)-Q(3))) \quad + \quad CL*\sin(Q(1)-Q(5))*(M(4)-M(5)-G*MLS*RLS*\cos(Q(6)))/(LSL*\sin(Q(5)-Q(6)))+CL*G*MCR*(\cos(Q(1))-(\cos(Q(2))*\sin(Q(1)-Q(3))-\cos(Q(3))*\sin(Q(1)-Q(2)))/\sin(Q(2)-Q(3)))+CL*G*MRP*(\cos(Q(3))*\sin(Q(1)-Q(2))/\sin(Q(2)-Q(3))-RRF*\cos(Q(2))*\sin(Q(1)-Q(3))/(RFL*\sin(Q(2)-Q(3)))) \quad + \quad CL*(MCR*(RFL*\sin(Q(1)-Q(2))*U(2)^2-RSL*\sin(Q(1)-Q(3))*U(3)^2-RTL*\sin(Q(1)-Q(4))*U(4)^2-(\cos(Q(1)-Q(2))*(RFL*\cos(Q(2)-Q(3))*U(2)^2-RSL*U(3)^2-CL*\cos(Q(1)-Q(3))*U(1)^2-RTL*\cos(Q(3)-Q(4))*U(4)^2)-\cos(Q(1)-Q(3))*(RFL*U(2)^2-CL*\cos(Q(1)-Q(2))*U(1)^2-RSL*\cos(Q(2)-Q(3))*U(3)^2-RTL*\cos(Q(2)-Q(4))*U(4)^2))/\sin(Q(2)-Q(3))+\sin(Q(1)-Q(5))*(ILS*(\cos(Q(5)-Q(6))*U(6)^2/\sin(Q(5)-Q(6))-(LFL*U(5)^2+CL*\cos(Q(1)-Q(5))*U(1)^2-LTL*\cos(Q(5)-Q(7))*U(7)^2)/(LSL*\sin(Q(5)-Q(6))))+MLS*RLS*(RTL*\sin(Q(6)-Q(7))*U(7)^2+RLS*(\cos(Q(5)-Q(6))*U(6)^2/\sin(Q(5)-Q(6))-(LFL*U(5)^2+CL*\cos(Q(1)-Q(5))*U(1)^2-LTL*\cos(Q(5)-Q(7))*U(7)^2)/(LSL*\sin(Q(5)-Q(6))))-LSL*MLF*((LFL*U(5)^2+CL*\cos(Q(1)-Q(5))*U(1)^2-LSL*\cos(Q(5)-Q(6))*U(6)^2-LTL*\cos(Q(5)-Q(7))*U(7)^2)/\sin(Q(5)-Q(6))-RLF*\sin(Q(5)-Q(6))*U(5)^2-RTL*\sin(Q(6)-Q(7))*U(7)^2-RLF*\cos(Q(5)-Q(6))*(\cos(Q(5)-Q(6))*U(5)^2/\sin(Q(5)-Q(6)))+(CL*\cos(Q(1)-Q(6))*U(1)^2-LSL*U(6)^2-LTL*\cos(Q(6)-Q(7))*U(7)^2)/(LFL*\sin(Q(5)-Q(6))))/(LSL*\sin(Q(5)-Q(6))));$$

$$\begin{aligned}
& Q(6))) + \sin(Q(1)-Q(3)) * (IRF * (\cos(Q(2)-Q(3)) * U(2)^2 / \sin(Q(2)-Q(3)) - \\
& (RSL * U(3)^2 + CL * \cos(Q(1)-Q(3)) * U(1)^2 + RTL * \cos(Q(3)-Q(4)) * U(4)^2) / (\\
& RFL * \sin(Q(2)-Q(3)))) - MCR * RFL * (CL * \sin(Q(1)-Q(2)) * U(1)^2 - RTL * \sin(Q(2)- \\
& Q(4)) * U(4)^2 - (RFL * \cos(Q(2)-Q(3)) * U(2)^2 - CL * \cos(Q(1)-Q(3)) * U(1)^2 - \\
& RTL * \cos(Q(3)-Q(4)) * U(4)^2 - RSL * \cos(Q(2)-Q(3)) * U(3)^2 - \cos(Q(2)- \\
& Q(3)) * (RFL * U(2)^2 - CL * \cos(Q(1)-Q(2)) * U(1)^2 - RSL * \cos(Q(2)-Q(3)) * U(3)^2 - \\
& RTL * \cos(Q(2)-Q(4)) * U(4)^2)) / \sin(Q(2)-Q(3))) - MRF * RRF * (\cos(Q(2)- \\
& Q(3)) * (RFL * U(2)^2 - CL * \cos(Q(1)-Q(2)) * U(1)^2 - RSL * \cos(Q(2)-Q(3)) * U(3)^2 - \\
& RTL * \cos(Q(2)-Q(4)) * U(4)^2) / \sin(Q(2)-Q(3)) - RSL * \sin(Q(2)-Q(3)) * U(3)^2 - \\
& RTL * \sin(Q(2)-Q(4)) * U(4)^2 - RRF * (\cos(Q(2)-Q(3)) * U(2)^2 / \sin(Q(2)-Q(3)) - (\\
& RSL * U(3)^2 + CL * \cos(Q(1)-Q(3)) * U(1)^2 + RTL * \cos(Q(3)- \\
& Q(4)) * U(4)^2) / (RFL * \sin(Q(2)-Q(3)))))) / (RFL * \sin(Q(2)-Q(3))) - \sin(Q(1)- \\
& Q(6)) * (ILF * (\cos(Q(5)-Q(6)) * U(5)^2 / \sin(Q(5)-Q(6)) + (CL * \cos(Q(1)- \\
& Q(6)) * U(1)^2 - LSL * U(6)^2 - LTL * \cos(Q(6)-Q(7)) * U(7)^2) / (LFL * \sin(Q(5)- \\
& Q(6)))) - MLF * RLF * (\cos(Q(5)-Q(6)) * (LFL * U(5)^2 + CL * \cos(Q(1)-Q(5)) * U(1)^2 - \\
& LSL * \cos(Q(5)-Q(6)) * U(6)^2 - LTL * \cos(Q(5)-Q(7)) * U(7)^2) / \sin(Q(5)-Q(6)) - \\
& LSL * \sin(Q(5)-Q(6)) * U(6)^2 - RTL * \sin(Q(5)-Q(7)) * U(7)^2 - RLF * (\cos(Q(5)- \\
& Q(6)) * U(5)^2 / \sin(Q(5)-Q(6)) + (CL * \cos(Q(1)-Q(6)) * U(1)^2 - LSL * U(6)^2 - \\
& LTL * \cos(Q(6)-Q(7)) * U(7)^2) / (LFL * \sin(Q(5)-Q(6)))))) / (LFL * \sin(Q(5)-Q(6))) - \\
& \sin(Q(1)-Q(2)) * (IRS * (\cos(Q(2)-Q(3)) * U(3)^2 / \sin(Q(2)-Q(3)) - (RFL * U(2)^2 - \\
& CL * \cos(Q(1)-Q(2)) * U(1)^2 - RTL * \cos(Q(2)-Q(4)) * U(4)^2) / (RSL * \sin(Q(2)- \\
& Q(3)))) + MRS * RRS * (RTL * \sin(Q(3)-Q(4)) * U(4)^2 + RRS * (\cos(Q(2)- \\
& Q(3)) * U(3)^2 / \sin(Q(2)-Q(3)) - (RFL * U(2)^2 - CL * \cos(Q(1)-Q(2)) * U(1)^2 - \\
& RTL * \cos(Q(2)-Q(4)) * U(4)^2) / (RSL * \sin(Q(2)- \\
& Q(3)))))) + MCR * RSL * (RTL * \sin(Q(3)-Q(4)) * U(4)^2 - CL * \sin(Q(1)-Q(3)) * U(1)^2 - \\
& (RFL * \cos(Q(2)-Q(3)) * U(2)^2 - CL * \cos(Q(1)-Q(2)) * U(1)^2 - RSL * \cos(Q(2)- \\
& Q(3)) * U(3)^2 - RTL * \cos(Q(2)-Q(4)) * U(4)^2 - \cos(Q(2)-Q(3)) * (RFL * \cos(Q(2)- \\
& Q(3)) * U(2)^2 - RSL * U(3)^2 - CL * \cos(Q(1)-Q(3)) * U(1)^2 - RTL * \cos(Q(3)- \\
& Q(4)) * U(4)^2) / \sin(Q(2)-Q(3))) - MRF * RSL * ((RFL * U(2)^2 - CL * \cos(Q(1)- \\
& Q(2)) * U(1)^2 - RSL * \cos(Q(2)-Q(3)) * U(3)^2 - RTL * \cos(Q(2)- \\
& Q(4)) * U(4)^2) / \sin(Q(2)-Q(3)) - RRF * \sin(Q(2)-Q(3)) * U(2)^2 - RTL * \sin(Q(3)- \\
& Q(4)) * U(4)^2 - RRF * \cos(Q(2)-Q(3)) * (\cos(Q(2)-Q(3)) * U(2)^2 / \sin(Q(2)-Q(3)) - \\
& (RSL * U(3)^2 + CL * \cos(Q(1)-Q(3)) * U(1)^2 + RTL * \cos(Q(3)- \\
& Q(4)) * U(4)^2) / (RFL * \sin(Q(2)-Q(3)))))) / (RSL * \sin(Q(2)-Q(3))) - \\
& CL * M(4) * \sin(Q(1)-Q(6)) / (LFL * \sin(Q(5)-Q(6))) - CL * \sin(Q(1)-Q(2)) * (M(1)- \\
& M(2)-G * MRS * RRS * \cos(Q(3))) / (RSL * \sin(Q(2)-Q(3))) - \\
& CL * G * MLF * (\cos(Q(6)) * \sin(Q(1)-Q(5)) / \sin(Q(5)-Q(6)) - \\
& RLF * \cos(Q(5)) * \sin(Q(1)-Q(6)) / (LFL * \sin(Q(5)-Q(6)))));
\end{aligned}$$

$$\begin{aligned}
T(1,2) = & M(3) + G * MRT * RRT * \cos(Q(4)) + RTL * (M(1) - M(2)) * \sin(Q(2)- \\
& Q(4)) / (RSL * \sin(Q(2)-Q(3))) + G * MRS * RTL * (\cos(Q(4)) - \\
& RRS * \cos(Q(3)) * \sin(Q(2)-Q(4)) / (RSL * \sin(Q(2)-Q(3)))) + G \\
& * MCR * RTL * (\cos(Q(4)) + (\cos(Q(2)) * \sin(Q(3)-Q(4)) - \cos(Q(3)) * \sin(Q(2)- \\
& Q(4))) / \sin(Q(2)-Q(3))) - M(2) - RTL * M(1) * \sin(Q(3)-Q(4)) / (RFL * \sin(Q(2)-Q(3))) \\
& - G * MRF * RTL * (\cos(Q(3)) * \sin(Q(2)-Q(4)) / \sin(Q(2)-Q(3)) - \cos(Q(4)) -
\end{aligned}$$

$$\begin{aligned}
& \text{RRF} * \cos(Q(2)) * \sin(Q(3) - Q(4)) / (\text{RFL} * \sin(Q(2) - Q(3))) - \text{RTL} * (\sin(Q(3) - \\
& Q(4)) * (\text{IRF} * (\cos(Q(2) - Q(3)) * U(2)^2 / \sin(Q(2) - Q(3)) - \\
& (\text{RSL} * U(3)^2 + \text{CL} * \cos(Q(1) - Q(3)) * U(1)^2 + \text{RTL} * \cos(Q(3) - Q(4)) * U(4)^2 / \\
& (\text{RFL} * \sin(Q(2) - Q(3)))) - \text{MCR} * \text{RFL} * (\text{CL} * \sin(Q(1) - Q(2)) * U(1)^2 - \text{RTL} * \sin(Q(2) - \\
& Q(4)) * U(4)^2 - (\text{RFL} * \cos(Q(2) - Q(3)) * U(2)^2 - \text{CL} * \cos(Q(1) - Q(3)) * U(1)^2 - \\
& \text{RTL} * \cos(Q(3) - Q(4)) * U(4)^2 - \text{RSL} * \cos(Q(2) - Q(3)) * U(3)^2 - \cos(Q(2) - \\
& Q(3)) * (\text{RFL} * U(2)^2 - \text{CL} * \cos(Q(1) - Q(2)) * U(1)^2 - \text{RSL} * \cos(Q(2) - Q(3)) * U(3)^2 - \\
& \text{RTL} * \cos(Q(2) - Q(4)) * U(4)^2)) / \sin(Q(2) - Q(3))) - \text{MRF} * \text{RRF} * (\cos(Q(2) - \\
& Q(3)) * (\text{RFL} * U(2)^2 - \text{CL} * \cos(Q(1) - Q(2)) * U(1)^2 - \text{RSL} * \cos(Q(2) - Q(3)) * U(3)^2 - \\
& \text{RTL} * \cos(Q(2) - Q(4)) * U(4)^2) / \sin(Q(2) - Q(3))) - \text{RSL} * \sin(Q(2) - Q(3)) * U(3)^2 - \\
& \text{RTL} * \sin(Q(2) - Q(4)) * U(4)^2 - \text{RRF} * (\cos(Q(2) - Q(3)) * U(2)^2 / \sin(Q(2) - Q(3)) - \\
& (\text{RSL} * U(3)^2 + \text{CL} * \cos(Q(1) - Q(3)) * U(1)^2 + \text{RTL} * \cos(Q(3) - Q(4)) * U(4)^2) / \\
& (\text{RFL} * \sin(Q(2) - Q(3)))))) / (\text{RFL} * \sin(Q(2) - Q(3))) - \\
& \text{MRS} * \text{RRS} * (\sin(Q(3) - Q(4)) * U(3)^2 - \cos(Q(3) - Q(4)) * (\cos(Q(2) - Q(3)) * U(3)^2 / \\
& \sin(Q(2) - Q(3)) - (\text{RFL} * U(2)^2 - \text{CL} * \cos(Q(1) - Q(2)) * U(1)^2 - \text{RTL} * \cos(Q(2) - \\
& Q(4)) * U(4)^2) / (\text{RSL} * \sin(Q(2) - Q(3)))) - \text{MCR} * (\text{CL} * \sin(Q(1) - \\
& Q(4)) * U(1)^2 + \text{RSL} * \sin(Q(3) - Q(4)) * U(3)^2 - \text{RFL} * \sin(Q(2) - Q(4)) * U(2)^2 - \\
& (\cos(Q(2) - Q(4)) * (\text{RFL} * \cos(Q(2) - Q(3)) * U(2)^2 - \text{RSL} * U(3)^2 - \text{CL} * \cos(Q(1) - \\
& Q(3)) * U(1)^2 - \text{RTL} * \cos(Q(3) - Q(4)) * U(4)^2) - \cos(Q(3) - Q(4)) * (\text{RFL} * U(2)^2 - \\
& \text{CL} * \cos(Q(1) - Q(2)) * U(1)^2 - \text{RSL} * \cos(Q(2) - Q(3)) * U(3)^2 - \text{RTL} * \cos(Q(2) - \\
& Q(4)) * U(4)^2)) / \sin(Q(2) - Q(3))) - \text{MRF} * (\text{RSL} * \sin(Q(3) - Q(4)) * U(3)^2 + \\
& \cos(Q(3) - Q(4)) * (\text{RFL} * U(2)^2 - \text{CL} * \cos(Q(1) - Q(2)) * U(1)^2 - \text{RSL} * \cos(Q(2) - \\
& Q(3)) * U(3)^2 - \text{RTL} * \cos(Q(2) - Q(4)) * U(4)^2) / \sin(Q(2) - Q(3))) - \text{RRF} * \sin(Q(2) - \\
& Q(4)) * U(2)^2 - \text{RRF} * \cos(Q(2) - Q(4)) * (\cos(Q(2) - Q(3)) * U(2)^2 / \sin(Q(2) - Q(3)) - \\
& (\text{RSL} * U(3)^2 + \text{CL} * \cos(Q(1) - Q(3)) * U(1)^2 + \text{RTL} * \cos(Q(3) - Q(4)) * U(4)^2) / \\
& (\text{RFL} * \sin(Q(2) - Q(3)))) - \sin(Q(2) - Q(4)) * (\text{IRS} * (\cos(Q(2) - Q(3)) * U(3)^2 / \sin(Q(2) - \\
& Q(3)) - (\text{RFL} * U(2)^2 - \text{CL} * \cos(Q(1) - Q(2)) * U(1)^2 - \text{RTL} * \cos(Q(2) - \\
& Q(4)) * U(4)^2) / (\text{RSL} * \sin(Q(2) - Q(3)))) + \text{MRS} * \text{RRS} * (\text{RTL} * \sin(Q(3) - \\
& Q(4)) * U(4)^2 + \text{RRS} * (\cos(Q(2) - Q(3)) * U(3)^2 / \sin(Q(2) - Q(3)) - (\text{RFL} * U(2)^2 - \\
& \text{CL} * \cos(Q(1) - Q(2)) * U(1)^2 - \text{RTL} * \cos(Q(2) - Q(4)) * U(4)^2) / (\text{RSL} * \sin(Q(2) - \\
& Q(3)))) + \text{MCR} * \text{RSL} * (\text{RTL} * \sin(Q(3) - Q(4)) * U(4)^2 - \text{CL} * \sin(Q(1) - Q(3)) * U(1)^2 - \\
& (\text{RFL} * \cos(Q(2) - Q(3)) * U(2)^2 - \text{CL} * \cos(Q(1) - Q(2)) * U(1)^2 - \text{RSL} * \cos(Q(2) - \\
& Q(3)) * U(3)^2 - \text{RTL} * \cos(Q(2) - Q(4)) * U(4)^2 - \cos(Q(2) - Q(3)) * (\text{RFL} * \cos(Q(2) - \\
& Q(3)) * U(2)^2 - \text{RSL} * U(3)^2 - \text{CL} * \cos(Q(1) - Q(3)) * U(1)^2 - \text{RTL} * \cos(Q(3) - \\
& Q(4)) * U(4)^2)) / \sin(Q(2) - Q(3))) - \text{MRF} * \text{RSL} * ((\text{RFL} * U(2)^2 - \text{CL} * \cos(Q(1) - \\
& Q(2)) * U(1)^2 - \text{RSL} * \cos(Q(2) - Q(3)) * U(3)^2 - \text{RTL} * \cos(Q(2) - \\
& Q(4)) * U(4)^2) / \sin(Q(2) - Q(3))) - \text{RRF} * \sin(Q(2) - Q(3)) * U(2)^2 - \text{RTL} * \sin(Q(3) - \\
& Q(4)) * U(4)^2 - \text{RRF} * \cos(Q(2) - Q(3)) * (\cos(Q(2) - Q(3)) * U(2)^2 / \sin(Q(2) - Q(3)) - \\
& (\text{RSL} * U(3)^2 + \text{CL} * \cos(Q(1) - Q(3)) * U(1)^2 + \text{RTL} * \cos(Q(3) - \\
& Q(4)) * U(4)^2) / (\text{RFL} * \sin(Q(2) - Q(3)))))) / (\text{RSL} * \sin(Q(2) - Q(3)));
\end{aligned}$$

$$\begin{aligned}
T(1,3)= & M(6)+G*MLT*RLT*\cos(Q(7))+G*MLS*(RTL*\cos(Q(7))- \\
& LTL*RLS*\cos(Q(6))*\sin(Q(5)-Q(7))/(LSL*\sin(Q(5)-Q(6))))+ \\
& MLS*RLS*RTL*(\sin(Q(6)-Q(7))*U(6)^2-\cos(Q(6)-Q(7))*(\cos(Q(5)- \\
& Q(6))*U(6)^2/\sin(Q(5)-Q(6))-(LFL*U(5)^2+CL*\cos(Q(1)-Q(5))*U(1)^2- \\
& LTL*\cos(Q(5)-Q(7))*U(7)^2)/(LSL*\sin(Q(5)-Q(6)))))+ \\
& MLF*RTL*(LSL*\sin(Q(6)-Q(7))*U(6)^2+\cos(Q(6)-Q(7)) \\
& *(LFL*U(5)^2+CL*\cos(Q(1)-Q(5))*U(1)^2-LSL*\cos(Q(5)-Q(6))*U(6)^2- \\
& LTL*\cos(Q(5)-Q(7))*U(7)^2)/\sin(Q(5)-Q(6))-RLF*\sin(Q(5)-Q(7))*U(5)^2- \\
& RLF*\cos(Q(5)-Q(7))*(\cos(Q(5)-Q(6))*U(5)^2/\sin(Q(5)-Q(6))+(CL*\cos(Q(1)- \\
& Q(6))*U(1)^2-LSL*U(6)^2-LTL*\cos(Q(6)-Q(7))*U(7)^2)/(LFL*\sin(Q(5)- \\
& Q(6))))+LTL*\sin(Q(5)-Q(7))*(M(4)+ILS*(\cos(Q(5)-Q(6))*U(6)^2/\sin(Q(5)- \\
& Q(6))-(LFL*U(5)^2+CL*\cos(Q(1)-Q(5))*U(1)^2-LTL*\cos(Q(5)- \\
& Q(7))*U(7)^2)/(LSL*\sin(Q(5)-Q(6))))+MLS*RLS*(RTL*\sin(Q(6)- \\
& Q(7))*U(7)^2+RLS*(\cos(Q(5)-Q(6))*U(6)^2/\sin(Q(5)-Q(6))- \\
& (LFL*U(5)^2+CL*\cos(Q(1)-Q(5))*U(1)^2-LTL*\cos(Q(5)- \\
& Q(7))*U(7)^2)/(LSL*\sin(Q(5)-Q(6))))-M(5)-LSL*MLF*((LFL*U(5)^2+ \\
& CL*\cos(Q(1)-Q(5))*U(1)^2-LSL*\cos(Q(5)-Q(6))*U(6)^2-LTL*\cos(Q(5)- \\
& Q(7))*U(7)^2)/\sin(Q(5)-Q(6))-RLF*\sin(Q(5)-Q(6))*U(5)^2-RTL*\sin(Q(6)- \\
& Q(7))*U(7)^2-RLF*\cos(Q(5)-Q(6))*(\cos(Q(5)-Q(6))*U(5)^2/\sin(Q(5)- \\
& Q(6))+(CL*\cos(Q(1)-Q(6))*U(1)^2-LSL*U(6)^2-LTL*\cos(Q(6)-Q(7))*U(7)^2)/(\\
& LFL*\sin(Q(5)-Q(6)))))/(LSL*\sin(Q(5)-Q(6)))-M(5)- \\
& G*MLF*(LTL*\cos(Q(6))*\sin(Q(5)-Q(7))/\sin(Q(5)-Q(6))-RTL*\cos(Q(7))- \\
& LTL*RLF*\cos(Q(5))*\sin(Q(6)-Q(7))/(LFL*\sin(Q(5)-Q(6))))-LTL*\sin(Q(6)- \\
& Q(7))*(M(4)+ILF*(\cos(Q(5)-Q(6))*U(5)^2/\sin(Q(5)-Q(6))+(CL*\cos(Q(1)-Q(6))* \\
& U(1)^2-LSL*U(6)^2-LTL*\cos(Q(6)-Q(7))*U(7)^2)/(LFL*\sin(Q(5)-Q(6))))- \\
& MLF*RLF*(\cos(Q(5)-Q(6))*(LFL*U(5)^2+CL*\cos(Q(1)-Q(5))*U(1)^2- \\
& LSL*\cos(Q(5)-Q(6))*U(6)^2-LTL*\cos(Q(5)-Q(7))*U(7)^2)/\sin(Q(5)-Q(6))- \\
& LSL*\sin(Q(5)-Q(6))*U(6)^2-RTL*\sin(Q(5)-Q(7))*U(7)^2-RLF*(\cos(Q(5)- \\
& Q(6))*U(5)^2/\sin(Q(5)-Q(6))+(CL*\cos(Q(1)-Q(6))*U(1)^2-LSL*U(6)^2- \\
& LTL*\cos(Q(6)-Q(7))*U(7)^2)/(LFL*\sin(Q(5)-Q(6)))))/(LFL*\sin(Q(5)-Q(6)));
\end{aligned}$$

The accelerations were calculated by solving equation D1 for $\ddot{\theta}$:

$$\ddot{\theta} = [M]^{-1} \cdot T(\theta, \dot{\theta}) \quad (D2)$$

The accelerations were decomposed into, muscular, velocity-dependent, gravity-dependent, and frictional components:

$$\ddot{\theta} = \ddot{\theta}_{muscle} + \ddot{\theta}_{velocity} + \ddot{\theta}_{gravity} + \ddot{\theta}_{friction} \quad (D3)$$

The muscular contribution of the acceleration can be further decomposed into contributions of the ankle, knee, and hip torques:

$$\ddot{\theta}_{muscle} = \ddot{\theta}_{ankle} + \ddot{\theta}_{knee} + \ddot{\theta}_{hip} \quad (D4)$$

The mechanical power of the entire mechanical system was calculated using equation D5:

$$P = [M\ddot{\theta} - V - G] \cdot \dot{\theta} \quad (D5)$$

where

P is the total power of the system

V is a 3 x 1 vector containing the velocity-dependent forces

G is a 3 x 1 vector containing the gravitational forces

$\dot{\theta}$ is a 3 x 1 vector containing the angular velocities

By setting to zero the mass and inertia of the crank, the mechanical power of the limbs can be found. By setting the masses and inertias of the limbs to zero, the mechanical power of the crank can be found. This way, the total power P can be decomposed into power of the crank and the remaining limbs of the bicycle rider:

$$P = P_{crank} + P_{limbs} \quad (D6)$$

The muscular component of each power component can be found using equation D7

$$P_{j_{muscle}} = [M_j \ddot{\theta}_{muscle}] \cdot \dot{\theta} \quad (D7)$$

where $P_{j_{muscle}}$ (j=crank or j=limbs) is the muscular contribution to crank or limb power. M_j (j=crank or j=limbs) is the moment arm matrix with the mass and inertia of the crank or the masses and inertias of the limbs set to zero.

These muscular power contributions can be further decomposed into individual joint torque components (Equations D8-D10).

$$P_{j_{ankle}} = [M_j \ddot{\theta}_{ankle}] \cdot \dot{\theta} \quad (D8)$$

$$P_{j_{knee}} = [M_j \ddot{\theta}_{knee}] \cdot \dot{\theta} \quad (D9)$$

$$P_{j_{hip}} = [M_j \ddot{\theta}_{hip}] \cdot \dot{\theta} \quad (D10)$$

Appendix E: Kautz and Hull's Decomposition Technique

Nomenclature

$i=h, k, a, p$	hip, knee, ankle, and pedal
$j=y, z$	horizontal and vertical components of force
$k=t, s, f$	thigh, shank, and foot segments
$l=m, g, md$	muscular, gravitational, and motion-dependent component of pedal force
F_{i_j}	reaction force at i^{th} joint acting in j^{th} direction
$F_{m_{p_j}}$	muscular component of pedal reaction force acting in j^{th} direction
rk_{ij}	j^{th} component of moment arm vector from the center of gravity of the k^{th} segment to the i^{th} joint
M_i	net muscle moment at i^{th} joint (i =hip, knee, and ankle)
M_{add}	Additional moment applied to the foot (A_1), shank (A_2), and thigh (A_3)
A	9x9 matrix of moment arms for intersegmental forces
x	9x1 vector of intersegmental forces
x_l	l^{th} component of force vector x
b	9x1 vector containing muscles moments, motion-dependent, and gravitational terms
b_l	l^{th} component of vector b
g	gravitational constant
A_{k_j}	Linear acceleration in j^{th} direction of the center of mass of the k^{th} segment
m_k	Mass of k^{th} segment
α_k	Angular acceleration of k^{th} segment
I_k	Moment of inertia of k^{th} segment

In Kautz and Hull's (1993) decomposition technique, the equations of motion are formulated in the following form:

$$Ax=b \quad (E1)$$

where

A is a 9x9 matrix of moment arms of intersegmental forces (see details below).

x is a 9x1 vector of intersegmental forces.

b is a 9x1 vector containing muscle moments, linear and angular accelerations, as well as gravitational forces.

$$\begin{aligned}
x = & \begin{bmatrix} F_{h_y} \\ F_{h_z} \\ F_{k_y} \\ F_{k_z} \\ F_{a_y} \\ F_{a_z} \\ F_{p_y} \\ F_{p_z} \\ M_{add} \end{bmatrix} \\
b = & \begin{bmatrix} m_t A_{t_y} \\ m_t A_{t_z} + m_t g \\ I_t \alpha_t - M_h + M_k \\ m_s A_{s_y} \\ m_s A_{s_z} + m_s g \\ I_s \alpha_s - M_k + M_a \\ m_f A_{f_y} \\ m_f A_{f_z} + m_f g \\ I_f \alpha_f - M_a \end{bmatrix}
\end{aligned}$$

The matrices of intersegmental forces as described in Kautz and Hull (1993) have the following form. Note that due to a slightly different formulation of the equations of motion, the matrix differs slightly from that described by Kautz and Hull (1993).

$$A_1 = \begin{bmatrix} 1 & 0 & -1 & 0 & 0 & 0 & 0 & 0 & 0 \\ 0 & 1 & 0 & -1 & 0 & 0 & 0 & 0 & 0 \\ -r_{thz} & r_{thy} & -r_{tkz} & r_{tky} & 0 & 0 & 0 & 0 & 0 \\ 0 & 0 & 1 & 0 & -1 & 0 & 0 & 0 & 0 \\ 0 & 0 & 0 & 1 & 0 & -1 & 0 & 0 & 0 \\ 0 & 0 & -r_{skz} & r_{sky} & -r_{saz} & r_{say} & 0 & 0 & 0 \\ 0 & 0 & 0 & 0 & 1 & 0 & 1 & 0 & 0 \\ 0 & 0 & 0 & 0 & 0 & 1 & 0 & 1 & 0 \\ 0 & 0 & 0 & 0 & r_{faz} & -r_{fay} & -r_{fpz} & r_{fpy} & 1 \end{bmatrix}$$

The vector b can be decomposed into muscular, gravitational, and motion-dependent components.

$$b_m = \begin{bmatrix} 0 \\ 0 \\ -M_h + M_k \\ 0 \\ 0 \\ -M_k + M_a \\ 0 \\ 0 \\ -M_a \end{bmatrix} \quad b_g = \begin{bmatrix} 0 \\ m_t g \\ 0 \\ 0 \\ m_s g \\ 0 \\ 0 \\ m_f g \\ 0 \end{bmatrix} \quad b_{md} = \begin{bmatrix} m_t A_{t_y} \\ m_t A_{t_z} \\ I_t \alpha_{t_k} \\ m_s A_{s_y} \\ m_s A_{s_z} \\ I_s \alpha_s \\ m_f A_{f_y} \\ m_f A_{f_z} \\ I_f \alpha_f \end{bmatrix}$$

Solving equation E1 for the force vector x and decomposing the vector b allows for decomposing the forces into muscular, gravitational, and motion-dependent components:

$$x_l = [A]^{-1} b_l \quad (E2)$$

where

$[A]^{-1}$ is the inverse of the 9x9 matrix A

x_l is the l^{th} component of force vector x ($l=m, g, \text{ or } md$)

b_l is the l^{th} component of force vector b ($l=m, g, \text{ or } md$)

Appendix F: Tracking Results – Studies 1 and 2

Figure F1. Experimental and simulated crank angle at 60 rpm. The relative absolute deviation between the two profiles is 0.0004%.

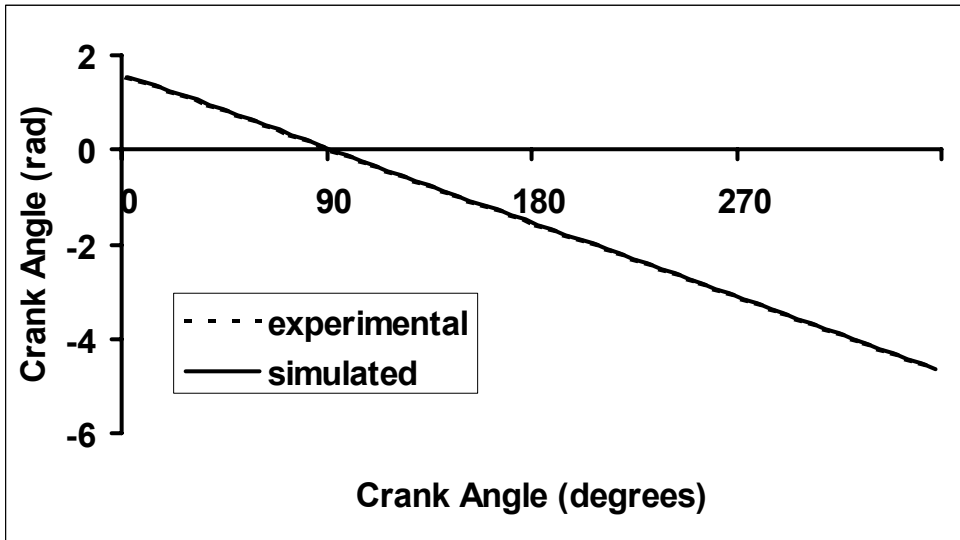


Figure F2. Experimental and simulated thigh angle at 60 rpm. The relative absolute deviation between the two profiles is 0.008%.

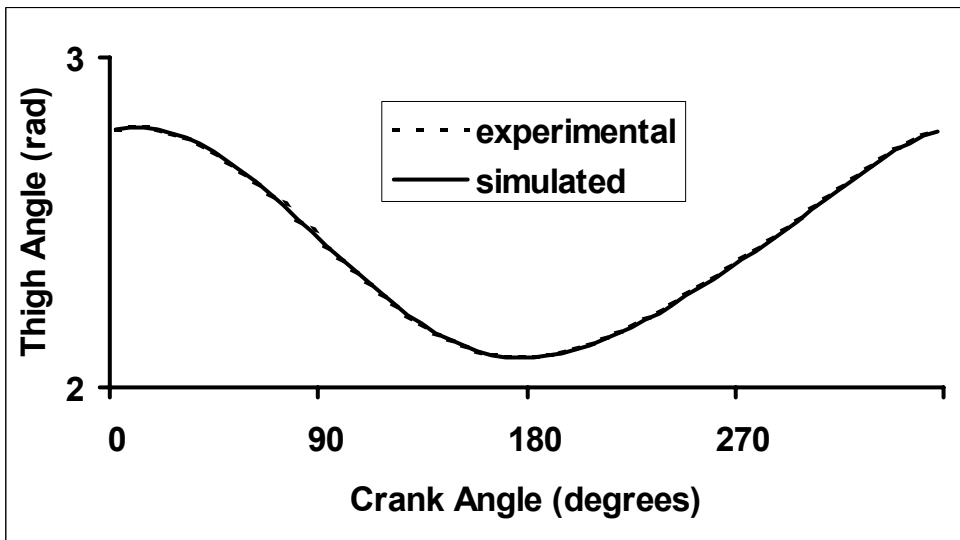


Figure F3. Experimental and simulated crank angular velocity at 60 rpm. The relative absolute deviation between the two profiles is 0.094%.

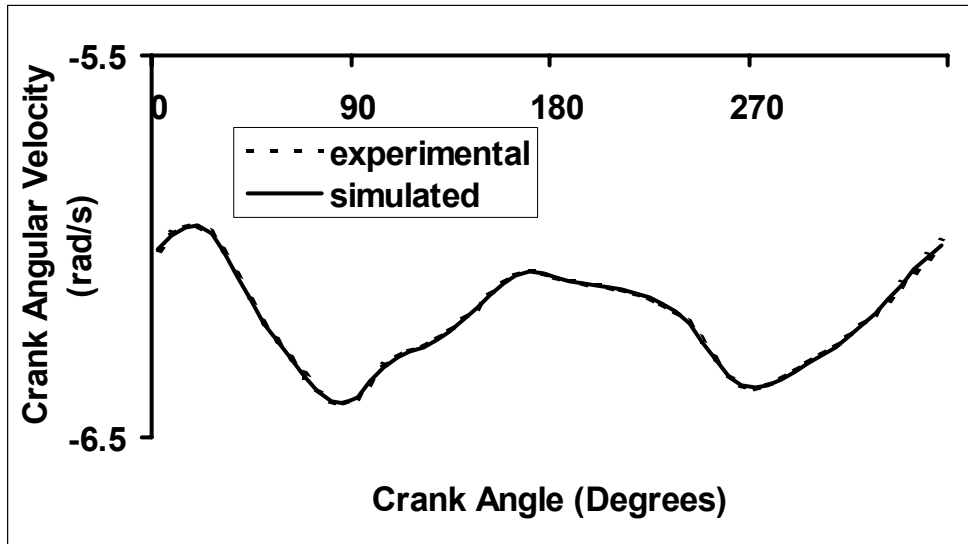


Figure F4. Experimental and simulated thigh angular velocity at 60 rpm. The relative absolute deviation between the two profiles is 0.027%.

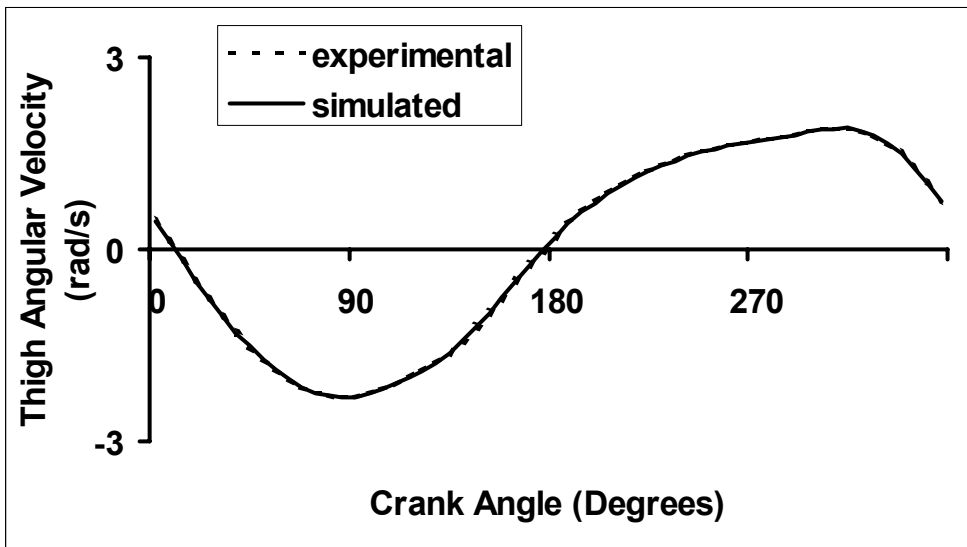


Figure F5. Experimental and simulated horizontal forces at 60 rpm. The relative absolute deviation between the two profiles is 1.518%.

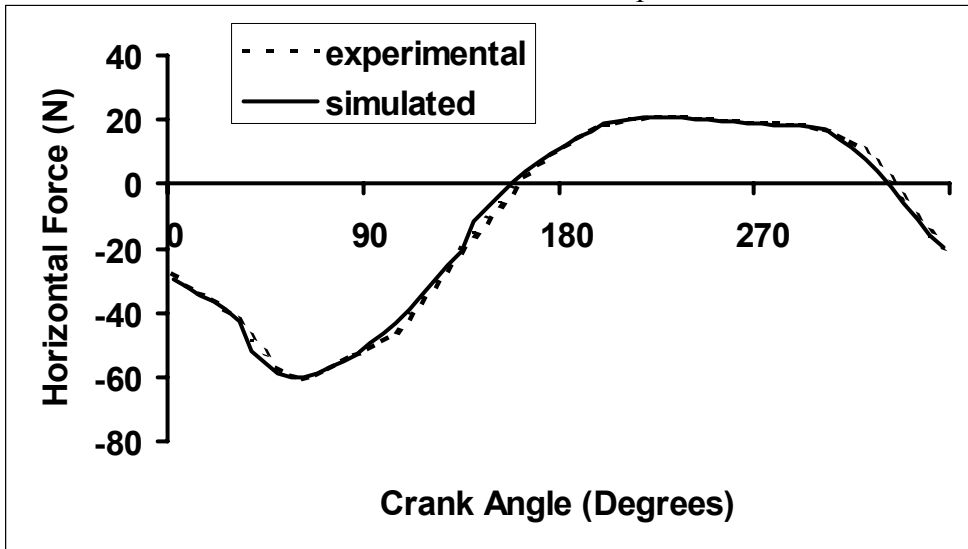


Figure F6. Experimental and simulated vertical forces at 60 rpm. The relative absolute deviation between the two profiles is 1.415%.

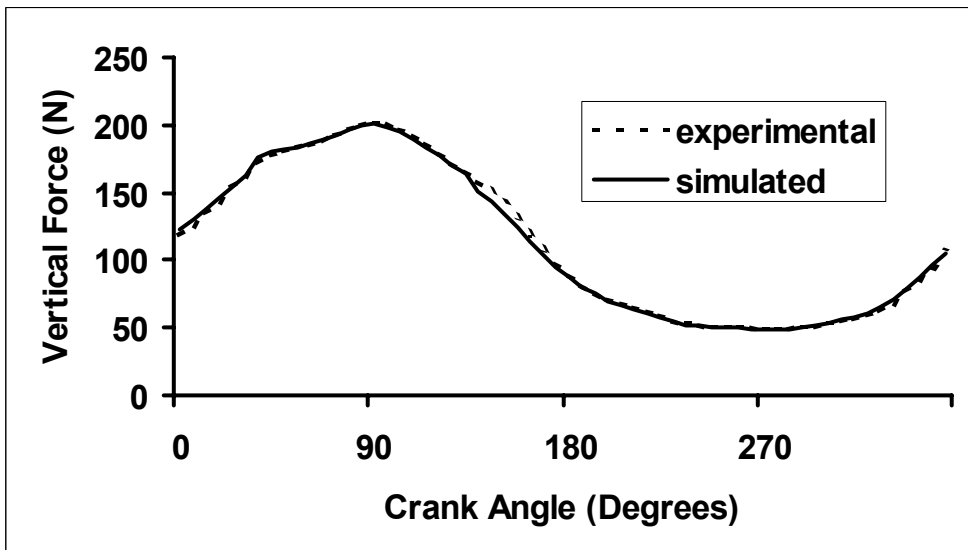


Figure F7. Experimental and simulated crank angle at 120 rpm. The relative absolute deviation between the two profiles is 0.0005%.

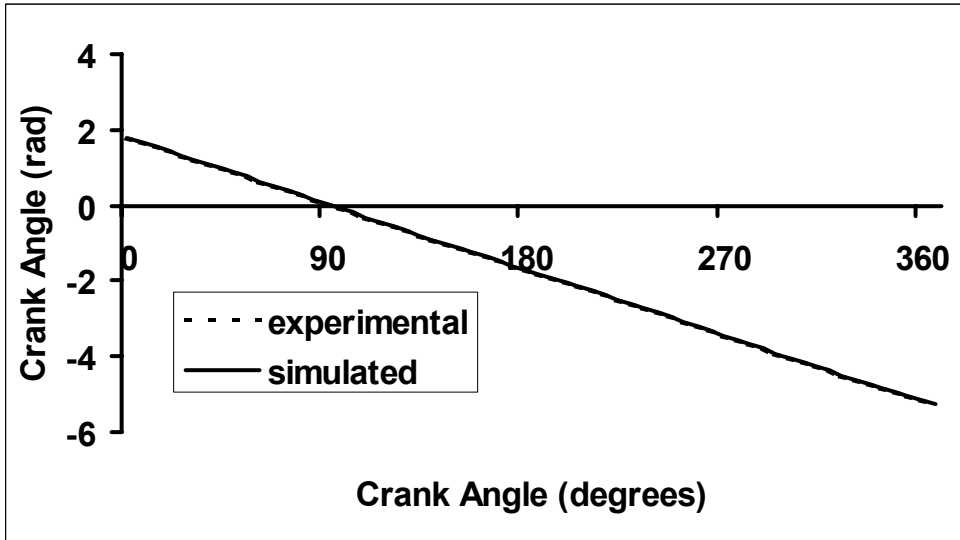


Figure F8. Experimental and simulated thigh angle at 120 rpm. The relative absolute deviation between the two profiles is 0.019%.

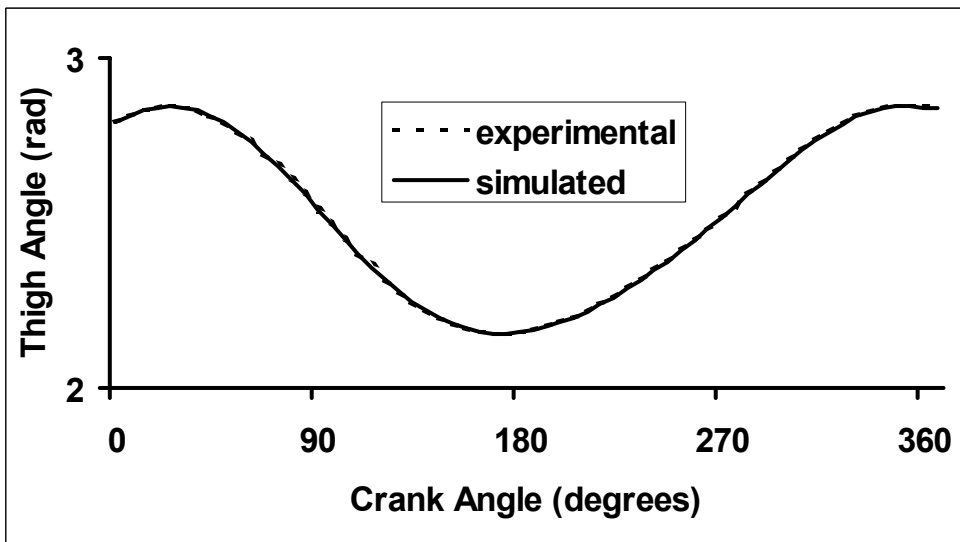


Figure F9. Experimental and simulated crank angular velocity at 120 rpm. The relative absolute deviation between the two profiles is 0.103%.

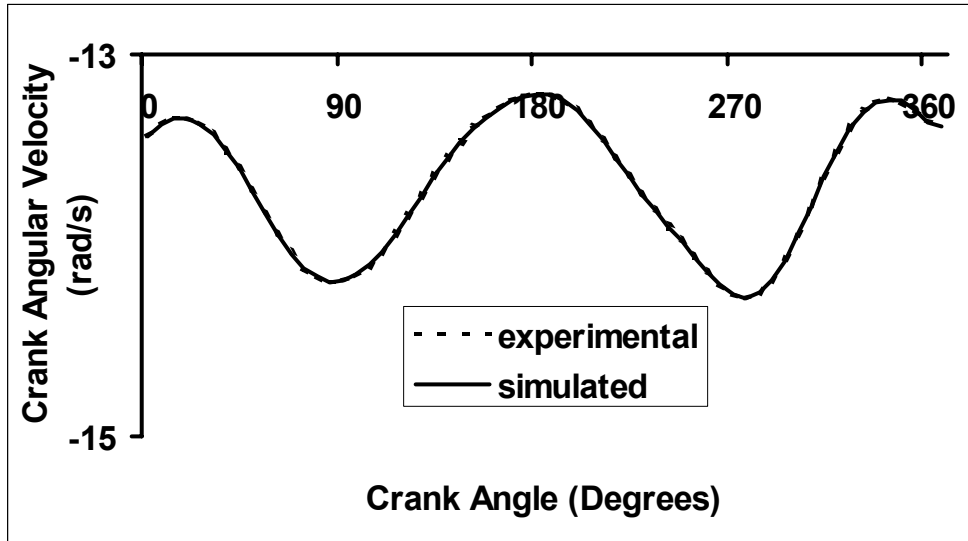


Figure F10. Experimental and simulated thigh angular velocity at 120 rpm. The relative absolute deviation between the two profiles is 0.028%.

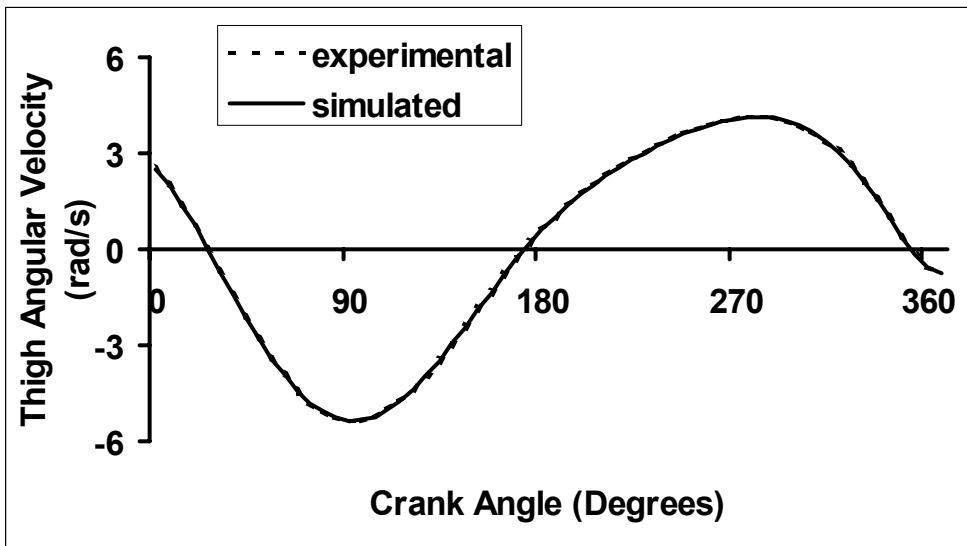


Figure F11. Experimental and simulated horizontal forces at 120 rpm. The relative absolute deviation between the two profiles is 1.432%.

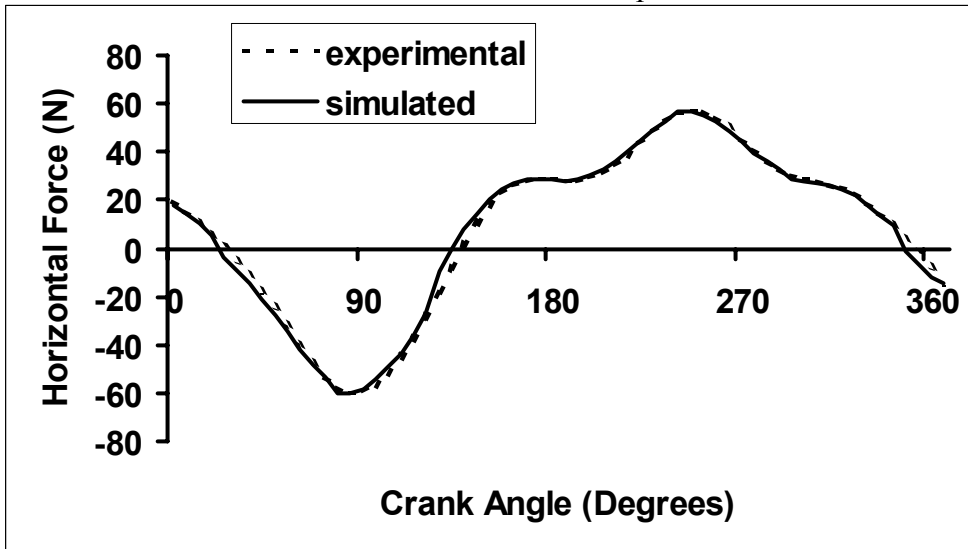
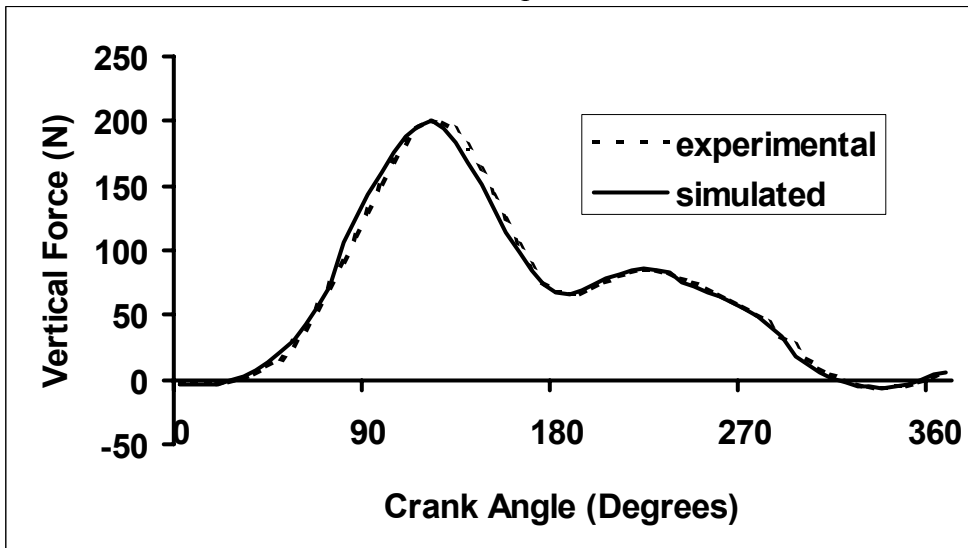


Figure F12. Experimental and simulated vertical forces at 120 rpm. The relative absolute deviation between the two profiles is 1.615%.



Appendix G: Extended Results – Study 2

Figure G1. Age-group differences in the muscular power contribution to crank power during the extensor phase. Means and standard deviations are shown for hypothetical preadolescents (anthro-PA), older children (anthro-OC) and younger children (anthro-YC) at 60 rpm and 120 rpm.

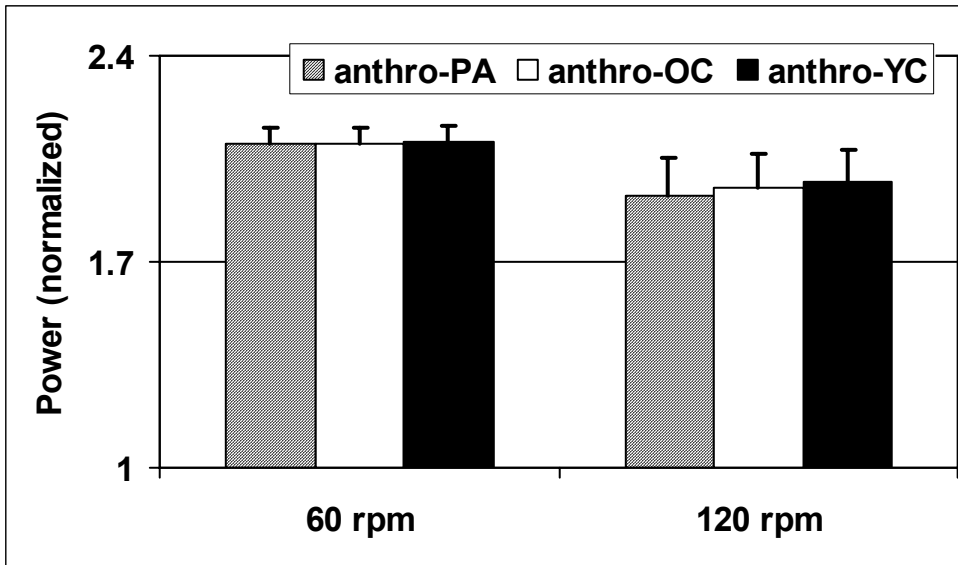


Figure G2. Age-group differences in the muscular power contribution to crank power during the flexor phase. Means and standard deviations are shown for hypothetical preadolescents (anthro-PA), older children (anthro-OC) and younger children (anthro-YC) at 60 rpm and 120 rpm.

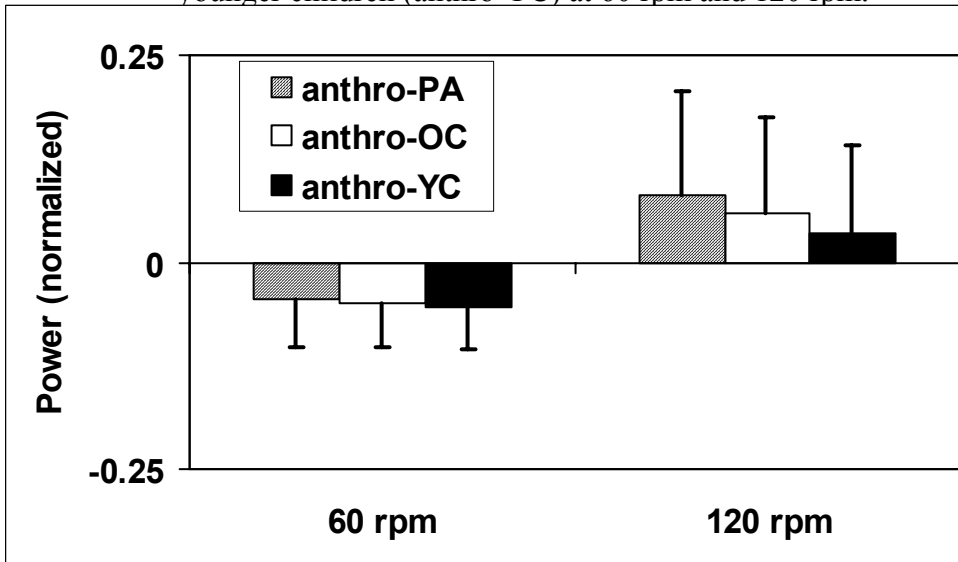


Figure G3. Age-group differences in the muscular power contribution to crank power during the top phase. Means and standard deviations are shown for hypothetical preadolescents (anthro-PA), older children (anthro-OC) and younger children (anthro-YC) at 60 rpm and 120 rpm.

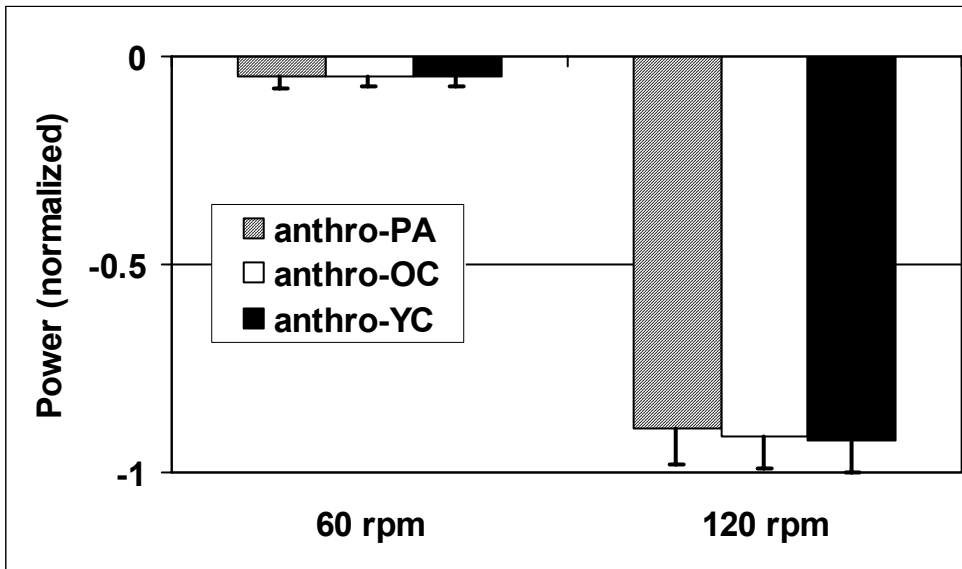


Figure G4. Age-group differences in the muscular power contribution to crank power during the bottom phase. Means and standard deviations are shown for hypothetical preadolescents (anthro-PA), older children (anthro-OC) and younger children (anthro-YC) at 60 rpm and 120 rpm.

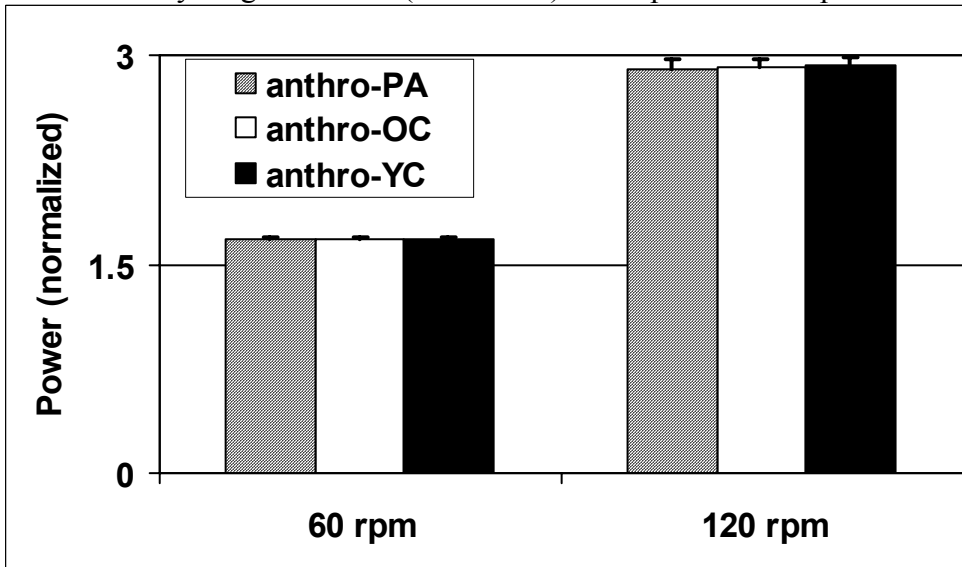


Figure G5. Age-group differences in the muscular power contribution to limb power during the extensor phase. Means and standard deviations are shown for hypothetical preadolescents (anthro-PA), older children (anthro-OC) and younger children (anthro-YC) at 60 rpm and 120 rpm.

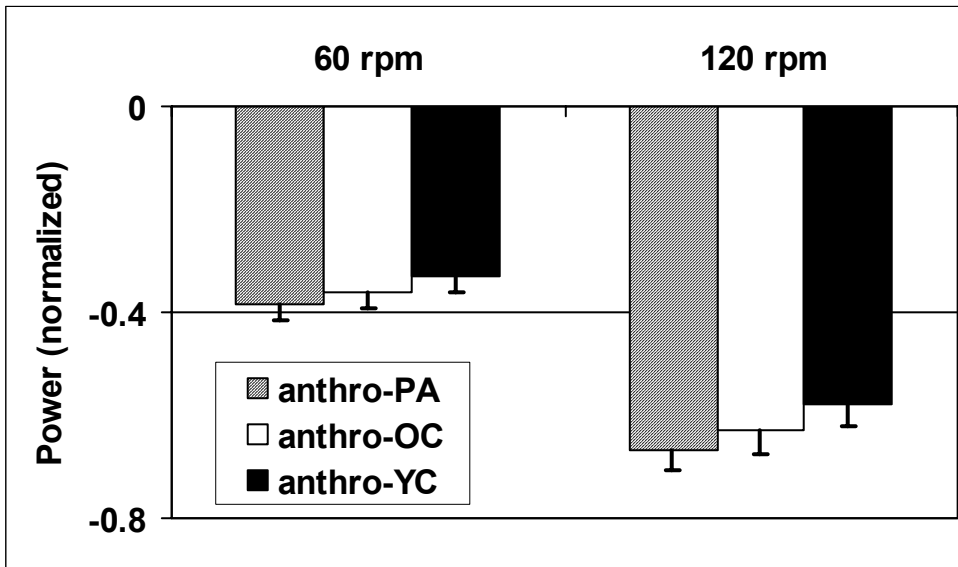


Figure G6. Age-group differences in the muscular power contribution to limb power during the flexor phase. Means and standard deviations are shown for hypothetical preadolescents (anthro-PA), older children (anthro-OC) and younger children (anthro-YC) at 60 rpm and 120 rpm.

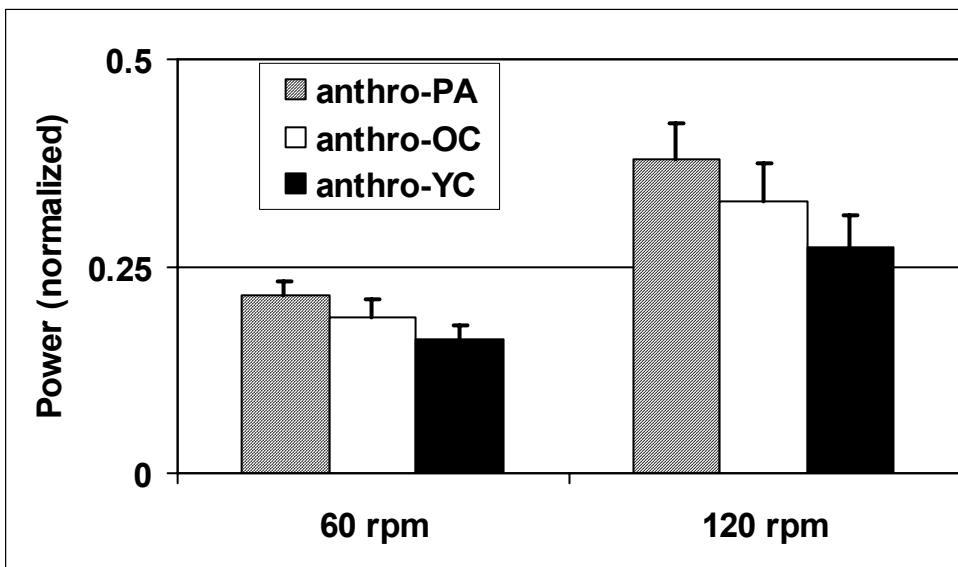


Figure G7. Age-group differences in the muscular power contribution to limb power during the top phase. Means and standard deviations are shown for hypothetical preadolescents (anthro-PA), older children (anthro-OC) and younger children (anthro-YC) at 60 rpm and 120 rpm.

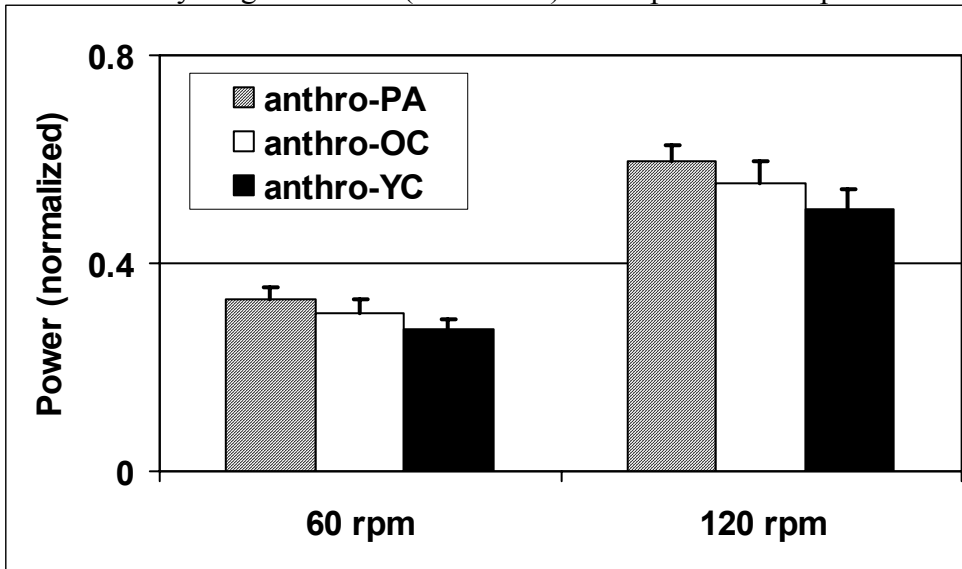
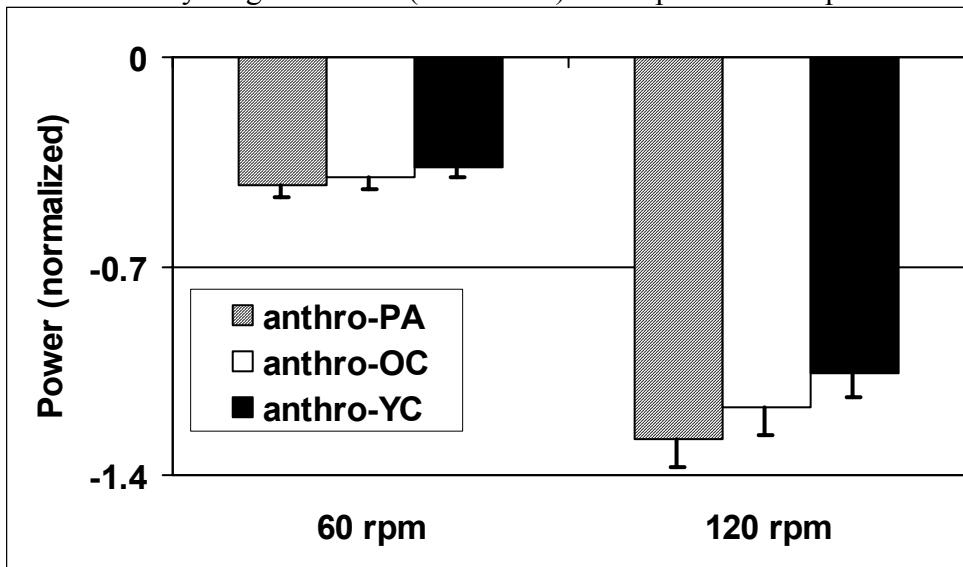


Figure G8. Age-group differences in the muscular power contribution to limb power during the bottom phase. Means and standard deviations are shown for hypothetical preadolescents (anthro-PA), older children (anthro-OC) and younger children (anthro-YC) at 60 rpm and 120 rpm.



Appendix H: Sensitivity Analysis for Bilateral Asymmetry – Study 3

To test the effect of bilateral asymmetry on the dependent measures, a sensitivity analysis was performed. For this sensitivity analysis, the trial with the greatest accepted bilateral asymmetry – observed in a YC at 60 rpm – was chosen. For this trial, the power produced by the ipsilateral leg was scaled to 50%, 42.5%, and 57.5% of the external power output. The following power profiles are presented:

- net ankle power (Figure H1)
- net knee power (Figure H2)
- net hip power (Figure H3)
- net muscular power (Figure H4)
- hip power contribution to limb power (Figure H4)
- indirect ankle power contribution to crank power (Figure H5)
- direct knee power contribution to crank power (Figure H6)

In addition, the dependent measures for all asymmetry conditions are presented in Table H1). In this table, the maximum deviation of the 42.5% and 57.5% conditions from the 50% condition is presented and compared to the standard deviation in the AD group for the corresponding dependent measure. The deviation of the 42.5% and 57.5% conditions from the 50% condition was always less than 50% of one standard deviation of the corresponding dependent variable in the adult group.

Figure H1. Net muscular power at the ankle joint for the three asymmetry conditions.

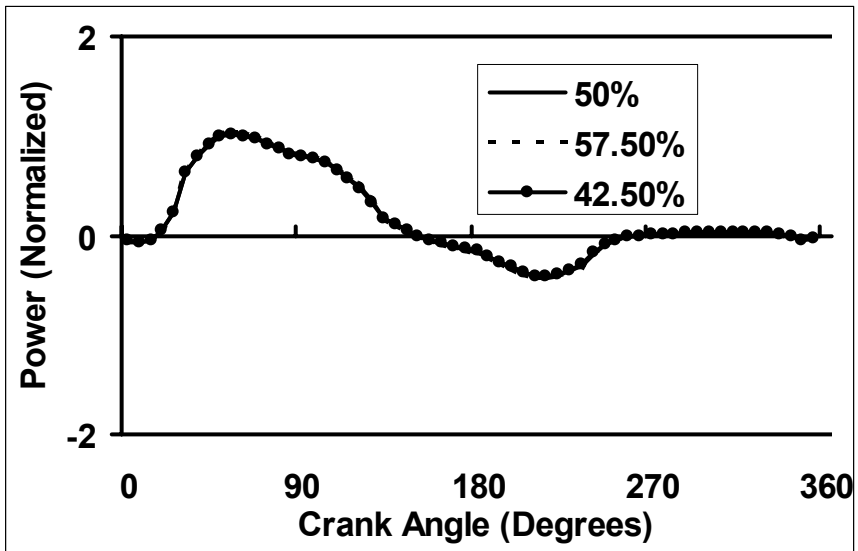


Figure H2. Net muscular power at the knee joint for the three asymmetry conditions.

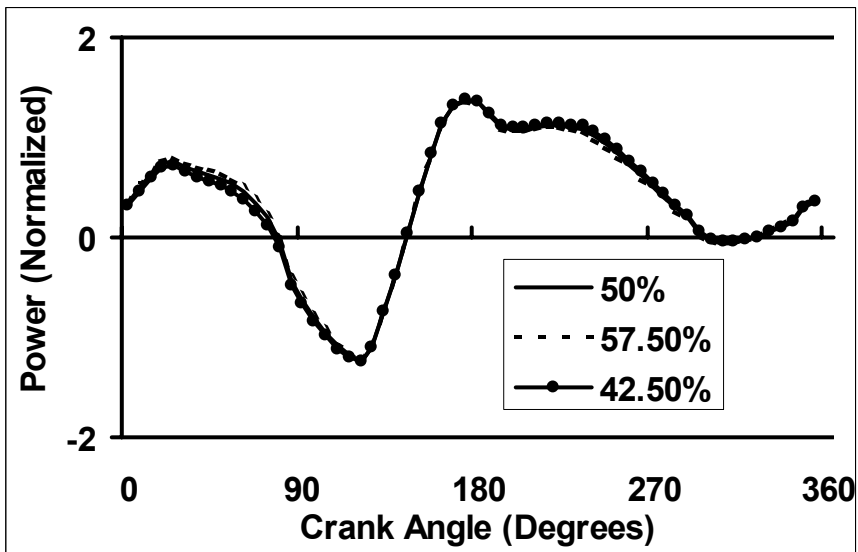


Figure H3. Net muscular power at the hip joint for the three asymmetry conditions.

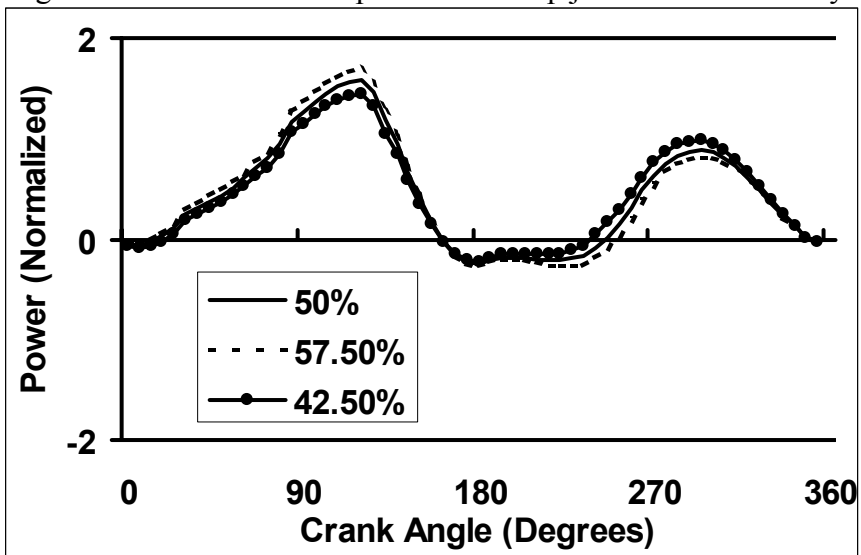


Figure H4. Net muscular power for the three asymmetry conditions.

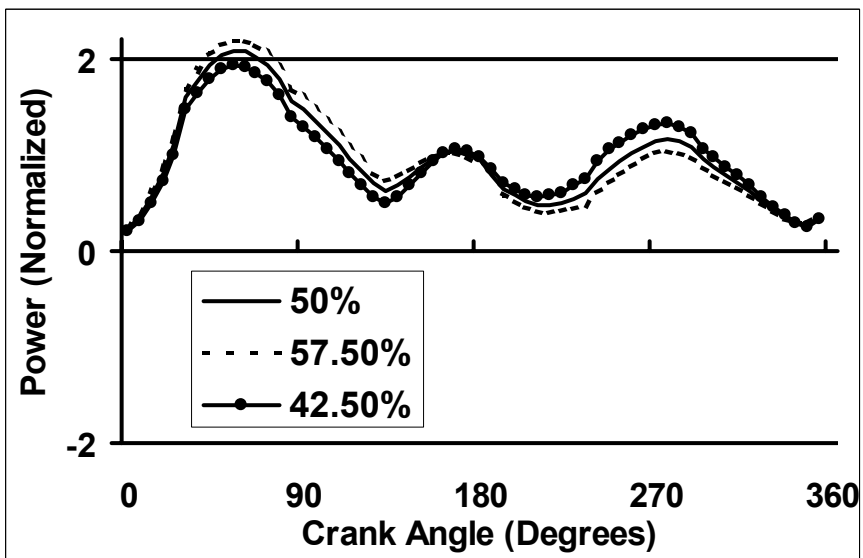


Figure H5. Hip power contribution to limb power for the three asymmetry conditions.

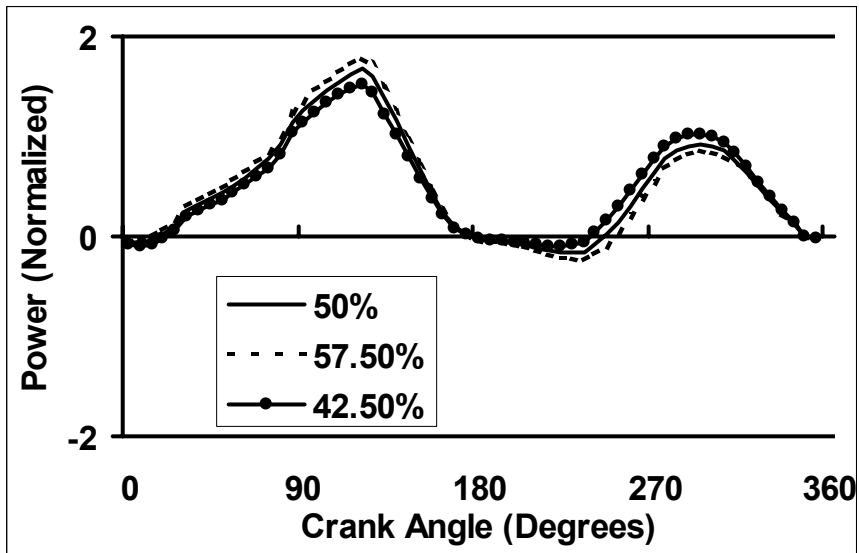


Figure H6. Ankle power contribution to limb power for the three asymmetry conditions.

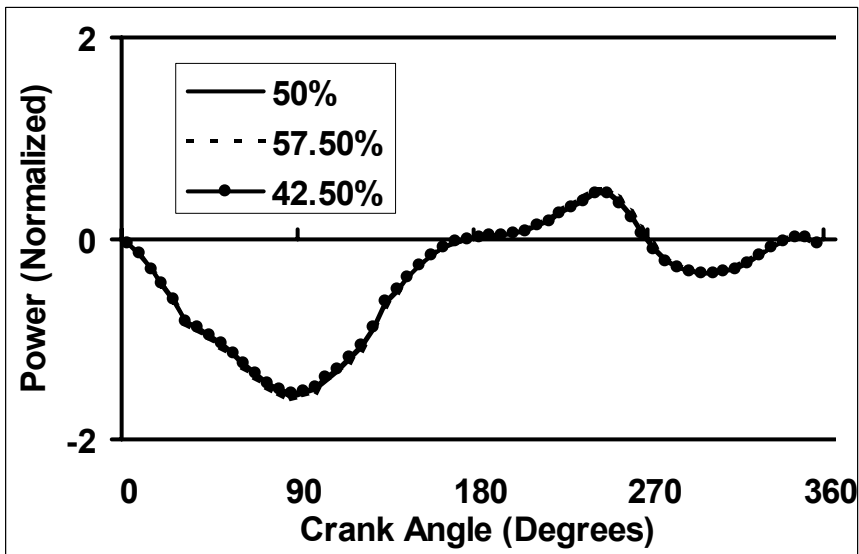


Figure H7. Direct knee power contribution to crank power for the three asymmetry conditions.

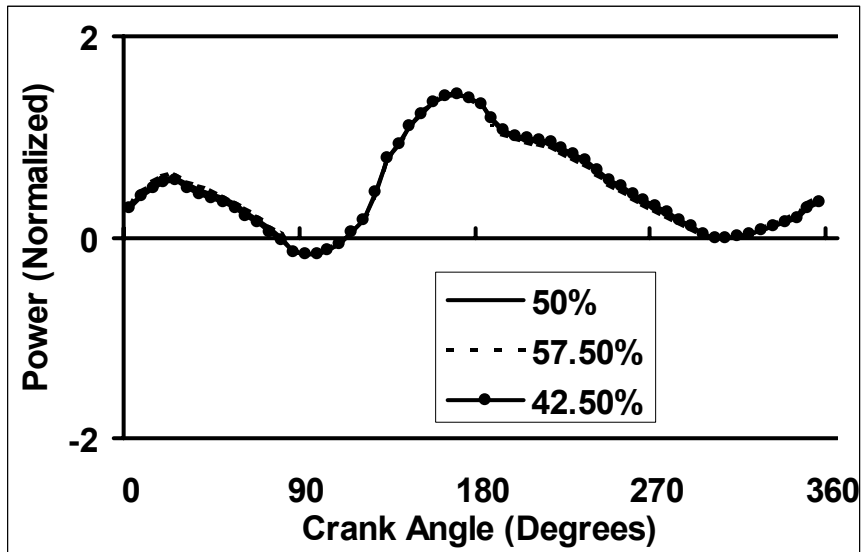


Table H1. Effect of bilateral asymmetry on the dependent variables used in Study 3. The unit for all values is normalized power, except for those in the last column which quantify the effect of bilateral asymmetry as a percentage of the standard deviation in the adult (AD) group. Power profiles were averaged across 4 regions of the crank cycle: extensor (EXT), flexor (FLEX), top (TOP), and bottom (BOT).

		50%	57.5%	42.5%	Maximum absolute deviation	Standard deviation (SD) in AD group	Maximum absolute deviation as a percentage of SD in AD group
Peak power ankle		1.03	1.04	1.02	0.01	0.38	3.90
Peak power knee		1.37	1.36	1.37	0.00	0.64	0.72
Peak power hip		1.58	1.68	1.45	0.13	0.38	35.10
Net muscular power	EXT	1.15	1.22	1.04	0.10	0.26	40.38
	FLEX	0.83	0.76	0.91	0.09	0.22	40.15
	TOP	0.72	0.66	0.80	0.07	0.17	42.90
	BOT	1.05	1.10	0.98	0.07	0.15	44.23
Hip power contribution to limb power	EXT	0.60	0.64	0.54	0.06	0.26	22.69
	FLEX	0.33	0.30	0.38	0.05	0.11	44.04
	TOP	0.33	0.29	0.40	0.06	0.15	42.64
	BOT	0.70	0.75	0.63	0.07	0.25	27.38
Ankle power contribution to limb power	EXT	-0.82	-0.83	-0.81	0.01	0.15	8.20
	FLEX	-0.02	-0.01	-0.03	0.01	0.12	5.93
	TOP	-0.07	-0.07	-0.08	0.01	0.17	4.52
	BOT	-0.66	-0.67	-0.65	0.01	0.18	5.82
Direct knee power contribution to crank power	EXT	0.22	0.23	0.20	0.02	0.22	9.73
	FLEX	0.73	0.72	0.74	0.01	0.19	7.04
	TOP	0.31	0.31	0.31	0.00	0.05	3.67
	BOT	0.65	0.65	0.64	0.00	0.13	2.00

Appendix I: Extended Results - Study 3

Figure I1. Net muscular power at the ankle joint for adults (AD), older children (OC), and younger children (YC) at 5 different cadences. The data for each age group are averaged across group members.

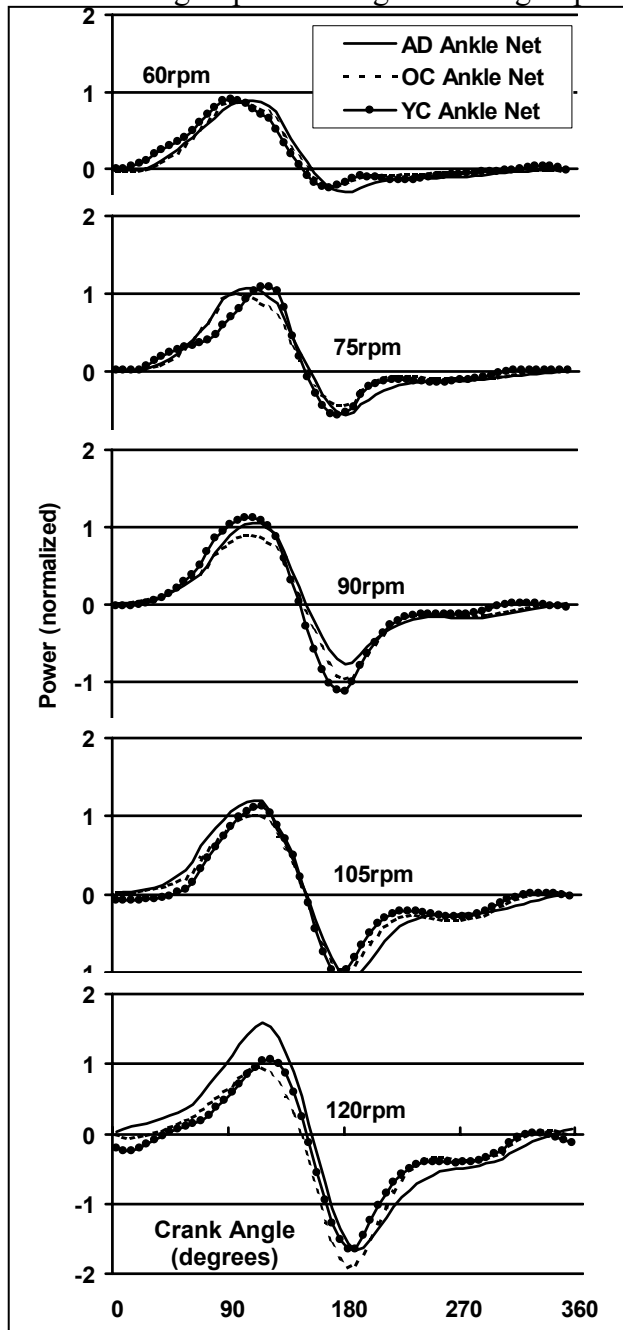


Figure I2. Net muscular power at the knee joint for adults (AD), older children (OC), and younger children (YC) at 5 different cadences. The data for each age group are averaged across group members.

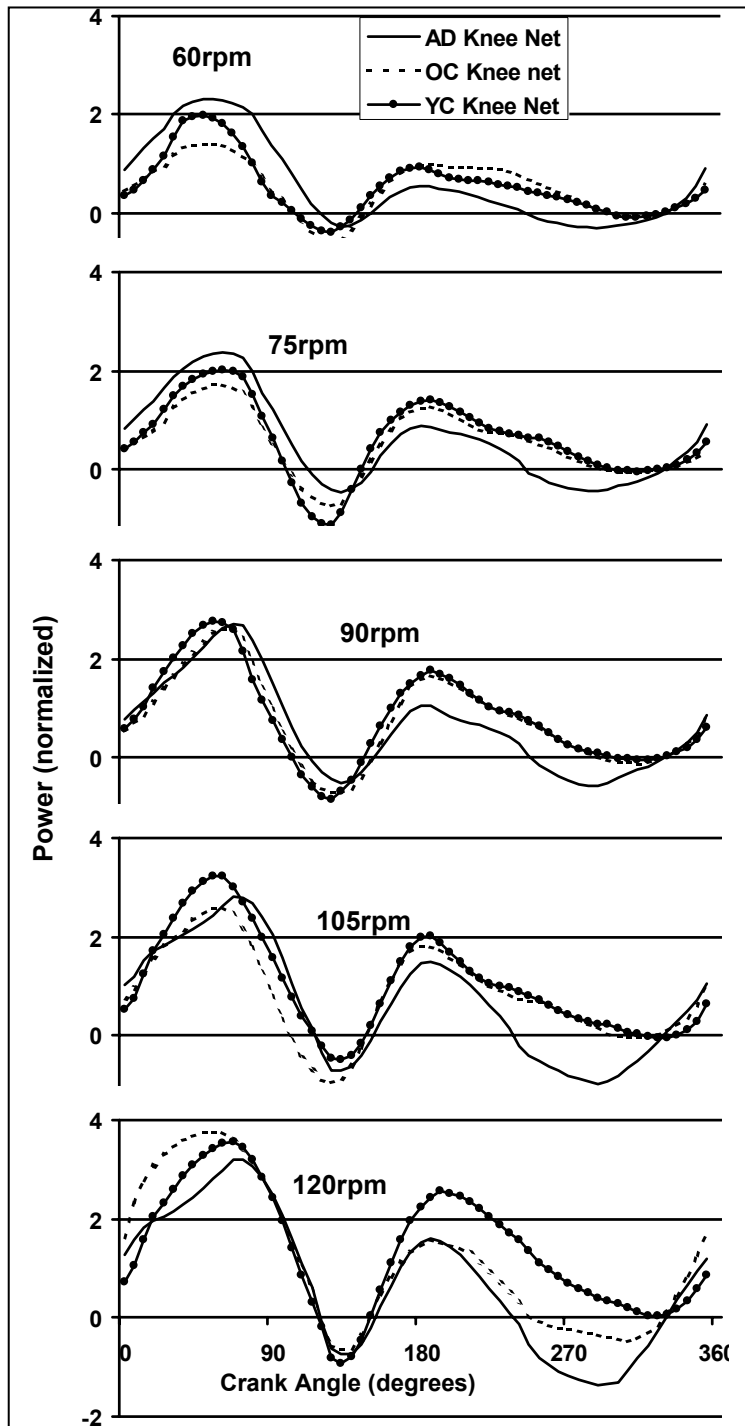


Figure I3. Net muscular power at the hip joint for adults (AD), older children (OC), and younger children (YC) at 5 different cadences. The data for each age group are averaged across group members.

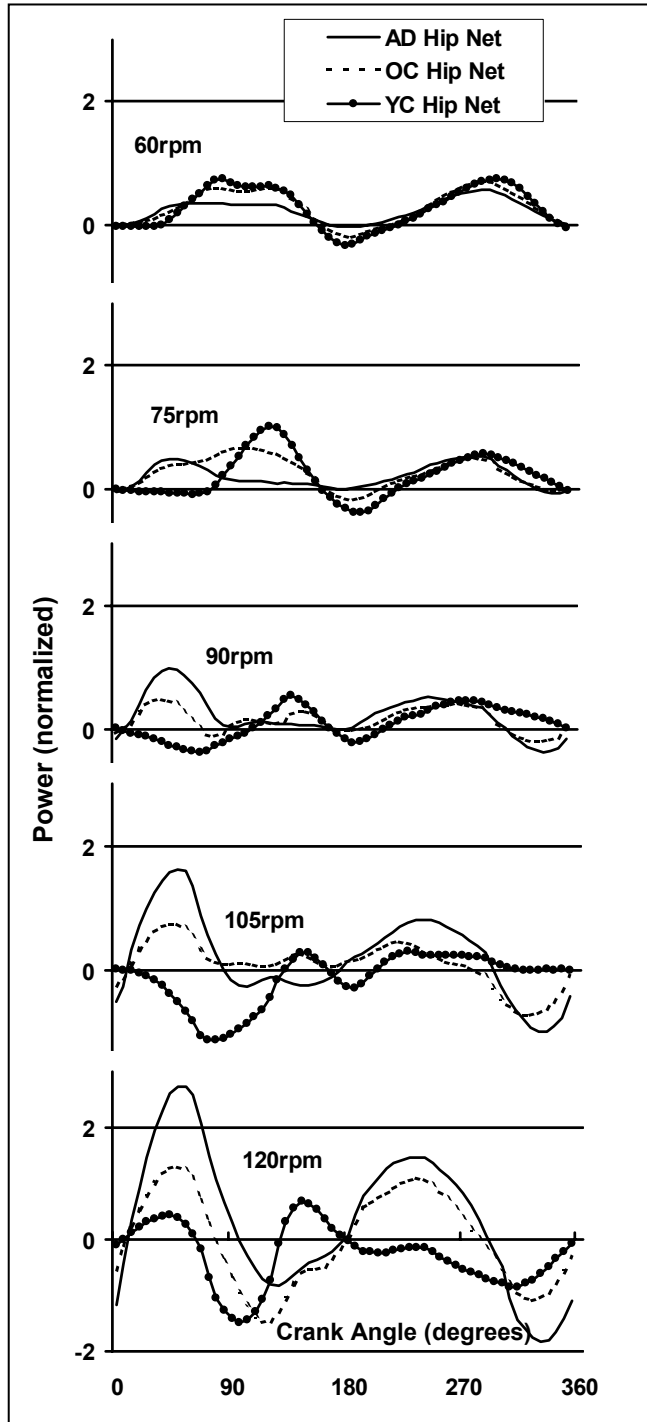


Figure I4. Effect of cadence on peak power at the ankle (A), knee (B), and hip (C) joints. The symbol “*” indicates a significant age-effect at the corresponding cadence. Means and standard deviations are plotted for adults (AD), older children (OC), and younger children (YC).

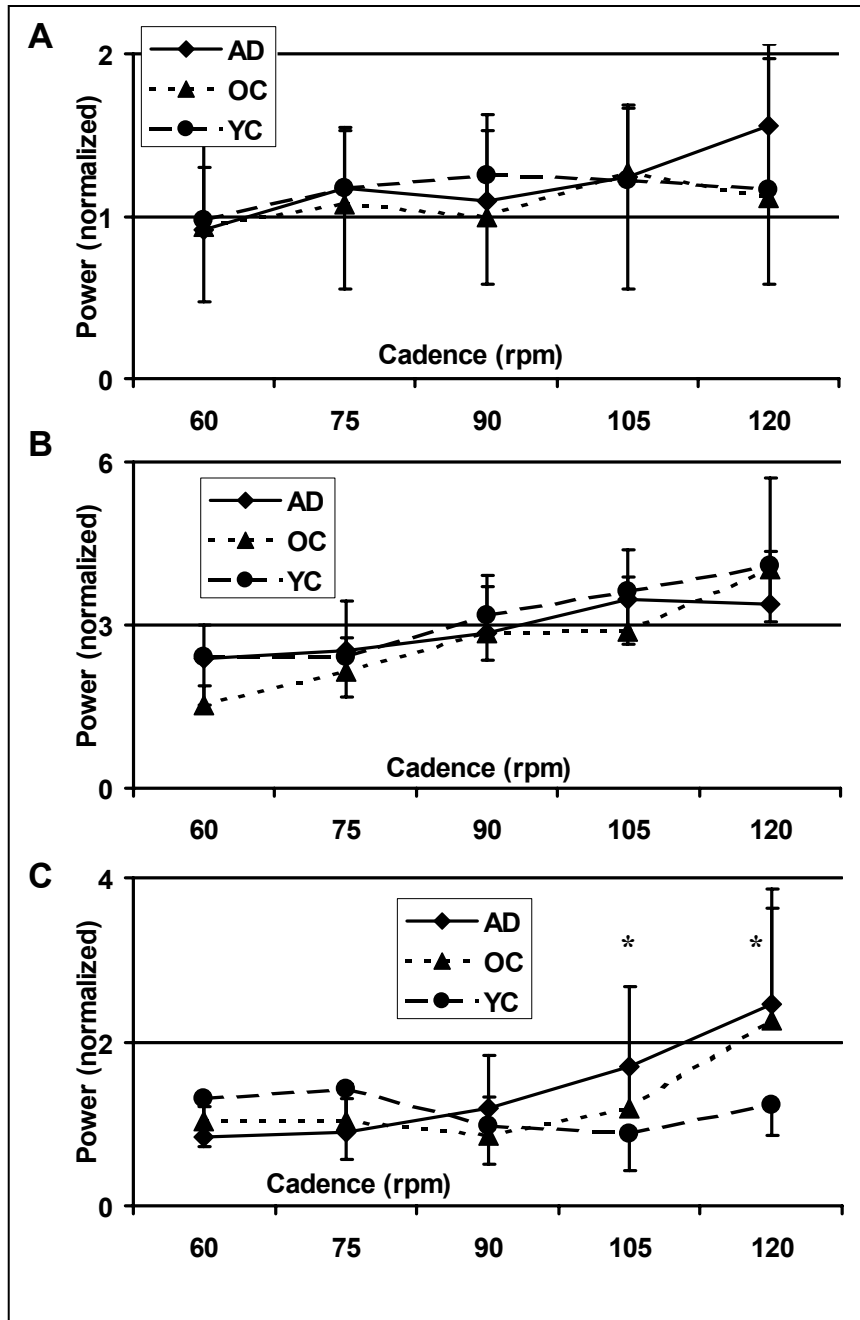


Figure I5. Net muscular power for adults (AD), older children (OC), and younger children (YC) at 5 different cadences. The data for each age group are averaged across participants.

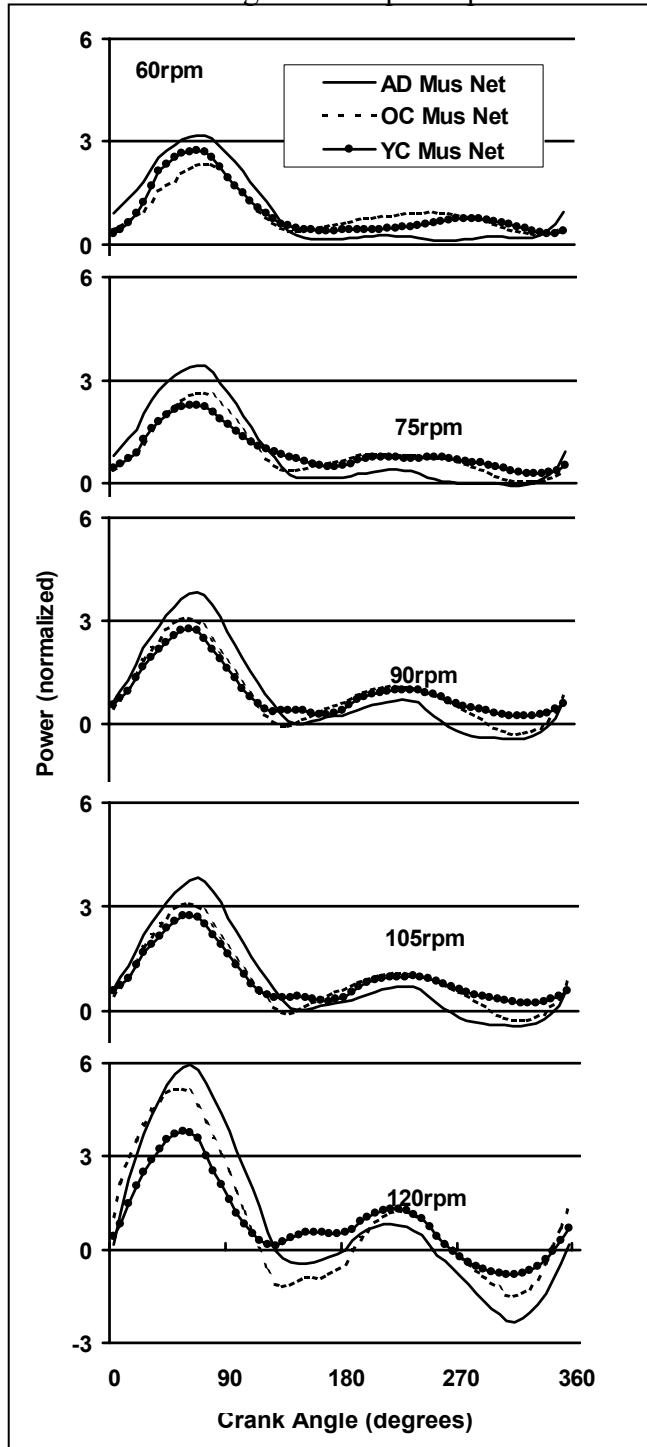


Figure I6. Effect of age and cadence on net muscular power during the extensor phase (EXT). The age-effect was statistically significant (“*”) at all cadences. Means and standard deviations are plotted for adults (AD), older children (OC), and younger children (YC).

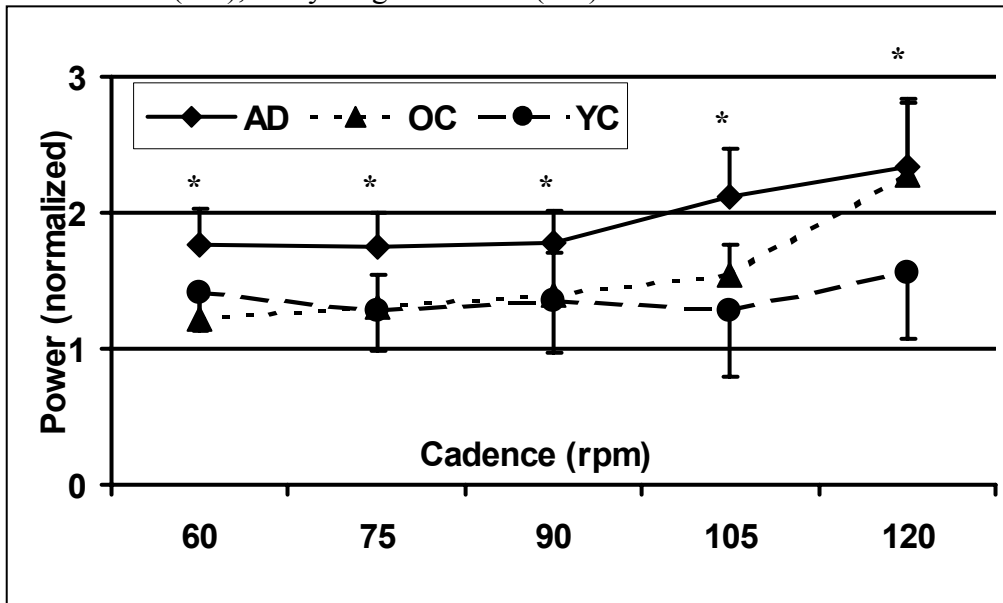


Figure I7. Effect of age and cadence on net muscular power during the flexor phase (FLEX). The Age x Cadence interaction was statistically non-significant. Means and standard deviations are plotted for adults (AD), older children (OC), and younger children (YC).

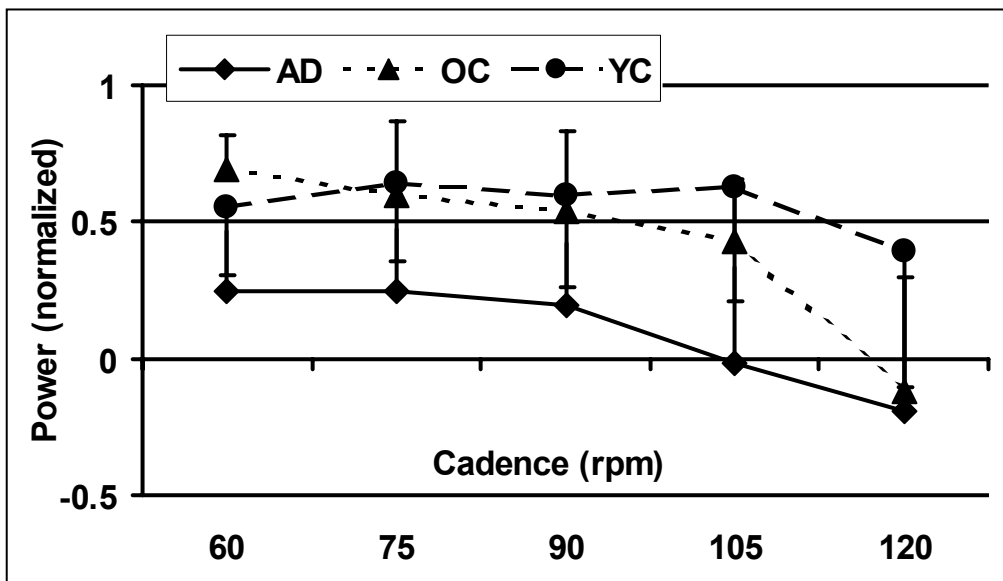


Figure I8. Effect of age and cadence on net muscular power during the top phase (TOP). The symbol “*” indicates a significant age-effect at the corresponding cadence. Means and standard deviations are plotted for adults (AD), older children (OC), and younger children (YC).

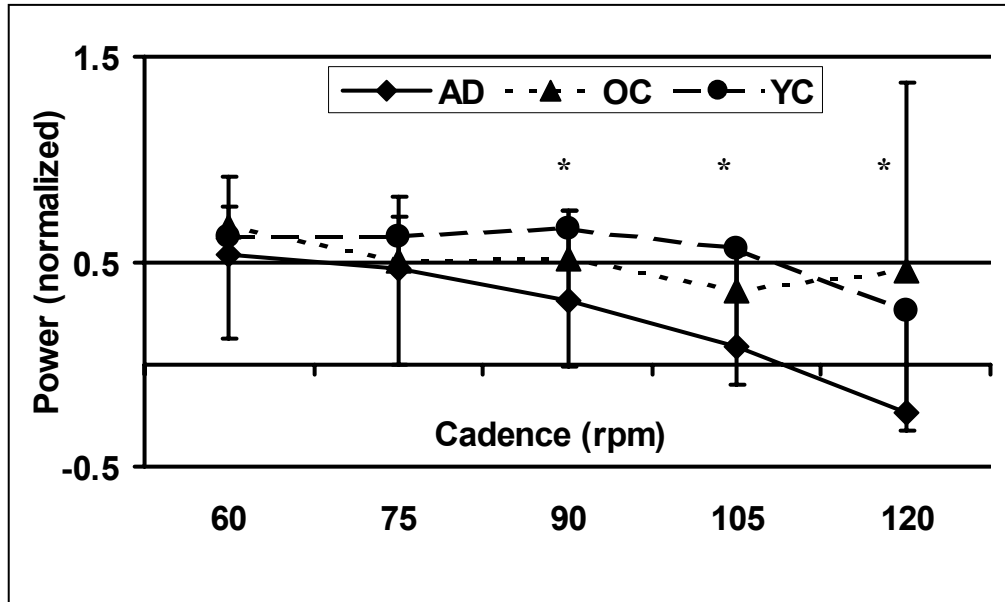


Figure I9. Effect of age and cadence on net muscular power during the bottom phase (BOT). The symbol “*” indicates a significant age-effect at the corresponding cadence. Means and standard deviations are plotted for adults (AD), older children (OC), and younger children (YC).

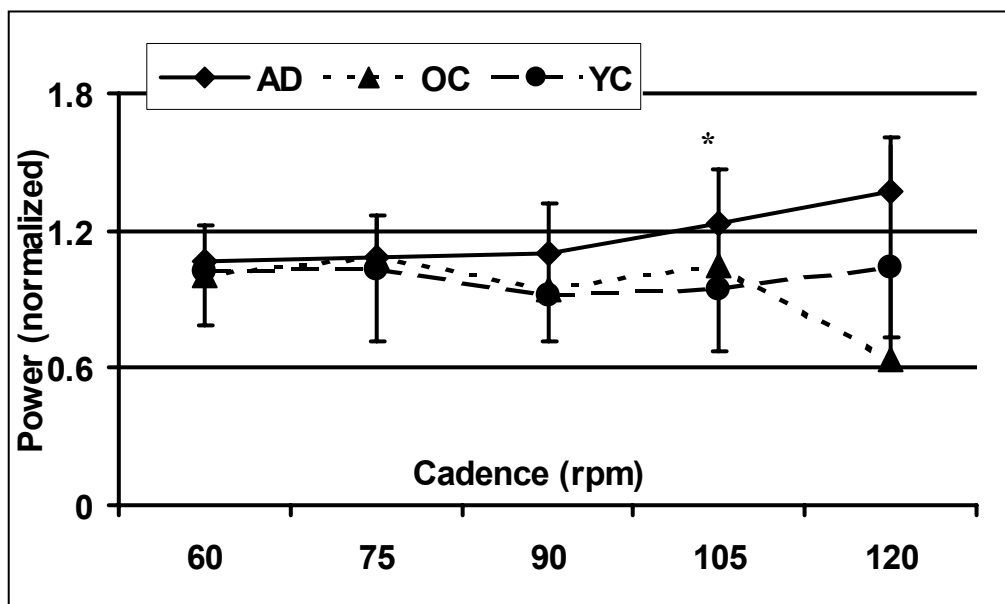


Figure I10. Hip power contribution to limb power for adults (AD), older children (OC), and younger children (YC) at 5 different cadences. The data for each age group are averaged across group members.

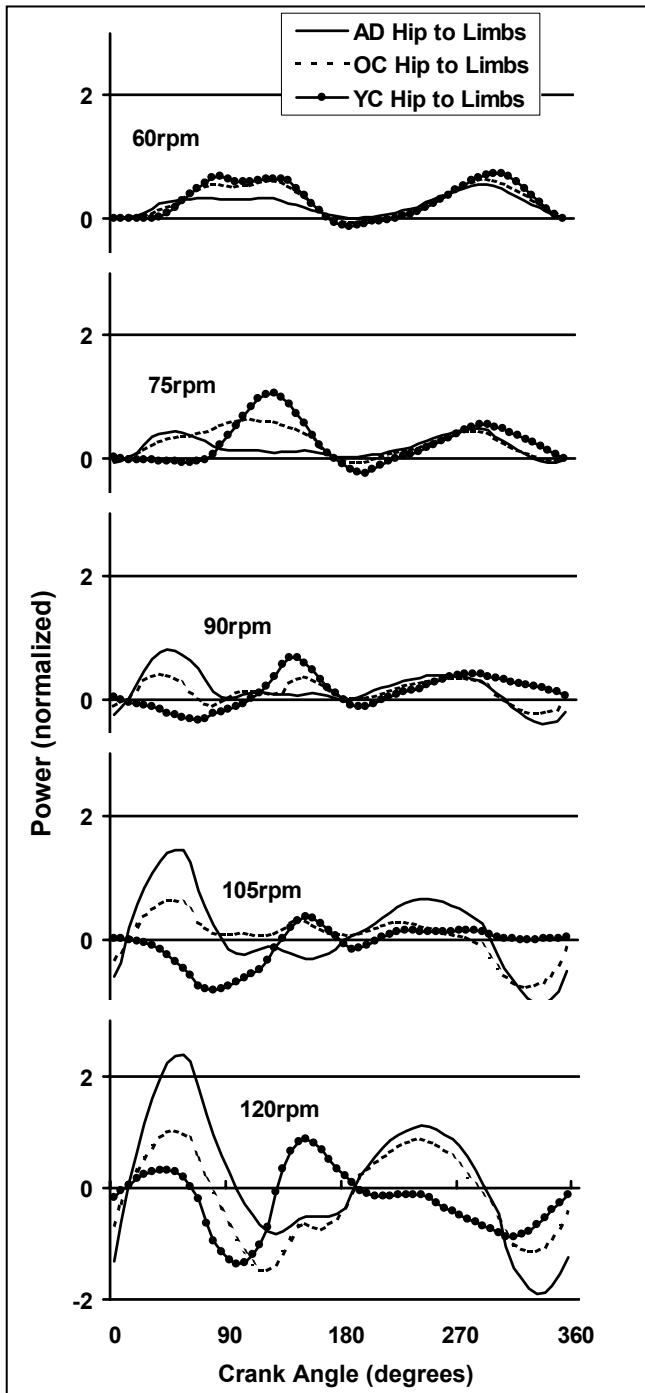


Figure I11. Effect of age and cadence on the hip power contribution to limb power during the extensor phase (EXT). The symbol “*” indicates a significant age-effect at the corresponding cadence. Means and standard deviations are plotted for adults (AD), older children (OC), and younger children (YC).

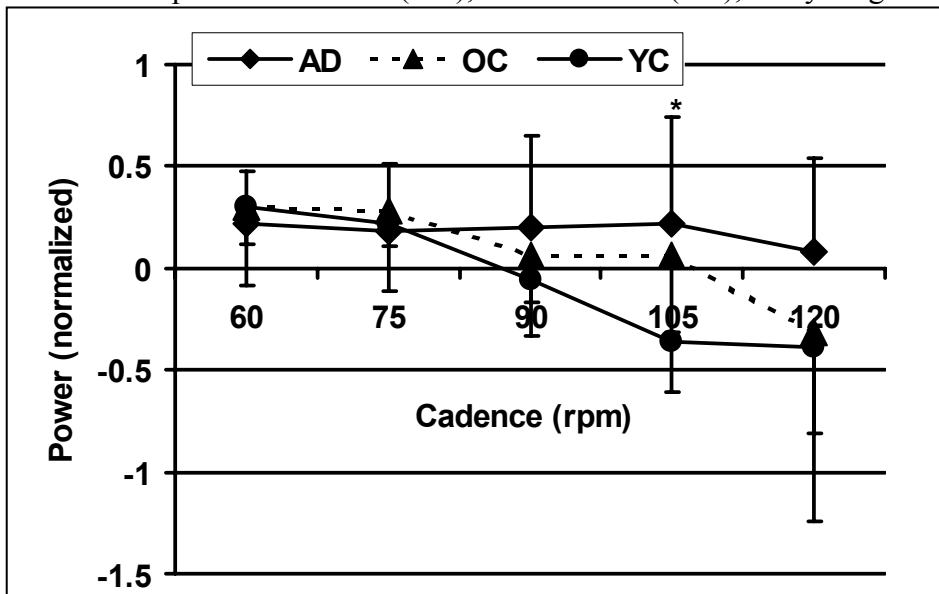


Figure I12. Effect of age and cadence on the hip power contribution to limb power during the flexor phase (FLEX). The Age x Cadence interaction was statistically non-significant. Means and standard deviations are plotted for adults (AD), older children (OC), and younger children (YC).

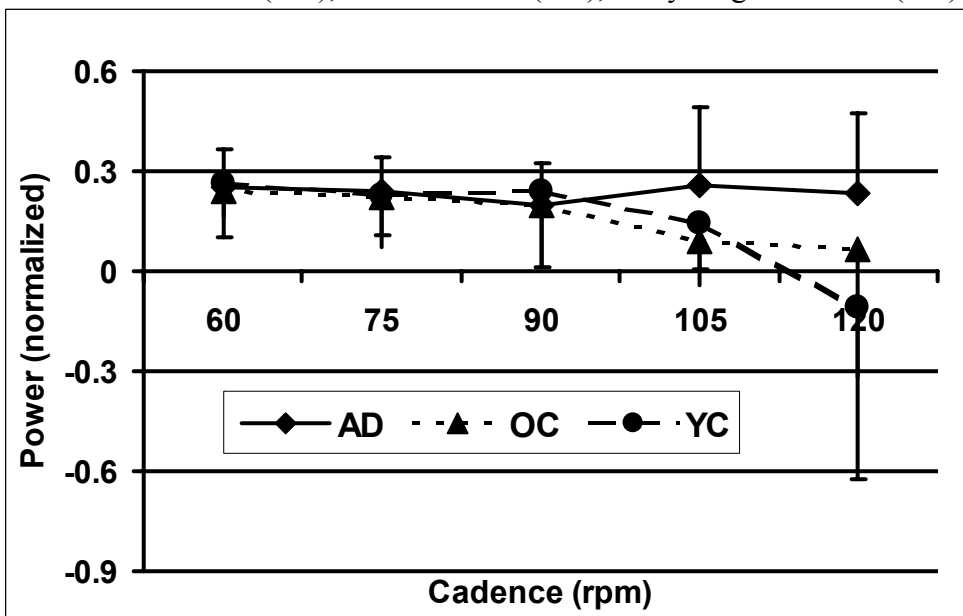


Figure I13. Effect of age and cadence on the hip power contribution to limb power during the top phase (TOP). The Age x Cadence interaction was statistically non-significant. Means and standard deviations are plotted for adults (AD), older children (OC), and younger children (YC).

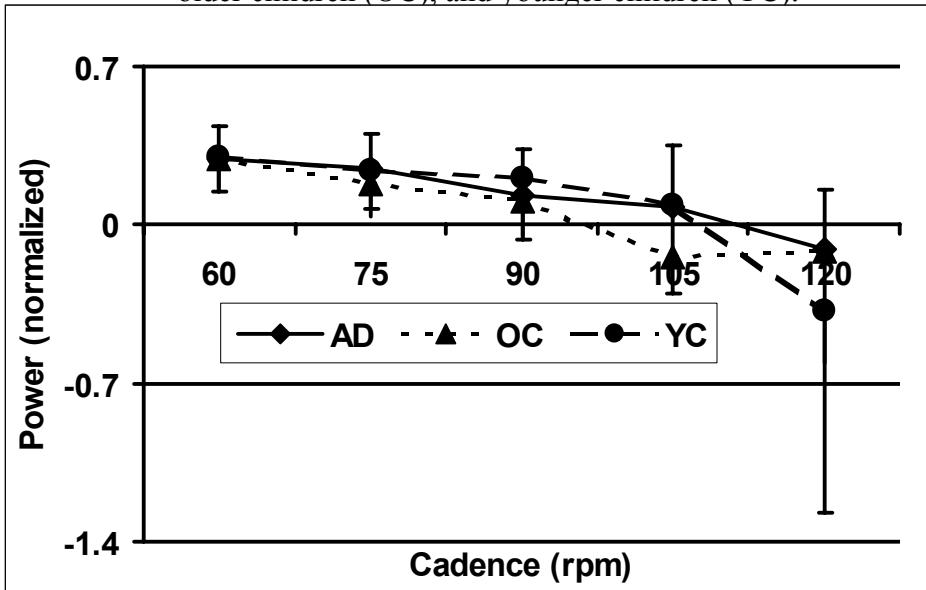


Figure I14. Effect of age and cadence on the hip power contribution to limb power during the bottom phase (BOT). The Age x Cadence interaction was statistically non-significant. Means and standard deviations are plotted for adults (AD), older children (OC), and younger children (YC).

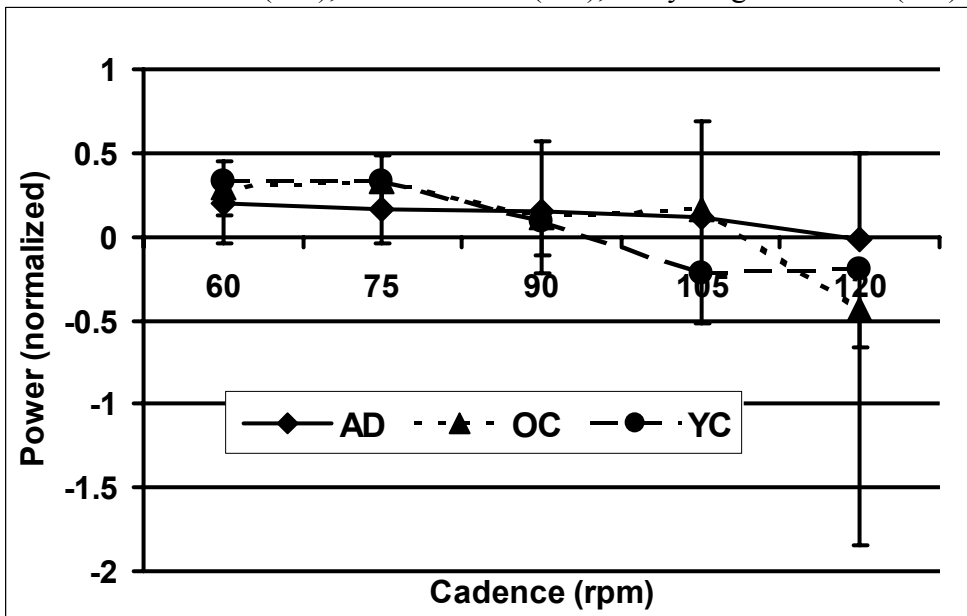


Figure I15. Knee joint power contribution to crank power for adults (AD), older children (OC), and younger children (YC) at 5 different cadences. The data for each age group are averaged across participants.

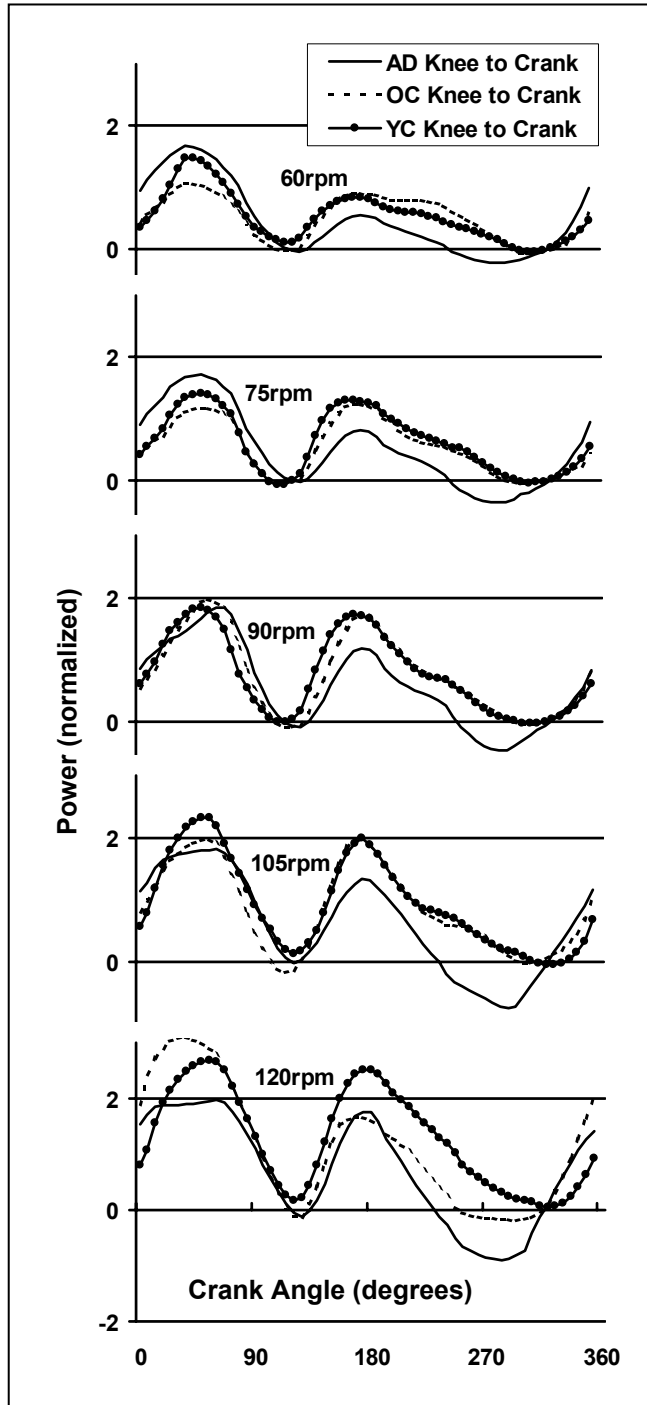


Figure I16. Effect of age and cadence on the knee power contribution to crank power during the extensor phase (EXT). The Age x Cadence interaction was statistically non-significant. Means and standard deviations are plotted for adults (AD), older children (OC), and younger children (YC).

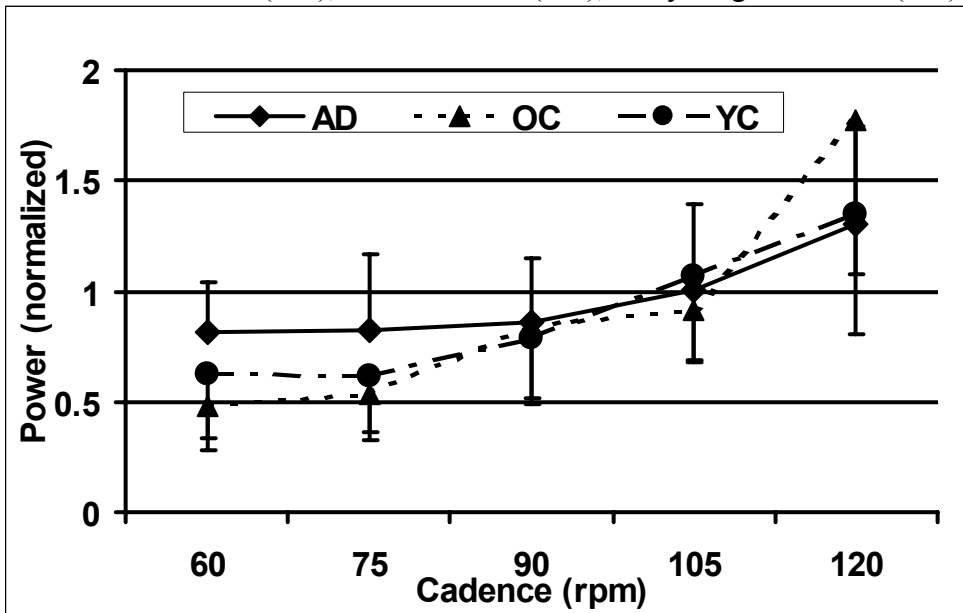


Figure I17. Effect of age and cadence on the knee power contribution to crank power during the flexor phase (FLEX). The Age x Cadence interaction was statistically non-significant. Means and standard deviations are plotted for adults (AD), older children (OC), and younger children (YC).

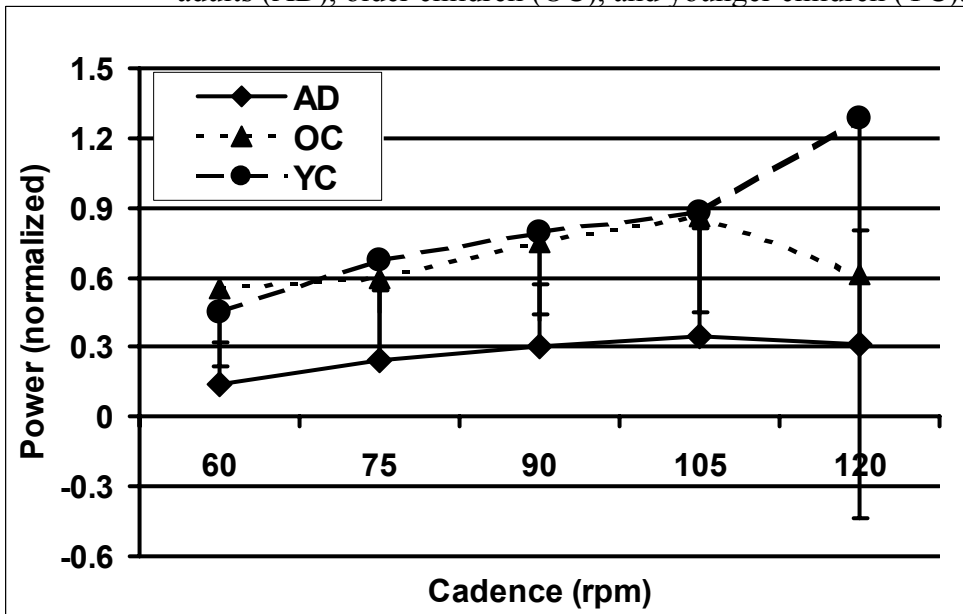


Figure I18. Effect of age and cadence on the knee power contribution to crank power during the top phase (TOP). The symbol “*” indicates a significant age-effect at the corresponding cadences. Means and standard deviations are plotted for adults (AD), older children (OC), and younger children (YC).

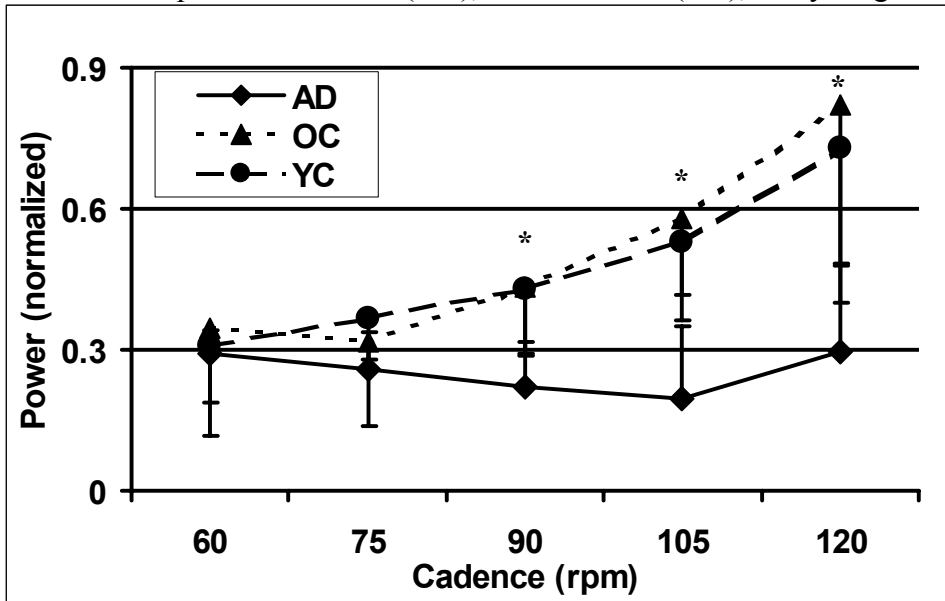


Figure I19. Effect of age and cadence on the knee power contribution to crank power during the bottom phase (BOT). The Age x Cadence interaction was statistically non-significant. Means and standard deviations are plotted for adults (AD), older children (OC), and younger children (YC).

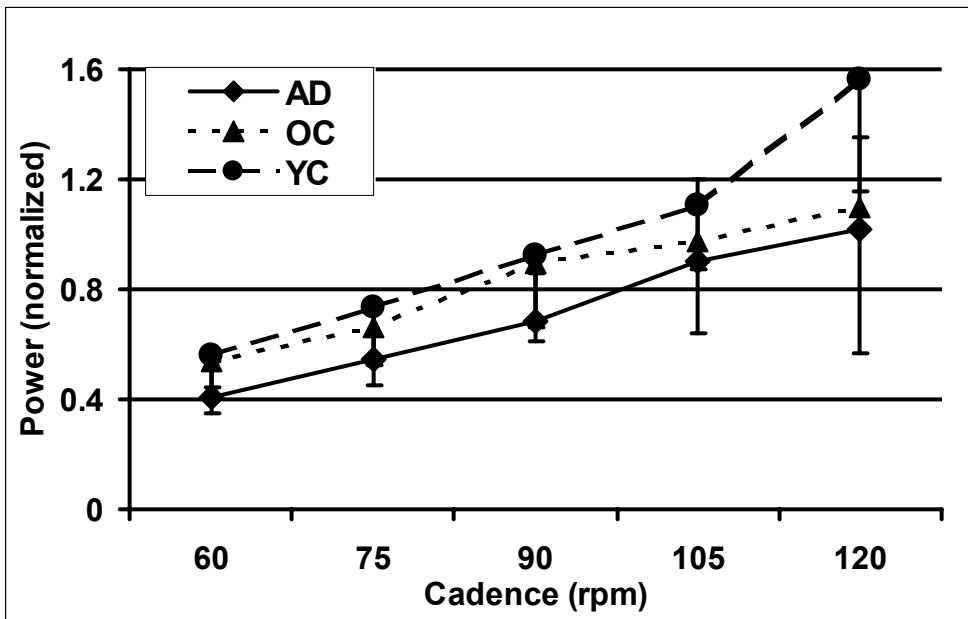


Figure I20. Ankle power contribution to limb power (AD), older children (OC), and younger children (YC) at 5 different cadences. The data for each age group are averaged across participants.

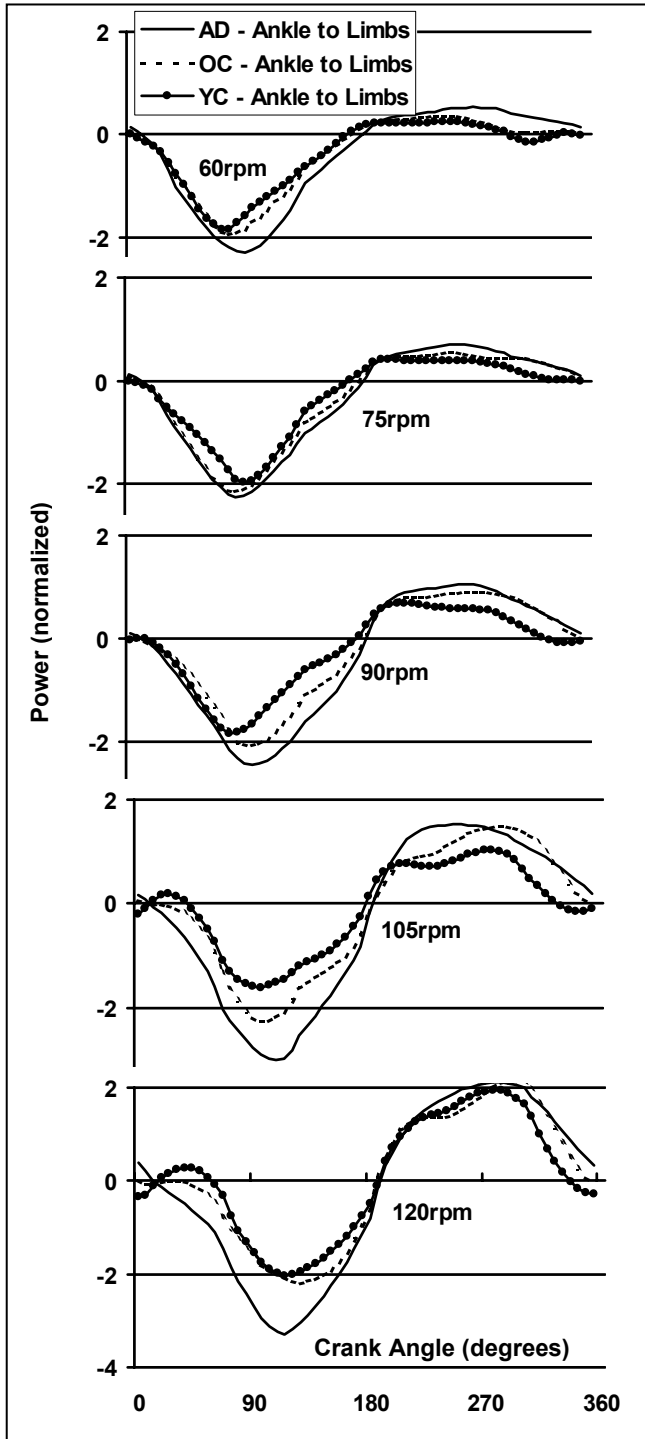


Figure I21. Effect of age and cadence on the ankle power contribution to limb power during the extensor phase (EXT). The negative numbers indicate that energy is absorbed from the limbs and transferred to the crank. The Age x Cadence interaction was non-significant. Means and standard deviations are plotted for adults (AD), older children (OC), and younger children (YC).

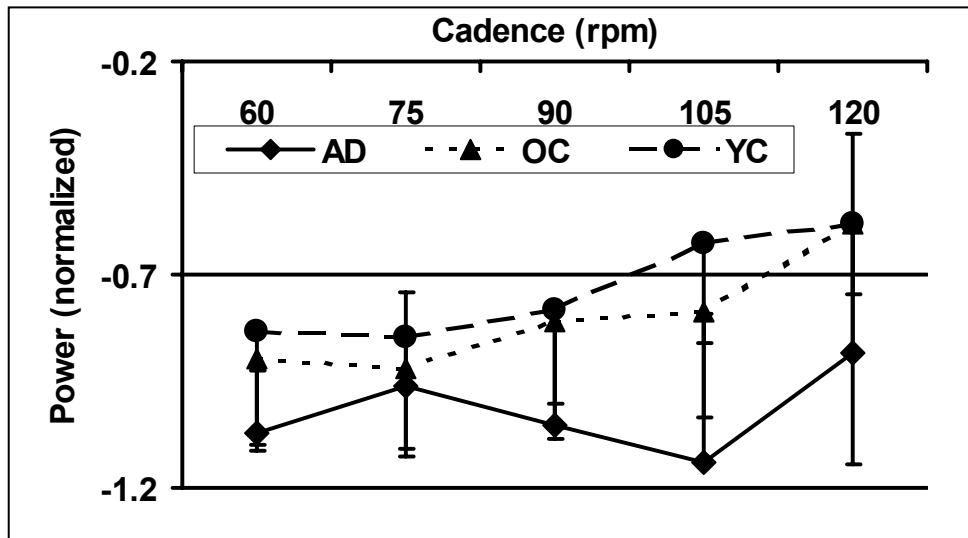


Figure I22. Effect of age and cadence on the ankle power contribution to limb power during the flexor phase (FLEX). The negative numbers indicate that energy is absorbed from the limbs and transferred to the crank. The Age x Cadence interaction was non-significant. Means and standard deviations are plotted for adults (AD), older children (OC), and younger children (YC).

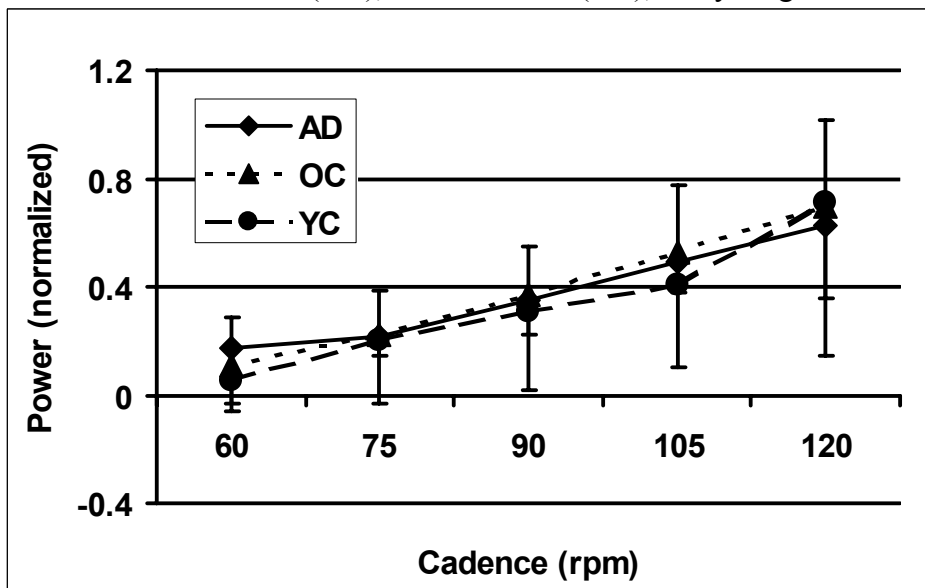


Figure I23. Effect of age and cadence on the ankle power contribution to limb power during the top phase (TOP). The Age x Cadence interaction was statistically non-significant. Means and standard deviations are plotted for adults (AD), older children (OC), and younger children (YC).

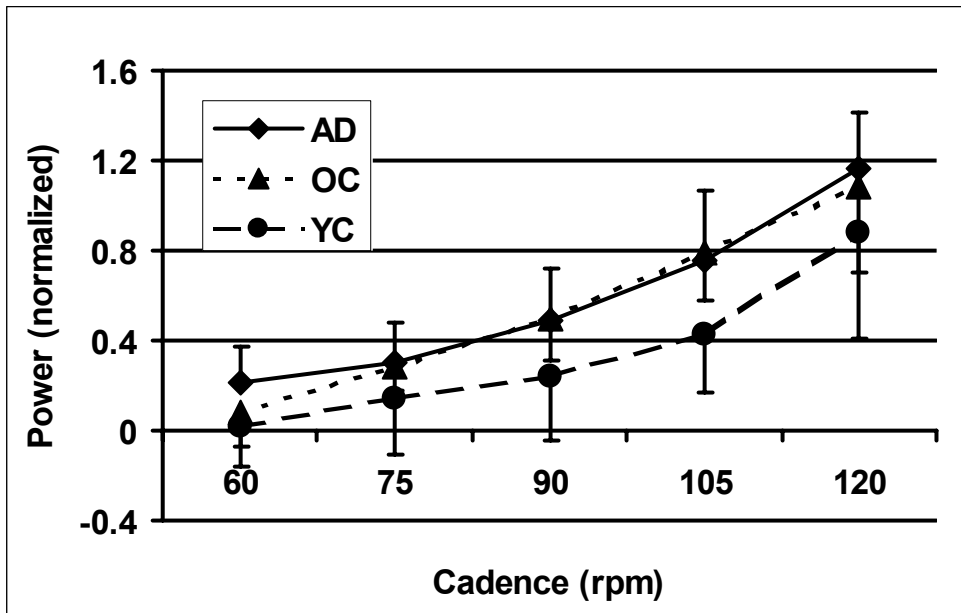


Figure I24. Effect of age and cadence on the ankle power contribution to limb power during the bottom phase (BOT). The symbol “*” indicates a significant age-effect at the corresponding cadences. Means and standard deviations are plotted for adults (AD), older children (OC), and younger children (YC).

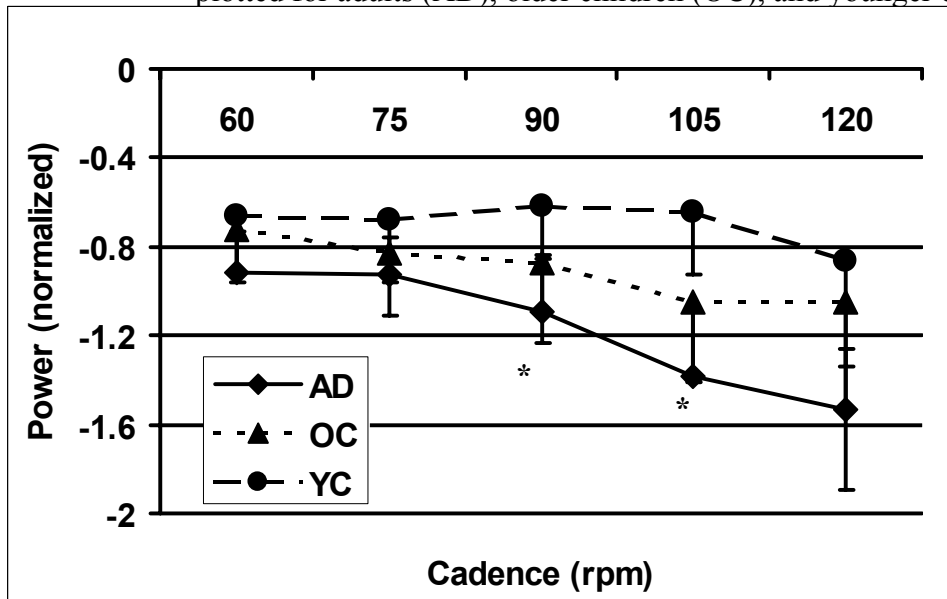


Table I1. Effect sizes describing the age group differences in peak power (AD: adults; OC: older children; YC: younger children).

Age group comparison			Cadence (rpm)	Joint
AD-OC	AD-YC	OC-YC		
-0.04	-0.12	-0.07	60	Ankle
0.22	-0.01	-0.17	75	
0.19	-0.27	-0.39	90	
-0.06	0.05	0.09	105	
0.64	0.72	-0.08	120	
1.62	-0.05	-1.24	60	Knee
0.49	0.17	-0.36	75	
-0.01	-0.35	-0.38	90	
0.62	-0.17	-0.76	105	
-0.46	-0.70	-0.04	120	
-0.55	-0.93	-0.57	60	Hip
-0.34	-0.76	-0.55	75	
0.60	0.39	-0.27	90	
0.65	1.15	0.64	105	
0.14	1.54	0.98	120	

Table I2. Effect sizes describing the age group differences in net muscular power during the extensor phase (EXT) and during the top phase (TOP) (AD: adults; OC: older children; YC: younger children).

Age group comparison			Cadence (rpm)	Crank Cycle Phase
AD-OC	AD-YC	OC-YC		
2.52	1.29	-0.74	60	EXT
1.84	1.72	0.10	75	
1.43	1.31	0.14	90	
1.91	1.94	0.67	105	
0.12	1.62	1.41	120	
-0.96	-0.42	0.22	60	TOP
-0.25	-0.66	-0.43	75	
-0.93	-1.46	-0.56	90	
-0.98	-1.47	-0.71	105	
-1.05	-1.78	0.31	120	

Table I3. Effect sizes describing the age group differences in the hip power contribution to limb power the during the extensor phase (EXT) and during the top phase (TOP) (AD: adults; OC: older children; YC: younger children).

Age group comparison			Cadence (rpm)	Crank Cycle Phase
AD-OC	AD-YC	OC-YC		
-0.36	-0.26	-0.01	60	EXT
-0.37	-0.09	0.19	75	
0.37	0.71	0.44	90	
0.33	1.35	1.16	105	
0.54	1.12	0.12	120	
0.01	-0.07	-0.07	60	TOP
0.52	0.06	-0.29	75	
0.14	-0.28	-0.38	90	
1.00	0.01	-1.05	105	
0.01	1.02	0.34	120	

Table I4. Effect sizes describing the age group differences in the ankle power contribution to limb power during the extensor phase (EXT) and during the top phase (TOP) (AD: adults; OC: older children; YC: younger children).

Age group comparison			Cadence (rpm)	Crank Cycle Phase
AD-OC	AD-YC	OC-YC		
-0.99	-1.04	-0.25	60	EXT
-0.19	-0.45	-0.30	75	
-0.87	-1.12	-0.11	90	
-1.17	-1.72	-0.62	105	
-0.56	-0.85	0.01	120	
0.80	1.11	0.36	60	TOP
0.11	0.73	0.71	75	
-0.07	0.92	0.99	90	
-0.13	1.18	1.47	105	
0.16	1.24	0.43	120	

Table I5. Effect sizes describing the age group differences in the knee power contribution to crank power the extensor phase (EXT) and during the top phase (TOP) (AD: adults; OC: older children; YC: younger children).

Age group comparison			Cadence (rpm)	Crank Cycle Phase
AD-OC	AD-YC	OC-YC		
1.55	0.69	-0.48	60	EXT
1.02	0.63	-0.29	75	
0.06	0.26	0.17	90	
0.27	-0.13	-0.34	105	
-0.62	-0.13	0.64	120	
-0.33	-0.18	0.22	60	TOP
-0.44	-1.23	-0.36	75	
-1.71	-1.75	0.06	90	
-2.42	-2.10	0.32	105	
-1.91	-1.51	0.26	120	

Appendix J: Tracking Results – Study 3

Table J1. Tracking errors for younger children quantified as the relative absolute deviation (RAD) in percent.

Subject	Cadence (rpm)	RAD: Crank Angle (%)	RAD: Thigh Angle (%)	RAD: Crank Angular Velocity (%)	RAD: Thigh Angular Velocity (%)	RAD: Horizontal Pedal Force (%)	RAD: Vertical Pedal Force (%)
mlz06	60	0.0006	0.0077	0.046	0.0268	1.6686	1.4618
mlz06	75	0.0007	0.0116	0.0991	0.0302	1.3655	1.3388
mlz06	90	0.0007	0.0097	0.1543	0.0204	1.3694	1.1901
mlz06	105	0.0006	0.0144	0.0714	0.0261	1.9512	1.6281
mlz06	120	0.0004	0.0185	0.0859	0.0275	1.5202	1.4395
mfb05	60	0.001	0.0096	0.0916	0.0415	1.5009	1.2647
mfb05	75	0.0003	0.0126	0.0995	0.0318	1.5493	1.4523
mfb05	90	0.0006	0.0159	0.125	0.0402	1.561	1.8833
mfb05	105	0.0006	0.0175	0.0956	0.0361	1.6544	1.9524
jdb05	75	0.0005	0.0148	0.1085	0.0381	1.5846	1.3406
jdb05	90	0.0005	0.013	0.093	0.0262	1.6953	1.5889
jdb05	120	0.001	0.0174	0.0799	0.0319	1.4916	1.5553
ecb05	60	0.0024	0.0138	0.3297	0.0385	1.4059	1.3876
ecb05	75	0.0029	0.0193	0.4828	0.0372	1.6741	1.5372
ecb05	90	0.0005	0.0152	0.0823	0.0346	1.5453	1.4001
ecb05	105	0.0006	0.02	0.0719	0.0359	1.7848	1.8263
ecb05	120	0.0006	0.0225	0.0491	0.0322	1.7008	1.9141
jjc06	75	0.0009	0.0114	0.0895	0.0323	1.4069	1.3232
jjc06	90	0.0004	0.0126	0.0913	0.0279	1.518	1.637
jjc06	105	0.0005	0.0159	0.1202	0.0284	1.9053	1.7537
jjc06	120	0.0004	0.0199	0.0871	0.0286	2.0139	1.6464
esh06	60	0.0005	0.012	0.1771	0.0385	1.4575	1.6911
esh06	75	0.0004	0.0091	0.1218	0.0207	1.3467	1.5566
esh06	90	0.0004	0.0133	0.1881	0.03	1.3251	2.0204
esh06	105	0.0005	0.0149	0.0816	0.023	1.8491	2.0688
esh06	120	0.0005	0.0189	0.0888	0.0248	1.6847	1.6935
jat05	60	0.0005	0.01	0.2443	0.0458	1.2812	1.5244
jat05	75	0.0006	0.0124	0.2194	0.0309	1.4302	1.6635
jat05	90	0.0005	0.0123	0.0883	0.023	1.8041	1.4331
jat05	105	0.0004	0.0154	0.1008	0.0263	1.7393	1.799
jat05	120	0.0005	0.0213	0.0833	0.0263	1.5483	1.4702
bbh05	60	0.0007	0.011	0.0415	0.0441	1.3761	1.7303

bbh05	75	0.0004	0.013	0.1	0.027	1.5398	1.5264
bbh05	90	0.0004	0.0125	0.1142	0.0239	1.6336	1.332
bbh05	105	0.0004	0.0176	0.0744	0.0279	1.8526	1.7178
bbh05	120	0.0005	0.0178	0.09	0.031	1.8149	1.6111
wdh07	60	0.0004	0.0097	0.155	0.0327	1.4077	1.3949
wdh07	75	0.0004	0.0102	0.0825	0.0214	1.343	1.3337
wdh07	90	0.0004	0.0144	0.1641	0.0253	1.5064	1.5257
wdh07	105	0.0004	0.0157	0.0839	0.0269	1.7887	1.7968
wdh07	120	0.0004	0.0178	0.0616	0.0296	1.7511	1.3579
csd05	60	0.0008	0.0089	0.1623	0.0302	1.196	1.5283
csd05	75	0.0006	0.0116	0.082	0.0306	1.5004	1.4945
csd05	90	0.0005	0.0159	0.0676	0.033	1.5697	1.7667
csd05	120	0.0005	0.0181	0.1266	0.0357	1.9047	1.9475
lmc05	60	0.0024	0.014	0.4264	0.037	1.4527	1.4421
lmc05	75	0.003	0.0176	0.4116	0.0287	1.356	1.3164
lmc05	90	0.0035	0.0213	0.2664	0.0261	1.3542	1.2697
lmc05	105	0.0082	0.0433	0.7361	0.0476	1.6733	1.5046
lmc05	120	0.0091	0.0448	0.8424	0.0442	1.7008	1.3888

Table J2. Tracking errors for older children quantified as the relative absolute deviation (RAD) in percent.

Subject	Cadence (rpm)	RAD: Crank Angle (%)	RAD: Thigh Angle (%)	RAD: Crank Angular Velocity (%)	RAD: Thigh Angular Velocity (%)	RAD: Horizontal Pedal Force (%)	RAD: Vertical Pedal Force (%)
jdt10	75	0.0004	0.0107	0.1411	0.0281	1.5305	1.7505
jdt10	90	0.0006	0.014	0.1268	0.0359	2.1542	1.944
jdt10	105	0.0007	0.016	0.0745	0.0274	2.0044	2.0298
jdt10	120	0.0006	0.0171	0.1143	0.0312	1.7725	1.674
pad10	60	0.0005	0.0089	0.1751	0.0288	1.4972	1.5926
pad10	75	0.0004	0.0117	0.11	0.0332	1.3332	1.7778
pad10	90	0.0005	0.0126	0.1203	0.0225	1.5743	2.3854
pad10	120	0.0007	0.0188	0.1209	0.039	1.9089	2.4315
jjw09	60	0.0005	0.0081	0.0965	0.0277	1.4098	1.5831
jjw09	75	0.0061	0.0278	0.3904	0.038	1.5147	1.1799
jjw09	90	0.0004	0.0139	0.0724	0.0235	1.4532	1.5157
jjw09	105	0.0082	0.0409	0.6577	0.0424	1.6485	1.2726
jjw09	120	0.0004	0.0197	0.0788	0.032	1.7929	1.3531
kis10	60	0.0004	0.0092	0.1293	0.0338	1.4329	1.1886
kis10	75	0.0004	0.0098	0.1303	0.023	1.3794	1.403

kis10	90	0.0004	0.0123	0.0791	0.0229	1.5979	1.5195
kis10	105	0.0004	0.0152	0.145	0.0303	1.8076	1.981
kis10	120	0.0004	0.0161	0.0926	0.0271	1.4905	1.4332
kme08	60	0.0006	0.0073	0.1886	0.0321	1.5001	1.3035
kme08	75	0.0005	0.0091	0.2294	0.0222	1.4554	1.3958
kme08	90	0.0004	0.0125	0.1491	0.0215	1.6598	1.5307
kme08	105	0.0004	0.0161	0.1016	0.0291	1.9684	1.7844
kme08	120	0.0005	0.0169	0.0787	0.0272	1.5985	1.1156
amh09	60	0.0024	0.0148	0.4577	0.0317	1.4647	1.5506
amh09	75	0.0004	0.0124	0.1119	0.0315	1.3656	1.6832
amh09	90	0.0005	0.0129	0.0879	0.0239	1.7097	1.6924
amh09	105	0.0004	0.0148	0.091	0.0259	1.8877	1.867
amh09	120	0.0005	0.0163	0.1372	0.0282	1.7185	1.5585
agb09	60	0.0004	0.0085	0.1741	0.0275	1.4657	1.5629
agb09	75	0.0004	0.0105	0.0998	0.0259	1.5026	1.7219
agb09	90	0.0004	0.0123	0.1035	0.0205	1.6178	1.8898
agb09	105	0.0005	0.0145	0.1262	0.0221	1.829	1.9778
agb09	120	0.0004	0.0185	0.1357	0.0247	1.6088	1.5348
jmc08	60	0.0004	0.0079	0.1076	0.0226	1.6764	1.6307
jmc08	75	0.0004	0.0114	0.0525	0.0256	1.3437	1.385
jmc08	90	0.0003	0.0148	0.083	0.0281	1.4536	1.4521
jmc08	105	0.0004	0.0164	0.0619	0.0275	1.6844	1.6744
jmc08	120	0.0004	0.0193	0.0688	0.0326	1.7743	1.5319
rth10	60	0.0004	0.0077	0.1317	0.0249	1.4401	1.4373
rth10	75	0.0004	0.0104	0.0608	0.0238	1.3931	1.2312
rth10	90	0.0004	0.0131	0.076	0.0307	1.689	1.4545
rth10	105	0.0005	0.017	0.081	0.0312	1.9238	1.9966
rth10	120	0.0004	0.0188	0.0898	0.0306	1.7166	1.5976

Table J3. Tracking errors for adults quantified as the relative absolute deviation (RAD) in percent.

Subject	Cadence (rpm)	RAD: Crank Angle (%)	RAD: Thigh Angle (%)	RAD: Crank Angular Velocity (%)	RAD: Thigh Angular Velocity (%)	RAD: Horizontal Pedal Force (%)	RAD: Vertical Pedal Force (%)
ama27	60	0.0004	0.0087	0.1313	0.0246	1.4778	1.5009
ama27	75	0.0004	0.0107	0.1373	0.0245	1.4257	1.3568
ama27	90	0.0003	0.0134	0.1138	0.0246	1.5287	1.3881
ama27	105	0.0004	0.0144	0.1487	0.0267	1.6125	1.5949
ama27	120	0.0006	0.0164	0.1029	0.0256	1.6838	1.3631

bgj27	60	0.0004	0.007	0.0924	0.0183	1.4312	1.3907
bgj27	75	0.0004	0.0093	0.1205	0.0181	1.376	1.376
bgj27	90	0.0004	0.0123	0.1218	0.02	1.3416	1.6706
bgj27	105	0.0004	0.0144	0.1196	0.0213	1.6215	1.5635
bgj27	120	0.0004	0.0188	0.1206	0.0219	1.5329	1.4658
dst30	60	0.0004	0.007	0.1903	0.018	1.5265	1.3993
dst30	75	0.0004	0.0095	0.1238	0.0203	1.5382	1.3078
dst30	90	0.0003	0.0114	0.1513	0.0221	1.6452	1.3606
dst30	105	0.0004	0.0147	0.1143	0.0246	1.7531	1.8268
dst30	120	0.0004	0.0178	0.123	0.0266	1.7217	1.3424
mjn26	60	0.0005	0.0074	0.1439	0.0207	1.4598	1.5254
mjn26	75	0.0004	0.0083	0.1483	0.0175	1.4156	1.4576
mjn26	90	0.0004	0.0108	0.1051	0.0164	1.3614	1.4447
mjn26	105	0.0005	0.0145	0.1287	0.021	1.5756	1.5596
mjn26	120	0.0005	0.0171	0.157	0.0232	1.5065	1.3791
mmb25	60	0.0004	0.0073	0.1007	0.0203	1.5808	1.6119
mmb25	75	0.0004	0.009	0.0899	0.0169	1.4316	1.2618
mmb25	90	0.0004	0.0119	0.1685	0.0191	1.478	1.4812
mmb25	105	0.0004	0.0145	0.1534	0.0212	1.8241	2.4276
mmb25	120	0.0004	0.0169	0.173	0.0231	1.6355	2.1392
nho25	60	0.0005	0.0074	0.1813	0.0203	1.3184	1.4044
nho25	75	0.0004	0.0089	0.168	0.0217	1.2673	1.3769
nho25	90	0.0071	0.0339	1.1744	0.0444	1.6537	1.841
nho25	105	0.0007	0.017	0.0897	0.0273	1.6293	1.8012
nho25	120	0.0005	0.0201	0.1209	0.0231	1.4539	1.5402
pkc26	60	0.0004	0.009	0.1525	0.0383	1.5667	1.8523
pkc26	75	0.0004	0.0111	0.0986	0.0352	1.5309	1.8155
pkc26	90	0.0005	0.0124	0.1594	0.029	1.6367	1.8651
pkc26	105	0.0004	0.0152	0.1146	0.0239	1.5575	2.0084
pkc26	120	0.0005	0.0154	0.106	0.0225	1.5338	2.0115
raw30	60	0.0004	0.0089	0.1249	0.0261	1.4399	1.4486
raw30	75	0.0004	0.0093	0.1015	0.0203	1.3544	1.3777
raw30	90	0.0004	0.0128	0.102	0.0212	1.379	1.4508
raw30	105	0.0004	0.0151	0.0977	0.0221	1.6524	1.5574
raw30	120	0.0005	0.0179	0.099	0.023	1.5316	1.2965

References

- Anderson, F. C., & Pandy, M. G. (2001). Static and dynamic optimization solutions for gait are practically equivalent. *Journal of Biomechanics*, 34, 153-161.
- Anderson, F. C., & Pandy, M. G. (2003). Individual muscle contributions to support in normal walking. *Gait & Posture*, 17, 159-169.
- Asai, H., & Aoki, J. (1996). Force development of dynamic and static contractions in children and adults. *International Journal of Sports Medicine*, 17, 170-174.
- Asmussen, E., & Heebøll-Nielsen, K. (1956). Physical performance and growth in children. Influence of sex, age and intelligence. *Journal of Applied Physiology*, 8, 371-380.
- Asmussen, E., & Heebøll-Nielsen, K. (1955). A dimensional analysis of physical performance and growth in boys. *Journal of Applied Physiology*, 7, 593-603.
- Bernardi, M., Solomonow, M., Nguyen, G., Smith, A., & Baratta, R. (1996). Motor unit recruitment strategy changes with skill acquisition. *European Journal of Applied Physiology and Occupational Physiology*, 74, 52-59.
- Bothner, K. E., & Jensen, J. L. (2001). How do non-muscular torques contribute to the kinetics of postural recovery following a support surface translation? *Journal of Biomechanics*, 34, 245-250.
- Brown, N. A., & Jensen, J. L. (2003). The development of contact force construction in the dynamic-contact task of cycling. *Journal of Biomechanics*, 36, 1-8.
- Clark, J. E., Whittall, J., & Phillips, S. J. (1988). Human interlimb coordination: The first 6 months of independent walking. *Developmental Psychobiology*, 21, 445-456.
- Chao, P., Rabago, C., Korff, T., & Jensen, J. L. (2002). Muscle activation adaptations in children in response to changes in cycling cadence [Abstract]. *Journal of Sport & Exercise Psychology*, 24(Suppl.), S42-S43.
- Delp, S. L., Loan, J. P., Hoy, M. G., Zajac, F. E., Topp, E. L., & Rosen, J. M. (1990). An interactive graphics-based model of the lower extremity to study orthopaedic surgical procedures. *IEEE Transactions of Biomedical Engineering*, 37, 757-767.
- Forssberg, H., & Nashner, L. M. (1982). Ontogenetic development of postural control in man: adaptation to altered support and visual conditions during stance. *Journal of Neuroscience*, 2, 545-552.

- Forssberg, H. (1985). Ontogeny of human locomotor control I. Infant stepping, supported locomotion and transition to independent locomotion. *Experimental Brain Research*, 57, 480-493.
- Fregly, B. J., & Zajac, F. E. (1996). A state-space analysis of mechanical energy generation, absorption, and transfer during pedaling. *Journal of Biomechanics*, 29, 81-90.
- Gibbs, J., Harrison, L. M., & Stephens, J. A. (1997). Cross-correlation analysis of motor unit activity recorded from two separate thumb muscles during development in man. *Journal of Physiology*, 499, 255-266.
- Hatze, H. (2000). The inverse dynamics problem of neuromuscular control. *Biological Cybernetics*, 82, 133-141.
- Hoy, M. G., & Zernicke, R. F. (1986). The role of intersegmental dynamics during rapid limb oscillations. *Journal of Biomechanics*, 19, 867-877.
- Haywood, K. M., & Getchell N. (2001). *Life span motor development* (3rd ed.). Champaign, IL: Human Kinetics.
- Hof, A. L. (1992). An explicit expression for the moment in multibody systems. *Journal of Biomechanics*, 25, 1209-1211.
- Hull, M. L., & Jorge, M. (1985). A method for biomechanical analysis of bicycle pedalling. *Journal of Biomechanics*, 18, 631-644.
- Jensen, J. L., & Korff, T. (2004). Adapting to changing task demands: variability in children's response to manipulations of resistance and cadence during pedaling. *Research Quarterly for Exercise and Sport*, 75, 361-369.
- Jensen, R. K. (1981). The effect of a 12-month growth period on the body moments of inertia of children. *Medicine and Science in Sports and Exercise*, 13, 238-242.
- Jensen, R. K. (1986). Body segment mass, radius and radius of gyration proportions of children. *Journal of Biomechanics*, 19, 359-368.
- Jensen, R. K. (1989). Changes in segment inertia proportions between 4 and 20 years. *Journal of Biomechanics*, 22, 529-536.
- Kautz, S. A., & Hull, M. L. (1993). A theoretical basis for interpreting the force applied to the pedal in cycling. *Journal of Biomechanics*, 26, 155-165.
- Korff, T., & Jensen, J. L. (2003a). Development of adaptation to changing speed requirements in terms of negative muscular work during bicycling [Abstract]. *Research Quarterly for Exercise and Sport*, 74(Suppl.), A32-A33.

- Korff, T., & Jensen, J.L. (2003b). Standardisierung beim Versuchsaufbau von Experimenten der motorischen Entwicklung und Auswirkungen auf deren Interpretation: Normalisierung der Kurbellänge beim Radfahren. [Abstract]. *Schriftenreihe der DVS*, 138, 200.
- Lexell, J., Sjostrom, M., Nordlund, A. S., & Taylor, C. C. (1992). Growth and development of human muscle: A quantitative morphological study of whole vastus lateralis from childhood to adult age. *Muscle & Nerve*, 15, 404-409.
- Lin, J. P., Brown, J. K., & Walsh, E. G. (1994). Physiological maturation of muscles in childhood. *Lancet*, 343, 1386-1389.
- Lin, J. P., Brown, J. K., & Walsh, E. G. (1997). Soleus muscle length, stretch reflex excitability, and the contractile properties of muscle in children and adults: A study of the functional joint angle. *Developmental Medicine and Child Neurology*, 39, 469-480.
- Marsh, A. P., Martin, P. E., & Sanderson, D. J. (2000). Is a joint moment-based cost function associated with preferred cycling cadence? *Journal of Biomechanics*, 33, 173-180.
- Martin, J. C., Farrar, R. P., Wagner, B. M., & Spirduso, W. W. (2000). Maximal power across the lifespan. *Journals of Gerontology Series A: Biological Sciences and Medical Sciences*, 55, M311-316.
- Neptune, R. R., & Hull, M. L. (1998). Evaluation of performance criteria for simulation of submaximal steady-state cycling using a forward dynamic model. *Journal of Biomechanical Engineering*, 120, 334-341.
- Newell, K.M. (1986). Constraints on the development of coordination. In M.G. Wade & H.T.A. Whiting (Eds.), *Motor development in children: Aspects of coordination and control* (pp.341-360). Boston: Martinus Nijhoff.
- Pandy, M. G. (2001). Computer Modeling and Simulation of Human Movement. *Annual Reviews of Biomedical Engineering*, 3, 245-273.
- Raasch, C. C., Zajac, F. E., Ma, B., & Levine, W. S. (1997). Muscle coordination of maximum-speed pedaling. *Journal of Biomechanics*, 30, 595-602.
- Schneider, K., Zernicke, R. F., Ulrich, B. D., Jensen, J. L., & Thelen, E. (1990). Understanding movement control in infants through the analysis of limb intersegmental dynamics. *Journal of Motor Behavior*, 22, 493-520.
- Schneider, K., & Zernicke, R. F. (1992). Mass, center of mass, and moment of inertia estimates for infant limb segments. *Journal of Biomechanics*, 25, 145-148.

- Sun, H., & Jensen, R. K. (1994). Body segment growth during infancy. *Journal of Biomechanics*, 27, 265-275.
- Teeple, J. B. (1978). Physical growth and maturation. In M. F. Ridenour (Ed.), *Motor development: Issues and applications* (pp. 3-27). Princeton, NJ: Princeton Book.
- Timiras, P. S. (1972). *Developmental physiology and aging*. New York: Macmillan.
- Van Ingen Schenau, G. J., Dorssers, W. M., Welter, T. G., Beelen, A., de Groot, G., & Jacobs, R. (1995). The control of mono-articular muscles in multijoint leg extensions in man. *Journal of Physiology*, 484, 247-254.
- Winter, D. A., & Eng, P. (1995). Kinetics: our window into the goals and strategies of the central nervous system. *Behavioral Brain Research*, 67, 111-120.
- Winter, D. A., & Robertson, D. G. (1978). Joint torque and energy patterns in normal gait. *Biological Cybernetics*, 29, 137-142.
- Winter, D. A. (1989). Biomechanics of normal and pathological gait: Implications for understanding human locomotor control. *Journal of Motor Behavior*, 21, 337-355.
- Winter, D. A. (1990). *Biomechanics and motor control of human movement*. (2nd ed.), New York: Wiley.
- Zajac, F. E., & Gordon, M. E. (1989). Determining muscle's force and action in multiarticular movement. *Exercise and Sport Sciences Reviews*, 17, 187-230.

Vita

Thomas Korff was born in Minden, Germany on February 26, 1973, the son of Heidemarie Korff and Wilhelm Korff. He entered the Westfälische Wilhelms Universität Münster, Germany in 1993. Between 1997 and 1998, he attended the University of Lethbridge, Alberta, Canada. He received his degree (1. Staatsexamen für die Sekundarstufen I und II) which is equivalent to a Master of Science (Majors: Mathematics and Physical Education) from the University of Münster in May 2000. In September 2000 he started his doctoral work in Biomechanics at The University of Texas at Austin.

Permanent address: 26, Frayslea, Uxbridge, Middlesex, UB8 2AT, United Kingdom

This dissertation was typed by the author.